博士論文番号：0981031

Molecular mechanism of CO_2-induced self-incompatibility overcome in the Brassicaceae

Lao Xintian

Laboratory of Intercellular Communications
Graduate School of Biological Sciences
Nara Institute of Science and Technology, JAPAN
(Prof. Seiji Takayama)
30 November 2013

Dedication

To my uncle, Shihong Lao, for all your strict but kind words, support and love.

TABLE OF CONTENTS

Abbreviations i

Preface 1

Chapter 1. Physiological and genetic analysis on CO_2-induced self-incompatibility overcome in *Brassica rapa*

1.1 Introduction 9
1.2 Materials and Methods 11
1.3 Results 15
1.4 Discussion 21
1.5 Figures and tables 24

Chapter 2. Self-incompatibility responses to CO_2 in different *Arabidopsis thaliana* accessions

2.1 Introduction 52
2.2 Materials and Methods 54
2.3 Results 57
2.4 Discussion 60
2.5 Figures and tables 62

Chapter 3. Mutant screening of downstream components of SI pathway

3.1 Introduction 69
3.2 Materials and Methods 70
3.3 Results 72
3.4 Discussion 74
3.5 Figures and tables 76

Conclusions 79

Acknowledgments 80

References 81

Abbreviations

CO_2;	carbon dioxide
CTAB;	cetyltrimethylammonium bromide
EDX;	Energy Dispersive X-ray spectroscopy
ETD;	Everhart-Thornley detector
IM;	interval mapping
InDel;	insert and delete
GSI;	gametophytic self-incompatibility
LET;	linear energy transfer
LG;	linkage group
LOD;	log of odds
MAS;	marker-associated selection
MS;	Murashige and Skoog
NIL;	near-isogenic line
QTL;	quantitative trait loci
RFLP;	resistant fragment length polymorphism
$RLSICO_2$;	reaction level of SI to CO_2
RT-PCR;	reverse transcription-PCR
SC;	self-compatibility
SI;	self-incompatibility
SSI;	sporophytic self-incompatibility
SSR;	simple sequence repeated

PREFACE

Sexual reproduction is a primary system to increase genetic diversity which is in place in most of the flora and fauna. However, the majority of flowering plants produce both male and female reproductive organs on the same flower (hermaphrodite) and are prone to self-pollination. Self-incompatibility (SI) systems allow hermaphroditic flowers to differentiate and reject self-pollen thus serving as a genetic barrier to prevent self-fertilization and ensure high rates of out-crossing.

SI in plants is based on specific cell-cell interactive events between pollen and pistil. Stigma efficiently screens and blocks self-pollen from hydrating, germinating and penetrating, therefore, inhibiting pollen tube growth. During the evolution of flowering plants, a diversity of SI mechanisms has arisen (Charlesworh *et al*., 2005; Shimizu *et al*., 2008). SI systems can be categorized into heteromorphic and homomorphic systems (Fig. 1). In heteromorphic SI systems, which can be found in the Primulaceae, Oxalidaceae and Polygonaceae, flowers have different style and anther length which are genetically controlled by a single *S*-locus (Lewis, 1949) or *S* and *M* loci (Mather, 1943). A compatible reaction occurs only when pollen is from an anther with the same length as the recipient stigma.

In homomorphic SI systems, flowers have identical form and self-recognition is controlled by a multi-allelic *S*-locus (de Nettancourt, 2001). Based on a genetic system that controls the self-incompatible phenotype of pollen, homomorphic SI systems can be classified into gametophytic SI (GSI) and sporophytic SI (SSI) systems. In the GSI system (found in, e.g., Solanaceae, Rosaceae, Plantaginaceae), the self-incompatible phenotype of the pollen is determined by its own haploid genotype (n), while in the SSI system (found in the Brassicaceae, Convolvulacae and Asteraceae), the self-incompatible phenotype is determined by the genotype of the diploid parent (2n) (Fig. 2). All plant materials used in this thesis belong to the Brassicaceae family, which uses the SSI system. Based on outcrossing studies using wild populations, over 50 and 30 different *S*-alleles have been identified from *Brassica oleracea* and *B. rapa*, respectively (Ockendon, 1985; Nou *et al*., 1993).

The stigma of the style in Brassicaceae plants is covered by a layer of cells called the papilla cells. The cell wall of a papilla cell consists of pellicle, cuticle and pectocellulose

layers. Mature pollen is in a highly desiccated condition with a packed pollen coat between the baculae of exine (Elleman and Dickinson, 1986). When pollen adheres to the stigma, the initial contact between pollen coat and papilla cell causes the pollen grain to change conformation. After pollination, a coating 'foot' forms between attached pollen and papilla surface which involved in water supply from papilla cell to pollen grain. Pollen grain placed on a compatible stigma is hydrated in 20-60 min and changes in shape from ellipsoidal to almost spherical. A fully hydrated pollen grain then produces a tube and enters the papilla cell wall at a site within the foot (Elleman and Dickinson, 1990). The tube elongates along a space between the outer and inner cell wall components, and is guided down the papilla into the middle lamella region of the stigmatic crow, where it grows to the transmitting tissue of the style and finally reaches the ovule, where fertilization then occurs (Stead *et al*., 1980; Elleman and Dickinson, 1990; Elleman *et al*., 1992). In the case of incompatible pollination, pollen hydration, germination and pollen tube penetration are arrested after foot formation.

This SI reaction occurs when the same *S*-allele (or *S*-haplotype) is expressed in both pollen and pistil, and male and female *S*-determinants have been identified as SP11/SCR (*S*-locus protein 11/*S*-locus cysteine-rich) (Schopfer *et al*., 1999; Takayama *et al*., 2000) and SRK (*S* receptor kinase) (Takasaki *et al*., 2000), respectively. SP11/SCR binding to SRK triggers a phosphorylation signaling cascade to reject self-pollen (Takayama *et al*., 2001). Another stigmatically expressed gene, *SLG* (*S* locus glycoprotein) gene is located within the *S* locus (Takayama *et al*., 1987; Nasrallah *et al*., 1987). *SLG* encodes a secreted glycoprotein, which has been shown to enhance the recognition process between the self-pollen and stigma (Takasaki *et al*., 2000).

Many studies have been performed focusing on the downstream components involved in this type of SI signaling pathway. Two components have been identified as positive effectors. ARC1 (arm-repeat containing protein 1) was identified as an interacting molecule of SRK kinase by a yeast two-hybrid screening (Gu *et al*., 1998). Suppression of ARC1 messenger RNA level correlates with a partial breakdown of self-incompatibility, resulting in seed production in *Brassica napus* (Stone *et al*., 1999). ARC1 has E3 ubiquitin ligase activity and promotes degradation of proteins essential in compatible pathway (Stone *et al*., 2003). MLPK (*M*-locus protein kinase) was identified as a positive mediator of the SI signaling

pathway through the positional cloning of the gene responsible for the self-compatible *B. rapa* var. Yellow sarson. It is a cytoplasmic protein kinase and has two different MLPK transcripts, *MLPKf1* and *MLPKf2*. Both MLPK isoforms localize to the papilla cell membrane and interact directly with SRK to transduce SI signaling (Kakita *et al*., 2007). Based on these results, a model of SI in *Brassica* is shown in Fig. 3.

SI is not always stable but can be overcome under external and physiological conditions. The most well known example is a SI breakdown by by 4-5% CO_2 gas treatment found in *Brassica* (Nakanishi *et al*., 1969; Nakanishi and Hinata, 1973). Not only in the Brassicaceae family, there are reports showing certain SI interruption by CO_2 treatment in other plants like *Petunia hybrida* (Solanaceae) (Takahashi, 1975) and *Theobroma cacao* (Malvaceae) (Aneja and Gianfagna, 1994). However, the mechanism by which CO_2 alters the SI pathway is unclear and none of the responsible genes have been identified so far.

In recent years, due to the rapid development of genomic databases and genetic markers, many genes across a broad spectrum of pathways in model plants such as *Arabidopsis thaliana, Oryza sativa*, and *Lotus japonicus* have been discovered. *A. thaliana* is a particularly advantageous model organism for functional studies because of characteristics such as, e.g., a small genome, short life cycle, and the availability of a transformation method. Moreover, it has very elongated and separated papilla cells which are easy to manipulate. *A. thaliana* belongs to the Brassicaceae family but it is self-compatible due to the loss-of-function of *S* genes, and therefore initially could not be used in SI-related research. Nasrallah's group introduced functional *S* locus genes from self-incompatible *Arabidopsis lyrata* (SRK_b *and* SCR_b) into *A. thaliana*, resulting in SI in transgenic plants of accession C24 (Nasrallah *et al*., 2002). In my laboratory, previous colleagues have generated different stable self-incompatible C24 transgenic lines by transferring cDNAs of two *S* genes (Kanatani, 2008; Takehisa, 2009), and these lines have been used for several studies (Ohara, 2010; Ito, 2011; Tanaka, 2011; Matsumoto, 2012). Additionally, Boggs *et al*. (2009) demonstrated variation in SI stability in different *A. thaliana* accessions and demonstrated a possible *S* locus-unlinked SI-modifier involved in SI stability. Despite this variety of studies in *A. thaliana*, there are no published reports regarding the CO_2 sensitivity mechanism in transgenic SI *A. thaliana* plants.

In this thesis, I focus on the SI reaction responding to CO_2 treatment in the Brassicaceae.

Biological responses were examined and genetic analysis was performed in *B. rapa* in Chapter 1. In Chapter 2, self-incompatible *A. thaliana* accessions with different CO_2-susceptability responses were established, which should be ideal lines to reveal the mechanism of SI breakdown by CO_2. A self-compatible mutant candidate was also obtained to study the downstream SI signaling pathway (Chapter 3).

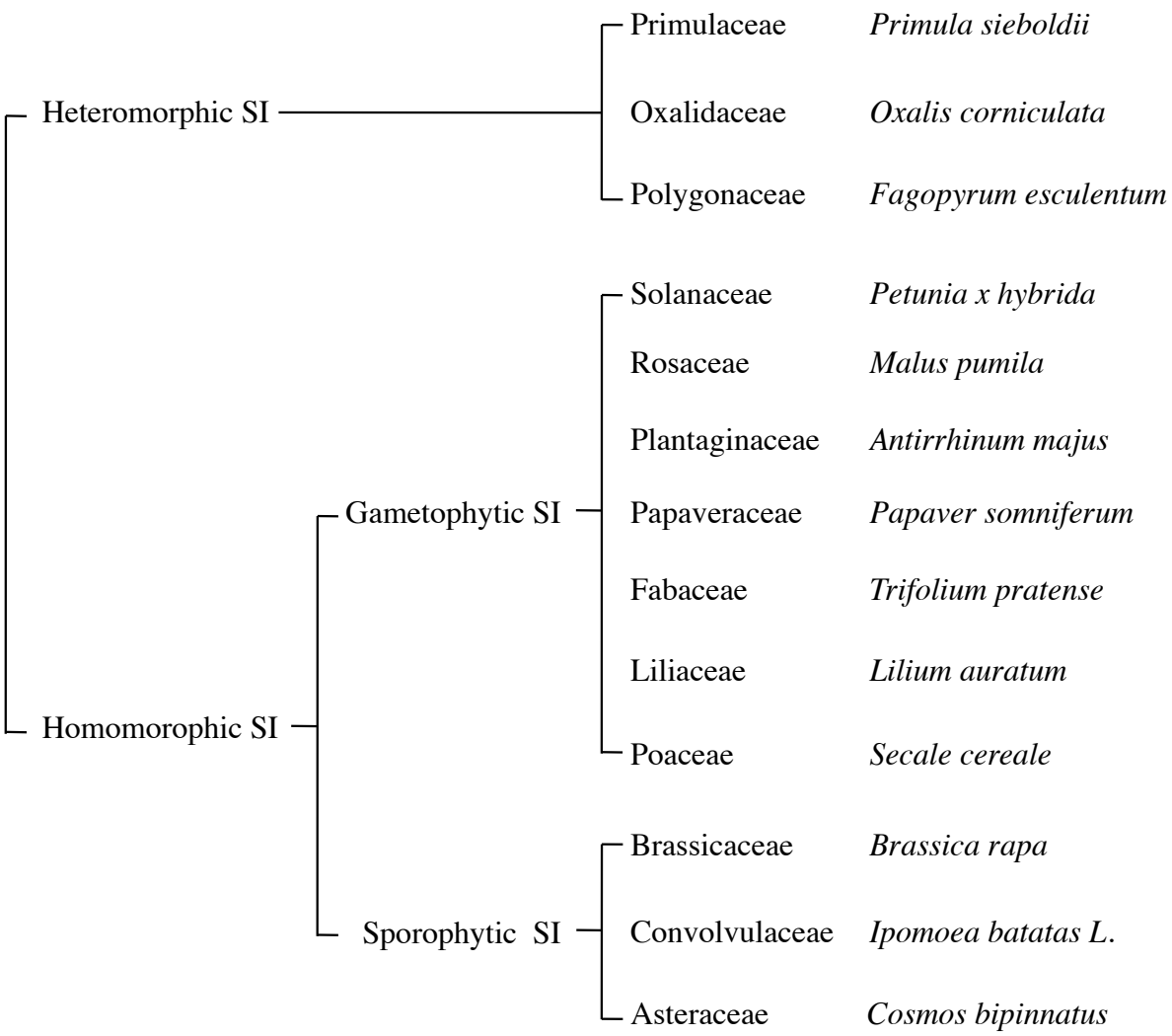

Fig. 1. Diversity of SI system

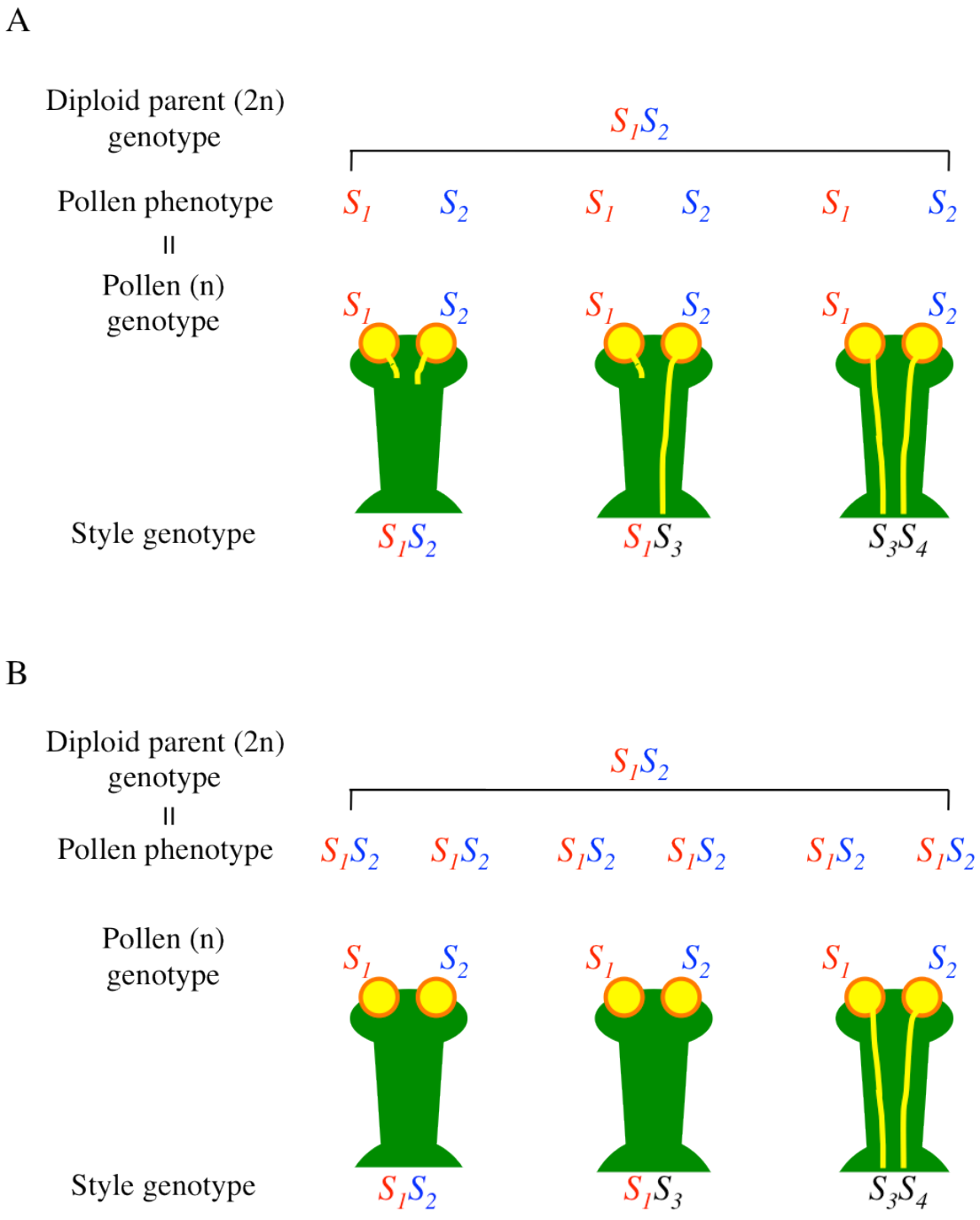

Fig. 2. Gametophytic SI (GSI) and sporophytic SI (SSI) systems

A, GSI system in Solanaceae, Rosaceae, Plantaginaceae etc. B, SSI system in the Brassicaceae, Convolvulacae and Asteraceae.

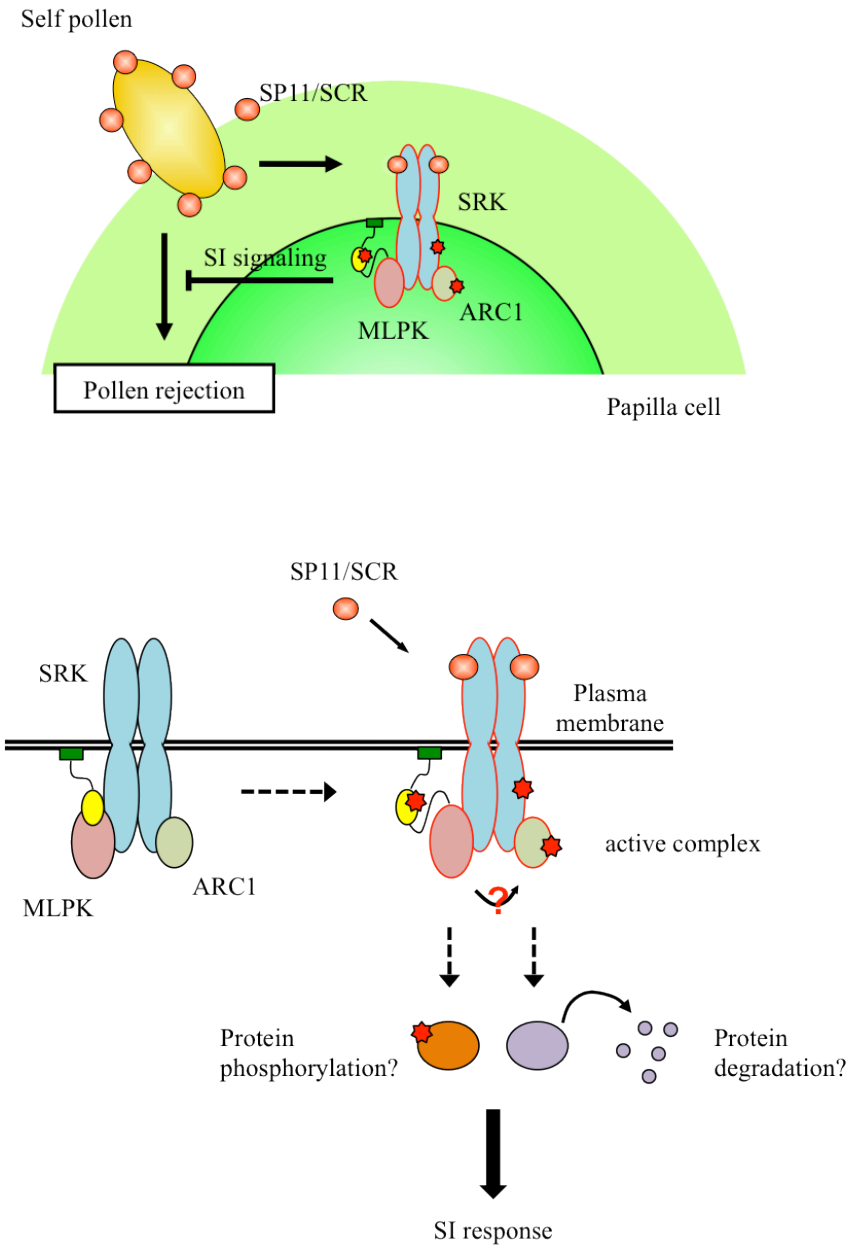

Fig. 3. SI model in the Brassicaceae

CHAPTER 1

Physiological and genetic analysis of the CO_2-induced self-incompatibility overcome in *Brassica rapa*

1.1 Introduction

When a stigma and an interacting pollen share an identical *S* haplotype, pollen hydration and/or pollen tube growth is inhibited, while when compatible pollen lands on the stigma, it can be hydrated and a pollen tube is allowed to grow. Previous studies in *Brassia* using an X-ray microanalysis (EDX) system showed that after cross-pollination, an increased calcium concentration near the site of pollen grain attachment (Iwano *et al*., 1999), and Ca^{2+} was transported from papilla cell to pollen with the hydrating water (Iwano, unpublished; Tateyama, 2010).

Hydrated pollen grains can sometimes be observed in *B. rapa* during self-pollination. In fact, the SI system in *Brassica* is not complete. Self-recognition can be interrupted by plant age (Ockendon, 1978; Horisaki and Niikura, 2008), chemical treatment such as organic solvent (Tatebe, 1968) or NaCl (Tao and Yong, 1986; Monterio and Gabelman, 1988), high temperature (Matsubara, 1980; Okazaki and Hinata 1987) or CO_2 treatment (Nakanishi *et al*., 1969). Because cultivated *Brassica* vegetables are very common in the world, especially in eastern Asia, and because of the advantage of heterosis, most *Brassica*, such as cabbage, Chinese cabbage and radish, are F_1 hybrids whose seeds are produced by taking advantage of SI. Genetically pure inbred parental lines are needed for the F_1 seeds production and CO_2 treatment is the most popular method used by many seed companies all over the world to obtain self-fertilized seeds. For *B. rapa* and *B. oleacea*, optimal CO_2 gas density, timing and humidity have been determined (Nakanishi and Hinata, 1973, 1975; Dhaliwal *et al.,* 1981; Palloix *et al.,* 1985). However, there is variation in SI response to CO_2 in *Brassica* vegetables and not all lines are CO_2-sensitive (Nakanishi and Hinata, 1973; Niikura and Matsuura, 2000). Niikura and Matsuura (2000) reported that CO_2-sensitive trait is controlled by a recessive gene that governs the construction and/or metabolism of the stigma. On the other hand, Hyun *et al*. (2007) reported a dominant, *S*-haplotype-linked CO_2-sensitive phenotype, and cDNA microarray analysis showed reduced expression of the *SLG* could be involved in overcoming SI in *B. rapa* (Kwun *et al*., 2004). Lee *et al*. (2001) reported a structural change on the surface of papilla cells in the CO_2-sensitive *Brassica campestris* (now *B. rapa*) line Hiratsuka after the CO_2 treatment, which could be the cause of SI breakdown. Despite these initial findings,

there is little knowledge about the physiological responses of the papilla cells to CO_2, and no responsible genes have been identified so far.

In this chapter, two inbred lines of *B. rapa* with different CO_2-sensitivity (HA-11621, CO_2-sensitive and HA-11623, CO_2-insensitive) were used. I performed X-ray microanalysis with a cryo-scanning electron microscope to examine changes of elemental distribution in papilla cells in response to CO_2 treatment. I evaluated the CO_2-sensitivity phenotype and investigated its relationship between *S*-haplotypes using a randomly chosen F_2 population of 110 individuals derived from these two lines. I found that the CO_2-sensitivity is a quantitative trait rather than a monogenic phenomenon. Therefore, I performed QTL analysis to identify response loci that control the high CO_2-sensitivity to overcome SI.

1.2 Materials and methods

All chemicals were purchased from Wako or Nacali without specific notification, and enzymes for genetics studies were from TAKARA.

1.2.1 Plant materials

Two inbred lines of *Brassica rapa* (2n = 20), a CO_2-sensitive line (HA-11621) and a CO_2-insensitive line (HA-11623), were established at Tohoku Seed Co., Ltd., and grown in the green house with 16-hr light and 8-hr dark conditions at 20 °C. Both lines show stable SI under normal (open-air) condition but have different CO_2-sensitivity; SI in HA-11621 breaks down following treatment with 4.5% CO_2 whereas SI in HA-11623 is unaffected. HA-11621 and HA-11623 are reciprocally compatible, and their F_1 progeny were obtained under normal condition. Buds (1-2 days before flowering) from a randomly chosen F_1 were used for F_2 production. Young petals and stamens were removed from the bud and the immature pistil was pollinated with pollen grains from mature flowers of the same plant (bud-pollination). Pollinated pistil was then covered with a paper bag for 3 days and seeds from the pistil were harvested. More than 20 pistils were pollinated and harvested seeds were used as F_2 population. 110 F_2 plants were used for phenotypic and genetic analysis.

1.2.2 Cryo-scanning electron microscopy and energy-dispersive X-ray analysis

A pistil was submersed in liquid nitrogen slush and frozen under vacuum. While under vacuum, the sample was transferred to the microscope cryo stage (ALTO 1000, Gatan), and then the stage temperature was increased to -95 °C to remove frost that had settled on top of the specimen as a result of condensation. When all the surface frost had been removed by sublimation and verified by electron microscope, the temperature was reduced to -140 °C. Imaging was performed using ETD (Everhart-Thornley Detector) by Quant 250 scanning electron microscope (FEI). The chamber pressure was 30 Pa and the accelerating voltage was 15 kV. EDX (Energy Dispersive X-ray spectroscopy) analysis of the element assay was performed on selected papilla cells using INCA X-ray analysis software (Oxford Instruments, http://www.oxinst.com/Pages/home.aspx), with the detector's process time set at 2. X-ray

data were collected with 4.5 nA probe current for 2 minutes.

1.2.3 Calcium Green assay

After removing the stamens, flowers cut at the peduncle were stood on a 1% (w/v) solid agar plate. 0.3 μL of 50 μM Calcium Green (cell impermeable type) (Invitrogen) in a solution containing 0.01% Tween 20 was applied on the stigma. After the stigma air-dried, place the pistil on the cover glass and 1% solid agar was used to cover the cut edge. The stigma was then pollinated using a manipulator, and observed using laser confocal microscope (LSM 710, Zeiss). Fluorescence was observed with a 488 nm excitation wavelength and emission collected at 500-550 nm.

1.2.4 Evaluation of the CO_2-sensitivity

Three to five flowers were cut at the peduncle and stood on a 1% (w/v) solid agar plate. Flowers were self-pollinated, placed into a CO_2 incubator, and treated with 4.5% CO_2 for 4 hr at 23 °C. After one day at room temperature, pistils were fixed in ethanol:acetic acid (3:1) overnight, softened in 1 N NaOH at 60 °C for 2 hr, then stained with 0.01% (w/v) decolorized aniline blue in 2% K_3PO_4 for 6 hr. Pollen-tube behavior was observed under a fluorescent microscope (Axiophot 2, Zeiss). CO_2-sensitivity was measured using $RLSICO_2$ index. $RLSICO_2$ was classified into five categories, based on the number of pollen tubes penetrating into the stigma: 1, 0; 2, 1-5; 3, 6-15; 4, 16-30; 5, >30. Three replicates were performed on each plant on different days. Non-CO_2-treated self-pollinated flowers were used as controls. In all cases, no pollen tubes penetrated into the control stigmas.

1.2.5 Genotype of *S*-haplotype

S-haplotypes of HA-11621 and HA-11623 were identified using primer PS5 (5'-ATGAAAGGCGTAAGAAAAACCTA-3') and PS15 (5'-CCGTGTTTTATTTTAAGAG AAAGAGCT-3') (Nisho *et al*., 1996) to amplify a fragment of the *SLG* gene. PCR-RFLP was used to distinguish the two *S*-haplotypes based on differential digest with restriction enzyme *Kpn*I. Digested DNA was electrophoresed on a 1.5% agarose gel.

1.2.6 Molecular markers and detection of DNA polymorphism

To screen for markers that show polymorphism between HA-11621 and HA-11623, primer sequences of the SSR markers from different sources (UK, prefixes Ra, Na, Ol and ENA (Lowe *et al*., 2004, http://www.brassica. bbscr.ac.uk); Japan, prefixes BRMS, KBr and EST (Suwabe *et al*., 2002, 2004, 2006; http://vegmarks.nivot.affrc.go.jp, NIVTS); Korea, prefix sau_um (Ramchiary *et al*., 2004); China, prefix AMCP (Ge *et al*., 2011)) were used. I also designed SSR, RFLP and InDel markers (prefixes XT and Bra) based on the *Brassica* database (http://brassicadb.org/brad/) (Table 1-1).

Total genomic DNA was extracted from young leaves of two parental lines and F_2 progeny using the cetyltrimethylammonium bromide (CTAB) method (Murray and Thompson 1980). DNA polymorphism analysis with SSRs was carried out using PCR with fluorescent dyes, performed according to Suwabe *et al*. (2008) with some modifications. The M13 (-21) universal primer sequence (18 bp) was fused to the 5' end of the original forward primer, and the M13 (-21) universal primer was labeled with 6-FAM, NED, VIC, or PET fluorescent dye (Applied Biosystems, California, USA). PCRs were performed in a 10 μL reaction volume containing 10 ng of template DNA, 4.7 μmol/L of labeled M13 (-21) universal primer and reverse primer, 0.3 μmol/L of forward primer, 1x PCR buffer, 1x dNTP, 1x $MgCl_2$ and 0.5 U of rTaq. Conditions for PCR were as follows: initial denaturing was carried out at 94 °C for 3 min followed by 37 cycles at 94 °C for 30 sec, 55 °C (slope of 0.5 °C/sec) for 30 sec, 72 °C (slope of 0.5 °C/sec) for 30 sec, and a final extension at 72 °C for 4 min. 1 μL of 50-fold diluted PCR product was added to 8.9 μL of Hi-Di™ Formamide and 0.1 μL of GeneScan™ 600 LIZ™ Size Standard (Applied Biosystems) and applied to an ABI 3730 DNA Analyzer (Applied Biosystems) Data were analyzed using ABI GeneMapper® software.

For polymorphism analysis with RFLP and InDel markers, PCR was carried out in 10 μL reaction volume with 5 pmol of forward and reverse primers instead of fluorescent dyes. For RFLP markers, amplified fragments were digested using restriction enzymes for 1 hr. Fragments or digested DNA were separated on 2-4% agarose gel.

1.2.7 Linkage map construction and QTL analysis

A genetic map was constructed using JoinMap® version 4 (Van Ooijen *et al*., 2006) utilizing the double pseudo-testcross strategy with a $\log_{10}$ of odds (LOD) threshold of 6.0 for linkage group identification. The best marker order was calculated with the regression mapping algorithm and marker order was retained from the first round only. Map distance units in centiMorgans (cM) were converted from recombination frequencies using the Kosambi mapping function (Kosambi, 1944). Interval mapping (IM) was performed to identify putative QTLs using the established linkage map and the observed phenotypic traits. This method was run using MapQTL® version 6 (Van Ooijen *et al*., 2009). With this software, a 0.05 significance threshold of LOD score was calculated by creating a group-wide distribution of the data based on a 1000 permutation test. LOD peaks were used to determine the estimated position of QTLs on the map.

1.2.8 Statistical analysis

Box plots were prepared by Ekuseru-Toukei 2012 software (Social Survey Research Information Co., Ltd.) to compare the phenotypic difference, as this plot type gives a good sense of environmental data distribution (Upton and Cook, 1996). Histogram was used to describe the variation of the phenotype. Kruskal-Wallis analysis was used between paired comparisons of markers to examine marker association.

1.3 Results

1.3.1 Phenotypic analysis of *B. rapa* lines in response to CO_2 treatment

Two inbred lines maintained in Tohoku Seed Co., Ltd. with different CO_2-sensitivity (HA-11621, CO_2-sensitive; HA-11623, CO_2-insensitive) were used (Fig. 1-1A, D). Flowers were self-pollinated by hand pollination and incubated in a CO_2 incubator for four hours. Both lines were self-incompatible under normal atmosphere conditions (control) (Fig. 1-1B, E), while they showed significantly different responses to a 4.5% CO_2 gas treatment (Fig. 1-1C, F). Specifically, in line HA-11621, many pollen tubes were seen to penetrate into papilla cells after treatment. This pollination test confirmed that line HA-11621 has a high sensitivity to CO_2 (CO_2-sensitive) but HA-11623 has a low sensitivity that hardly response to CO_2 (CO_2-insensitive). Cross-pollination was performed as a positive control (Fig. 1-1G).

1.3.2 Physiological changes in papilla cells after CO_2 treatment

Lee *et al*. (2001) showed a shrunken and distorted stigmatic papilla cell surface in CO_2-sensitive line after CO_2 treatment but aside from this, no other physical or biological effects of CO_2 treatment have been reported. Previous work has implicated the involvement of Ca^{2+} in self-compatible pathway (Iwano *et al*., 1999; Tateyama, 2010). I performed X-ray microanalysis of papilla cells using cryo-scanning electron microscope to examine surface structure and Ca^{2+} changes after CO_2 treatment. As shown in Fig. 1-2, the surface of papilla cells was very smooth after four hours of CO_2 treatment and did not differ from non-treated papilla in both HA-11621 and HA-11623 lines. Without CO_2, though few pollen grains hydrated on the papilla surface, no germination or penetration was observed in either line. However, in HA-11621, pollen grains hydrated and germinated on papilla cells after treatment (Fig. 1-2C, arrows). Next, the emission of elements in the tip of the papilla cell was analyzed. The area was with depth of 2-3 μm. The emissions of P-Kα, S-Kα, K-Kα and Ca-Kα were detected. The emission of Cl-Kα was under the limit of the detection and the detected emission of Al-Kα should be from the stub that held the samples. Fig. 1-3A shows the X-ray spectrum of an HA-11621 papilla cell after self-pollination. The increase of Ca-Kα emission in HA-11621 was remarkable when compared to the spectrum without CO_2

treatment in HA-11621 line (Fig. 1-3C), while such a massive intensity change could not be detected in HA-11623 line (Fig. 1-3B, D). The Calcium Green assay showed increased Ca^{2+} at the attachment site of the hydrated self-pollen after treatment in HA-11621 line (Fig. 1-4). These results suggest that in HA-11621 line, a high Ca accumulation on the pollinated papilla cell surface is induced and Ca^{2+} is exported from papilla cell to pollen after CO_2 treatment.

1.3.3 The efficiency of CO_2 treatment

The efficiency of CO_2 treatment is dependent on the treatment timing (Nakanishi and Hinata, 1973). Using the pollination assay, I showed that SI could still be overcome three hours after self-pollination (Fig. 1-5A). When only pollen or stigma was pre-treated with CO_2, SI could not be overcome after the pollination (Fig. 1-5B b, c); and no pollen penetration could be observed when both pollen and stigma were treated separately prior to pollination (Fig. 1-5B d), indicating that CO_2 treatment is effective only after pollination.

Non-pollinated papilla cells were subjected to X-ray microanalysis (Fig. 1-6). No significant difference was shown with or without CO_2 treatment, which supports the results of the pollination experiment, which indicate that pollination is essential for CO_2 to be effective.

1.3.4 *S*-allele characterization and Phenotype of CO_2-sensitivity in F_1 and F_2

I first determined the *S*-haplotypes of the two parental inbred lines by amplifying their *SLG* genes (Nishio *et al.*, 1996). The sequence data suggested that the *S*-haplotypes of CO_2-sensitive and CO_2-insensitive lines were $S_{55}S_{55}$ and $S_{46}S_{46}$, respectively. To genetically dissect the gene(s) that determines sensitivity to CO_2 treatment, six F_1 plants ($S_{46}S_{55}$) were produced by crossing CO_2-sensitive and CO_2-insensitive lines, and an F_2 population of 110 individuals derived from a bud-pollinated F_1 plant was made and used for further genetic analyses of the CO_2-sensitivity. F_2 individuals were genotyped using PCR-RFLP (restriction fragment length polymorphism) to distinguish *SLG* alleles (Fig. 1-7). S_{55}- and S_{46}-haplotypes were segregated in the F_2 population according to Mendelian transmission (Table 1-2). Pollen tube behaviour after CO_2 treatment varied among individuals, and in order to quantify the strength of CO_2-sensitivity, I employed the modified $RLSICO_2$ (reaction level of

self-incompatibility to a high CO_2 gas treatment) index (Niikura and Matsuura, 2000) to calculates CO_2-sensitivity based on the number of penetrating pollen tubes after self-pollination under high CO_2 conditions (see Materials and methods 1.2.4, Fig.1-8). The $RLSICO_2$ of 110 F_2 individuals is presented in Fig. 1-9 and the summarized box-plot data are shown in Fig. 1-10, together with the $RLSICO_2$ of F_1 and the parental inbred lines. F_1 had an $RLSICO_2$ score intermediate to the two parental lines, suggesting the high CO_2-sensitivity is a semi-dominant (incompletely dominant) trait in these inbred lines. Furthermore, the $RLSICO_2$ of F_2 individuals was continuously distributed, did not follow a simple one-locus biallelic Mendelian distribution (Fig. 1-9). These results suggest that CO_2-sensitivity in our inbred lines could be a quantitative trait which is controlled by more than one gene.

1.3.5 Relationship between *S*-haplotpyes and CO_2-sensitivity

To investigate whether CO_2-sensitivity is related to *S*-haplotypes, I grouped the 110 F_2 individuals into three genotypes ($S_{55}S_{55}$, $S_{46}S_{46}$, and $S_{46}S_{55}$). The $RLSICO_2$ of each group is shown in Fig. 1-10. In the three F_2 groups, $RLSICO_2$ scores were distributed from 1 to 5 and interquartile ranges overlapped, indicating that CO_2-sensitivity is not linked to the *S*-locus in these two lines.

1.3.6 Expressed organ of the gene that controls high CO_2-sensitivity

From the genotype and phenotype data I obtained two S_{46} homozygotes with different $RLSICO_2$ from the F_2 population: F_2-16 $RLSICO_2$=1±0 (CO_2-insensitive), and F_2-26, $RLSICO_2$=4.78±0.42 (CO_2-sensitive). These two plants were used to determine which organ controls the CO_2-sensitive trait. I performed reciprocal crosses between the two lines. The crossing using F_2-26 as the pistil pollinated with CO_2-insensitive F_2-16 pollen showed CO_2-sensitive trait, with many pollen tubes penetrated into stigma (Fig. 1-11A, C). When CO_2-insensitive F_2-16 pistil was pollinated with CO_2-sensitive F_2-26 pollen, SI could not be overcome (Fig. 1-11B, D). This suggests that CO_2-sensitivity could be controlled by gene(s) expressed in the female organ (stigma).

1.3.7 Marker analysis and construction of linkage map

To construct a linkage map for this F_2 population for QTL analysis, a total of 911 primer combinations of different genetic markers were used to screen the parental lines (see Materials and methods 1.2.6, Fig.1-12). To analyze the relationship between SI-related genes and high CO_2-sensitivity, *SLG* (marker for *S*-locus), *MLPK* and *ARC1* were also selected as markers. Though a very low level of polymorphism (14.7%) was found for all types of markers, a linkage map spanning 947.49 centiMorgans (cM) was built that consisting of 123 markers (113 SSRs, 5 RFLPs and 5 InDels) corresponding to 10 linkage groups (chromosome A01-A10) using JoinMap® version 4 with a threshold LOD=6.0 for the linkage group identification (Fig. 1-13). The distances between markers varied from 0 to 29.3 cM with an average distance of 7.70 cM. *MLPK*, *ARC1* and *SLG* were mapped to A07, A03 and A04 respectively, which is consistent with previous reports (Ajisaka *et al*., 2001; Hatakeyama *et al*., 2010).

1.3.8 QTL analysis and associations of markers to high CO_2-sensitivity

QTL analysis was performed using MapQTL® version 6. Three QTLs were identified on LG3 and 5 (A03 and 05) based on LOD threshold of 3.40 (1000 permutation test, $p<0.05$). These QTLs were tentatively named as *Brassica rapa SI Overcome (BrSIO) 1-3* (Fig. 1-14) and this result indicates that high CO_2-sensitivity is controlled by a polygenic system. Among these, *BrSIO1* on A05 and *BrSIO2* on A03 are two major QTL that explain 19.3% and 19.0% phenotypic variation, respectively. *BrSIO3* is a minor QTL which accounts for 14.5% of the variance and is located near to *BrSIO2* (Table 1-3).

To examine the significance and effect of major QTLs *BrSIO1* and *BrSIO2*, F_2 progeny were grouped by all the marker genotype at each QTL and the CO_2-sensitivity index ($RLSICO_2$) was compared using Kruskal-Wallis analysis (of variance by ranks) (Table 1-4). Alleles from line HA-11621 and HA-11623 are presented as S and I, respectively. Almost all of the interval markers showed significance at $p<0.01$ level in SS-II groups, except marker BRMS-114, which had significance at $p<0.05$ level. Marker association effect was examined with combinations of *BrSIO1* and *BrSIO2*. The groups that combined the allele from HA-11621 at *BrSIO1* with the allele from HA-11621 at *BrSIO2* showed higher $RLSICO_2$

(groups 1, 2 and 4 vs. groups 6, 8 and 9) (Table 1-5). Significance (p<0.05) was detected from group 1-8, 2-6 and 2-8. These data suggest that *BrSIO1* and *BrSIO2* work additively in overcoming SI during CO_2 treatment in the HA-11621 line. It was difficult to identify *BrSIO3* as an independent QTL and did not used in further discussion.

1.3.9 Associated gene prediction by *in silico* comparative mapping

Using the *B. rapa* genome sequence (Cheng *et al*., 2011), I could map *BrSIO1* to a 569 kb region flanked by InDel marker XT05-004 and SSR marker BRMS-034, and *BrSIO2* to a 1469 kb region flanked by SSR markers BRMS-042-2 and KBrH110I17R. These two regions include 121 and 280 genes annotated in the *Brassica* database (BRAD), respectively (Table S3, S4). Comparison of the *A. thaliana* genome to the Brassicaceae genome (reviewed by Schranz *et al*., 2006) suggests that *BrSIO1* has synteny on *A. thaliana* chromosome 2 and *BrSIO2* has synteny on both chromosomes 3 and 4. I assume that these two QTL do not have the same genetic origin and could be two independent regions controlling high CO_2-sensitivity. Based on reciprocal cross results, the CO_2-sensitivity trait may be controlled by genes expressed in the female organ (Fig. 1-11). 121 and 280 annotated genes in *BrSIO1* and *BrSIO2* have 103 and 243 homologues in *A. thaliana*, respectively, and 54 and 141 of these genes are expressing in *A. thaliana* pistil (Microarray data of Carpel at stage 12, http://affymetrix.arabidopsis.info/narrays/search.pl?f1=1&s1=ATGE_37, Table 1-6, 1-7).

Genes involved in related biological processes are often expressed cooperatively and their co-expression information is important for understanding biological systems (Eisen *et al*., 1998). ATTED-II (http://atted.jp/) is a gene co-expression database useful for identifying the potential partners working in the same biological processes (Obayashi *et al*., 2007). I performed co-expression analysis using ATTED-II with these 195 genes and found that *MAP kinase 6* (At2g43790 in *BrSIO1*) and *ethylene overproducer 1* (At3g511770 in *BrSIO2*) showed the strongest co-expression and *calmodulin-like 41* (At3g50770 in *BrSIO2*) has weak co-expression with *cytochrome c oxidase 10* (At2g44520in *BrSIO1*) and *beta glucosidase 28* (At2g44460 in *BrSIO1*). In addition to these co-expressed genes, these two regions encode highly homologous family member proteins: *e.g*., matrixin proteins (At2g45040 in *BrSIO1* and At4g16640 in *BrSIO2*), and senescence-associated proteins (At2g44670 in *BrSIO1* and

At4g17670 in *BrSIO2*). All these can be candidate responsible genes, although the biological functions of these genes mostly unknown.

1.4 Discussion

It has been more than 40 years since Nakanishi *et al*. reported SI could be overcome by CO_2 (1969), yet we still have very limited information about the breakdown mechanism.

Lee *et al*. (2001) showed a shrunken and distorted papilla cell surface in the CO_2-sensitive *Brassica campestris* (now *B. rapa*) line Hiratsuka, and suggested these structure changes could cause the overcoming of SI. The cryo-scanning electron microscopy data reported here did not show any structural changes in CO_2-sensitive or CO_2-sensitive lines (Fig. 1-2). Additionally, pretreatment of non-pollinated pistils with high CO_2 gas did not cause the SI breakdown (Fig. 1-5). Therefore, a completely different SI breakdown mechanism must be present, at least in our CO_2-sensitive line HA-11621. By contrast, massive Ca accumulation was observed at the pollen/stigma interface specifically in CO_2-sensitive plants under high CO_2 condition (Fig. 1-3) and I showed that Ca^{2+} exported from the papilla cell when self-incompatible pollen was hydrated during CO_2 treatment (Fig. 1-4), Brewbaker and Kwack (1963) were the first to describe the necessity of a high concentration of Ca^{2+} for pollen germination and pollen tube growth. Iwano *et al*. (1999) reported that in *B. rapa*, three hours after cross-pollination, a remarkable Ca-Kα emission increase is observed by X-ray microanalysis. Moreover, Ca^{2+} is transported from papilla cell to pollen together with the hydrating water in cross-pollination (Iwano, unpublished; Tateyama, 2010). The high concentration of Ca^{2+} could be needed for activating pectinase to loose the papilla cell wall, allowing the pollen tube to penetrate (Black and Charlwood, 1995), or for keeping the pollen tube cell wall rigid enough not to burst (Hepler and Winship, 2010). Although causal relationships remain unclear, the data suggest that CO_2 treatment induces a certain compatible reaction leading to Ca^{2+} accumulation at the pollen/stigma interface.

Because CO_2 treatment to induce self-fertilization is one of the best methods to obtain genetically pure inbred parental lines for large-scale commercial F_1 hybrid seed production, to date, several genetic studies have been performed to understand the mechanism of SI breakdown for breeding purposes. Niikura and Matsuura (2002) reported that in Japanese radish high CO_2-sensitivity is controlled by a recessive gene that governs the construction and/or metabolism of the stigma, which reacts to CO_2 without any changes in gene expression.

In contrast, Hyun *et al*. (2007) reported a dominant and *S*-haplotype-linked high CO_2-sensitive phenotype in *B. rapa*. In the present study, CO_2-sensitivity in lines HA-11621, HA-11623 and their F_1 and F_2 progenies were evaluated based on the degree of pollen tube penetration into the stigma ($RLSICO_2$). Different from these previous studies, F_1 had an intermediate CO_2-sensitivity (Fig. 1-10) and the F_2 population had a continuous frequency distribution of $RLSICO_2$ (Fig. 1-9). These results suggest that in the lines I used for this study, the CO_2-sensitivity is quantitative trait, which could be controlled by more than one gene(s).

Genetic linkage maps based upon frequency of recombination in segregating populations are fundamental and powerful tools for associating phenotypic traits specific genetic regions. Linkage mapping can be used to understand the biological basis of complex traits and to dissect genetic determinants underlying the expression of agronomically important breeding traits (Paran and Zamir, 2003). Very recently, five QTLs associated with stability of SI in *B. rapa* have been identified. Two of them co-localized with *SLG* (A07) and *MLPK* (A03) and the other three were on A02, A06 and A10 (Hatakeyama *et al*., 2010). In the present study, none of the other reported loci co-localized with QTLs detected (Fig. 1-14) and CO_2-sensitivity did not link with the *S*-haplotype in our study (Fig. 1-10), indicating that CO_2-sensitivity of the lines in this study is determined by novel genes different from those known to affect SI stability. I successfully identified three QTLs for high CO_2-sensitivity (*BrSIO1*, *BrSIO2* and *BrSIO3*). *BrSIO1* and *BrSIO2* had similar LOD scores with similar explained amounts of phenotypic variation and they could be two major factors controlling high CO_2-sensitivity (Fig. 1-14). Genes in *BrSIO1* and *BrSIO2* regions have 103 and 243 homologues in *A. thaliana* respectively, and 54 and 141 of these genes are expressing in *A. thaliana* pistil. *In silico* comparative analyses identified several co-expressing genes and highly homologous genes encoded in these two regions. All these can be candidate responsible genes, however, to more accurately identify the genes responsible for high CO_2-sensitivity in the QTL regions in *B. rapa*, it would be necessary to narrow down the regions by developing near-isogenic lines (NIL).

To maintain F_1 seed quality inbred lines with strong SI and high CO_2-sensitivity are ideal for breeding, and it is very important to understand the genetic relationships between SI-related genes and CO_2-sensitivity phenotypes. My results could be useful for the

maker-assisted selection (MAS) of parental lines with both stable SI and high CO_2-sensitivity.

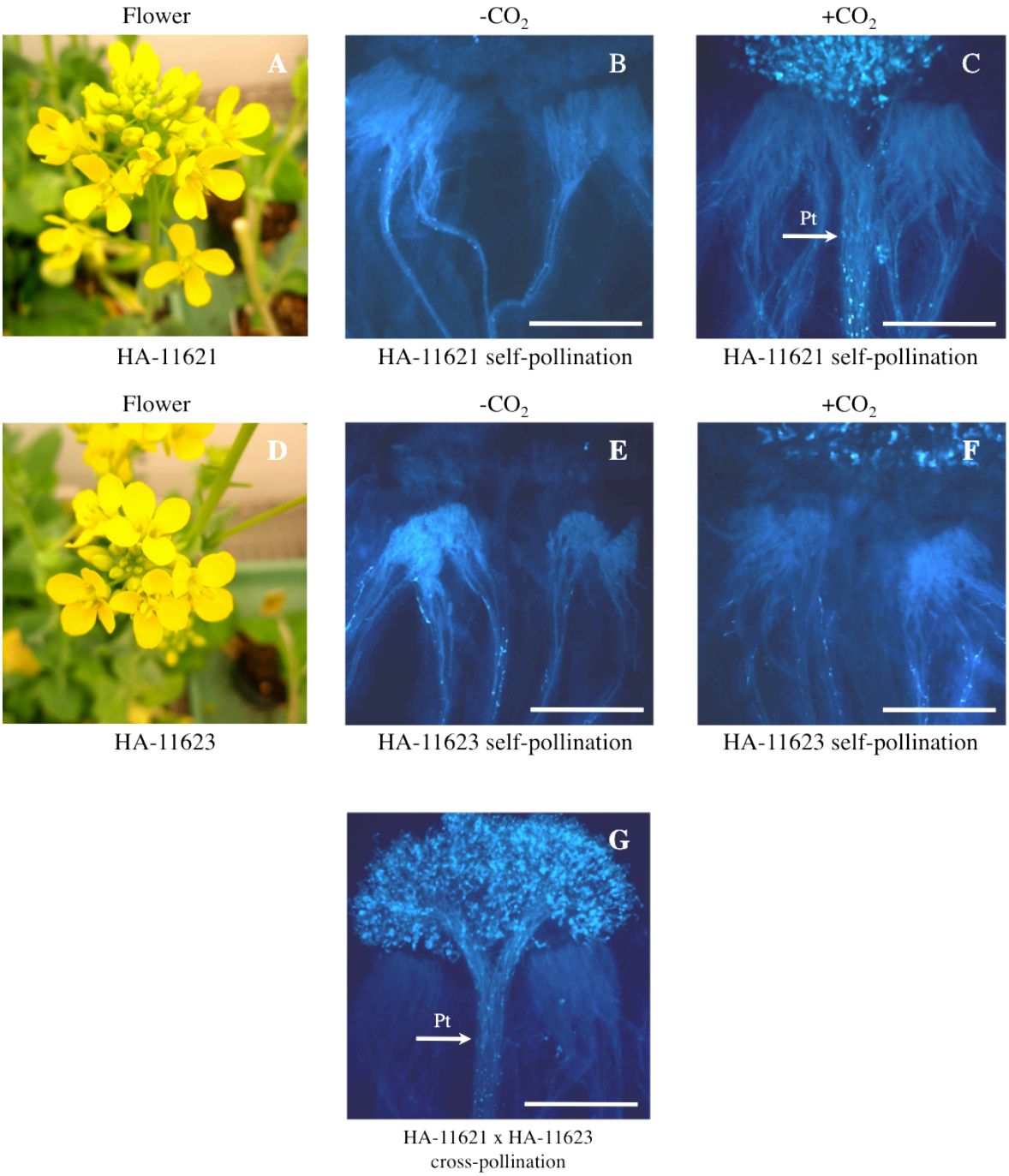

Fig. 1-1. Phenotype of two inbred lines of *Brassica rapa* used in this study

Flower morphology (A, D) and pollination assay with air or 4.5 % CO_2 treatment from HA-11621 line (B, C) and HA-11623 line (E, F). G is the cross pollination between these two lines as a positive control. Pt, pollen tubes. Bar=1000 μm.

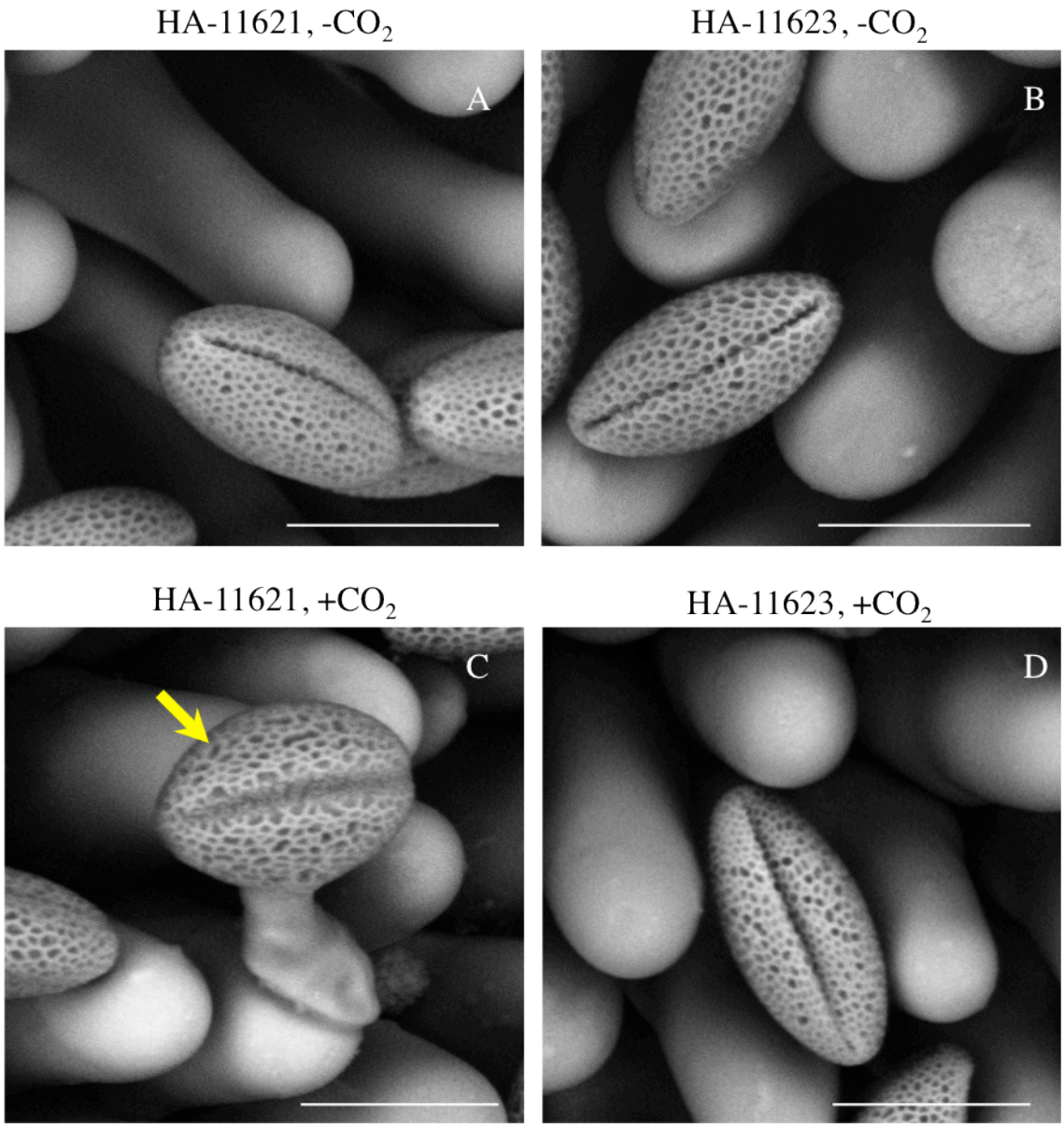

Fig. 1-2. Electron micrographs of self-pollinated papilla cell taken by cryo-scanning electron microscope

Pollen grain hydrates and germinates (arrows) in HA-11621 after CO_2 treatment. No significant papilla structural change is observed in HA-11621 and HA-11623 lines after CO_2 treatment. Bar= 25 μm.

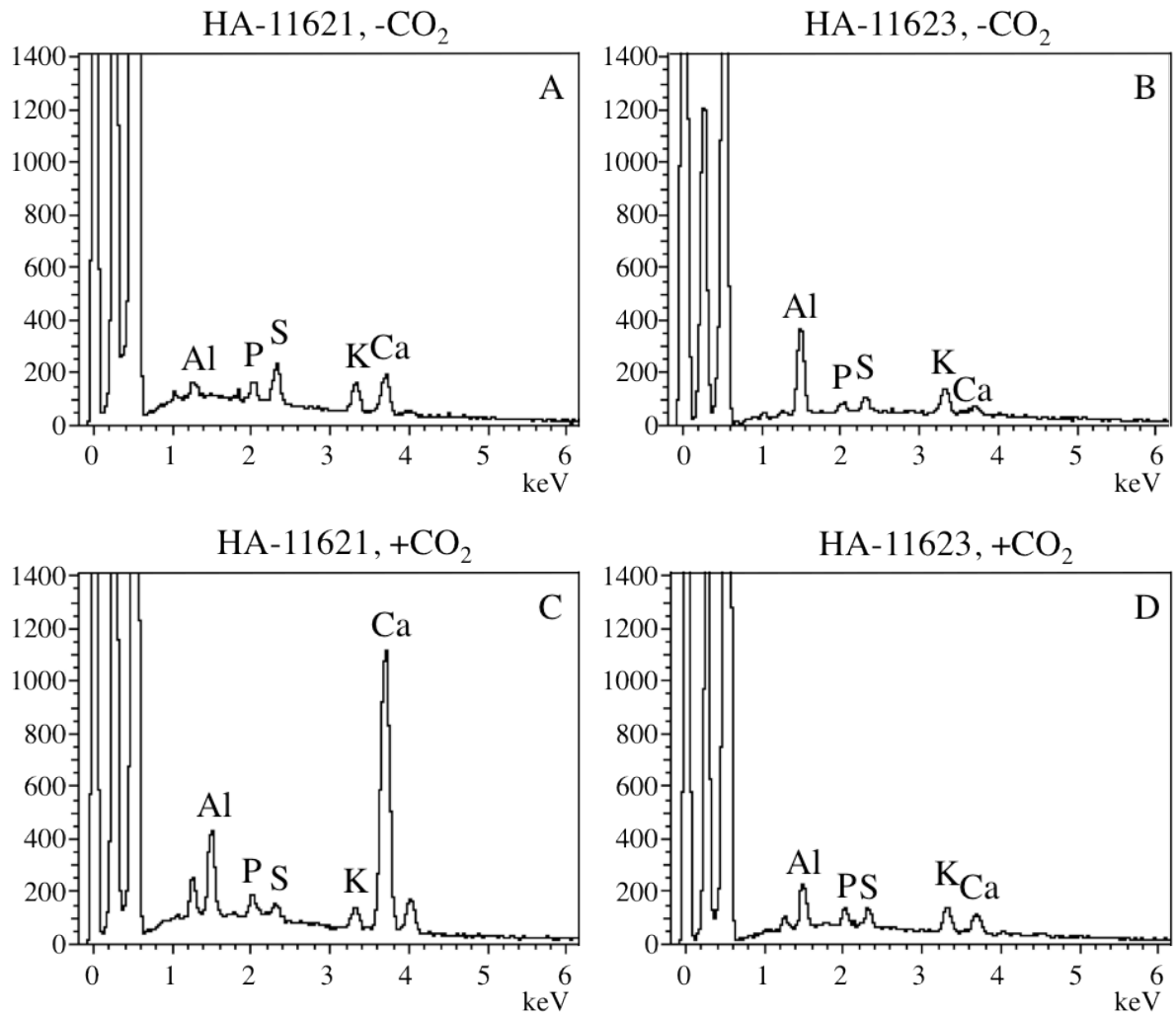

Fig. 1-3. Energy Dispersive X-ray spectrum of self-pollinated papilla cell

Pollinated papilla cell from HA-11621 (A), HA-11623 (B) without CO_2 treatment, and with CO_2 treatment (C), (D) were analyzed. Intensity of Ca emission is remarkably increased in HA-11621 line after the CO_2 treatment. These spectrum patterns are reproducible in three individual experiment sets.

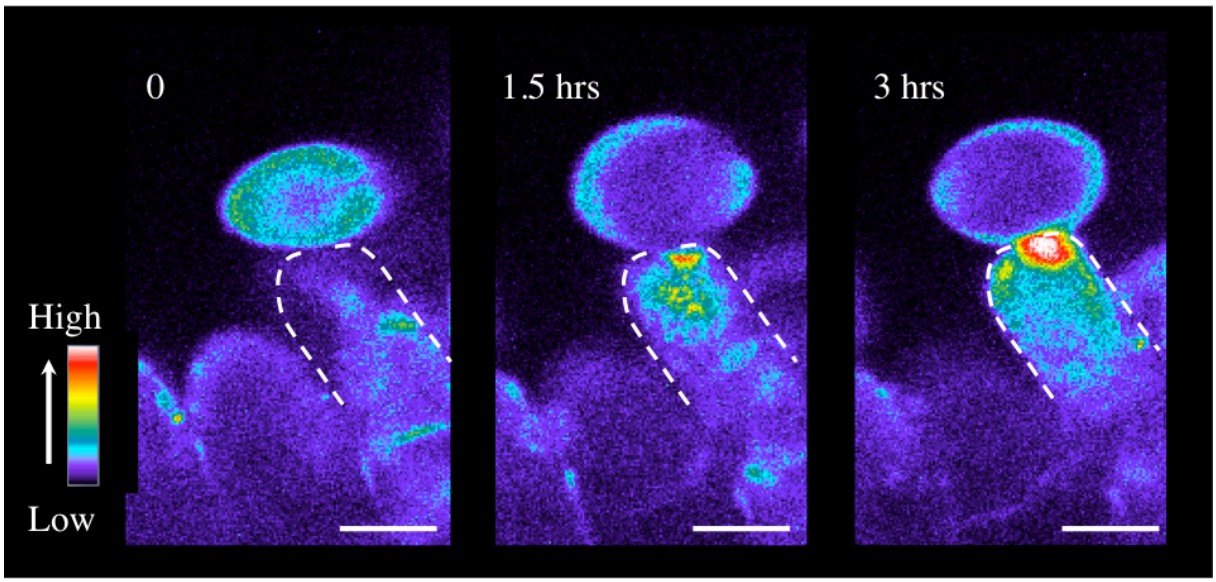

Fig. 1-4. Ca^{2+} dynamics during self-pollen hydration with CO_2 treatment in HA-11621 line
Calcium Green was applied to the surface of papilla cell and its signal was visualized in a rainbow colour. High Ca^{2+} concentration at the attachment site of self-pollen was observed after three hours. Bar=20 μm.

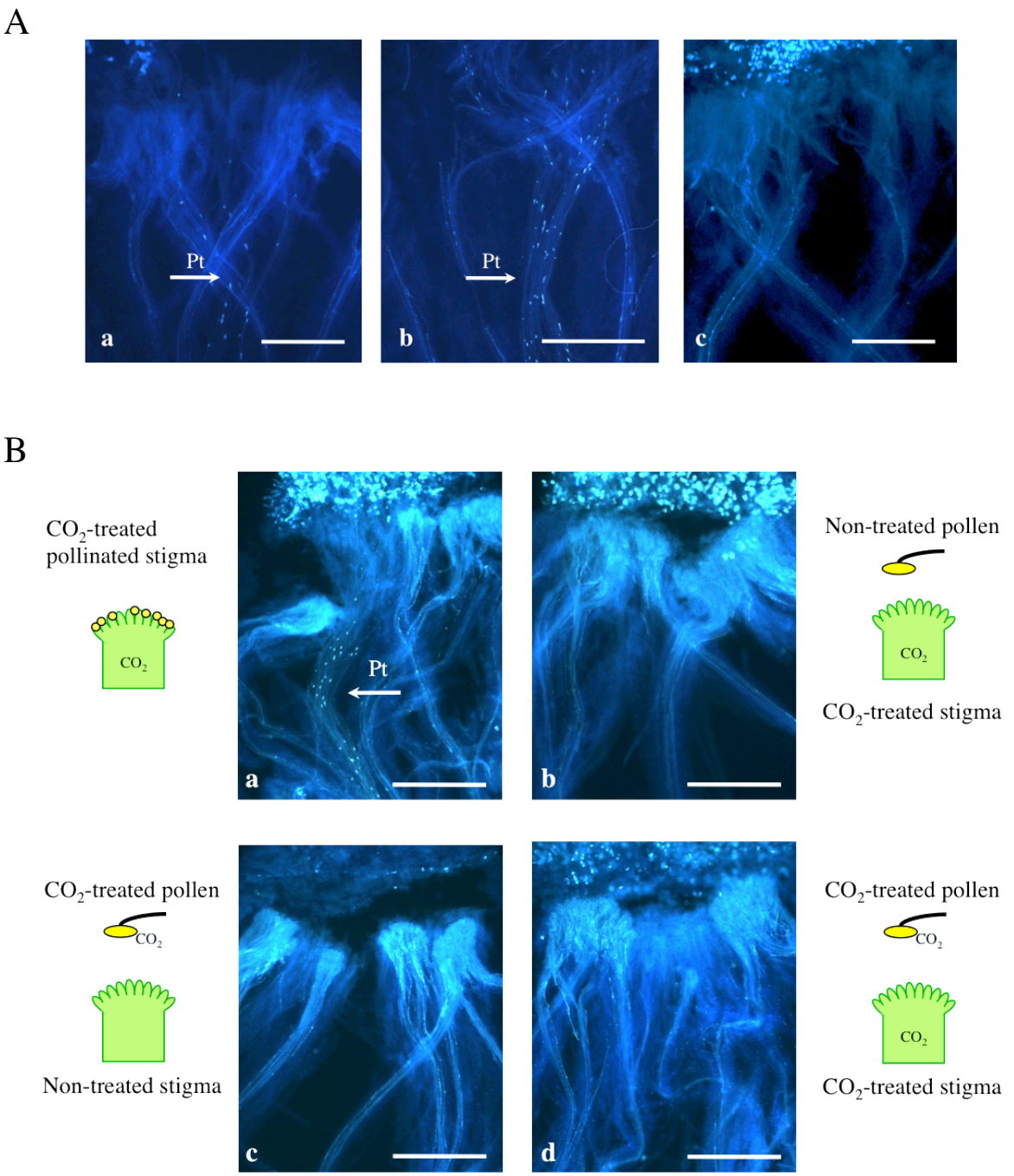

Fig. 1-5. The efficiency of CO_2 treatment

(A) SI can be overcome after 3 hours self-pollination CO_2 treatment. CO_2 treatment 0 hour (a), 3 hours (b) and 6 hours (c) after self-pollination.

(B) Pollination using separately CO_2-treated female and male organs. No pollen tube penetration is observed in CO_2-treated stigma and non-treated pollen (b), non-treated stigma and CO_2-treated pollen (c), CO_2-treated stigma and pollen (d) and only when they treated together after pollination pollen tubes (Pt) can be observed (a). Bar=1000 μm.

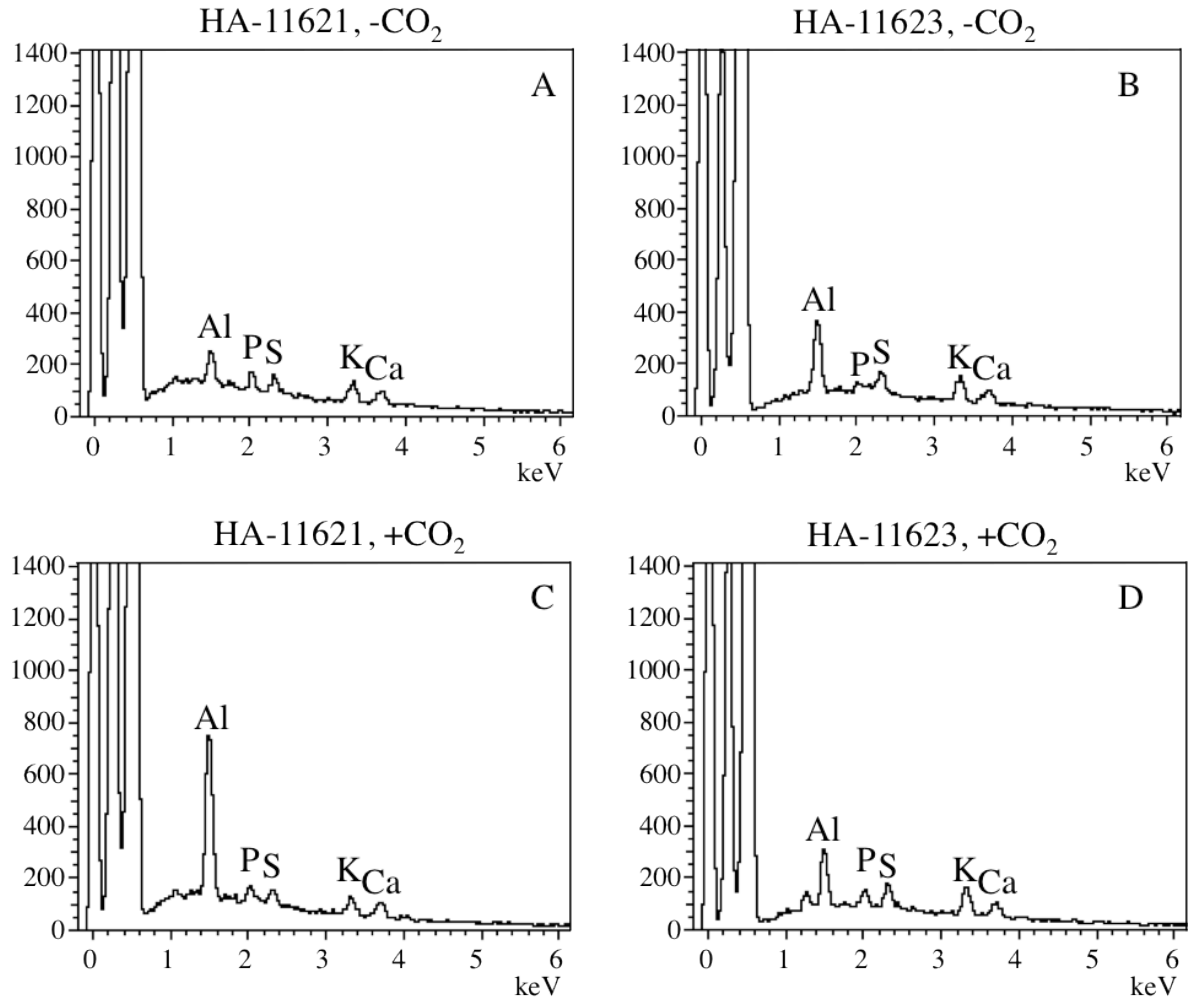

Fig. 1-6. Energy Dispersive X-ray spectrum of non-pollinated papilla cell

Non-pollinated papilla cell from HA-11621 (A), HA-11623 (B) without CO_2 treatment, and with CO_2 treatment (C), (D) were analyzed. No significant differences are observed between HA-11621 and HA-11623 and no significant differences are observed after treatment.

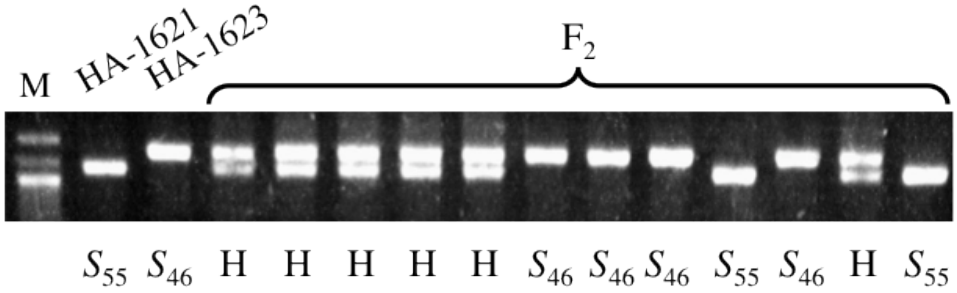

Fig. 1-7. *S*-haplotype analysis of F_2 plants by PCR-RFLP

M, marker; S_{55}, $S_{55}S_{55}$-homozygote; S_{46}, $S_{46}S_{46}$-homozygote, H, $S_{46}S_{55}$-heterozygote.

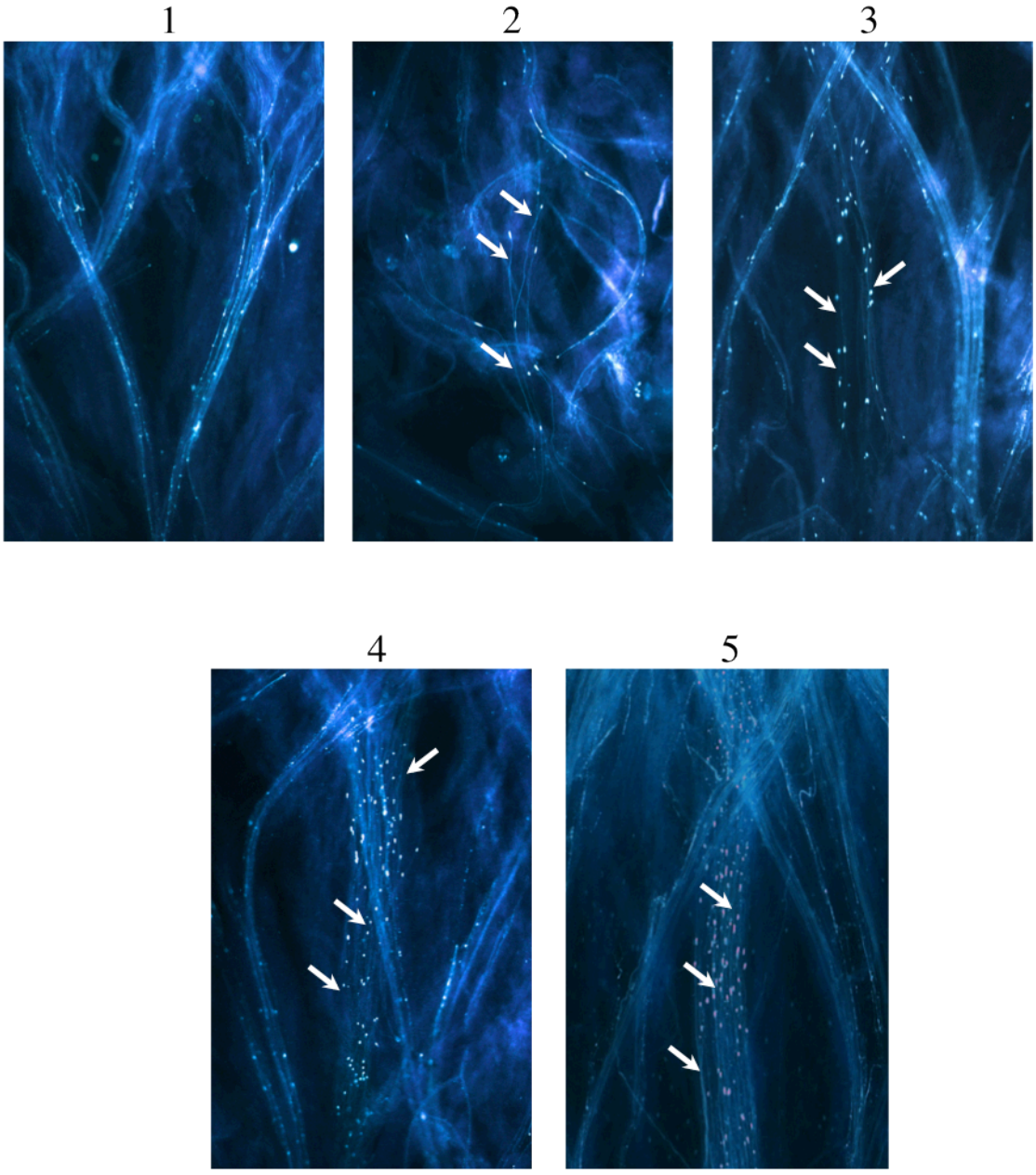

Fig. 1-8. RLSICO$_2$ index based on the pollen tubes (arrows) penetrated into the stigma (1) 0; (2) 1-5; (3) 6-15; (4) 16-30; (5) >30.

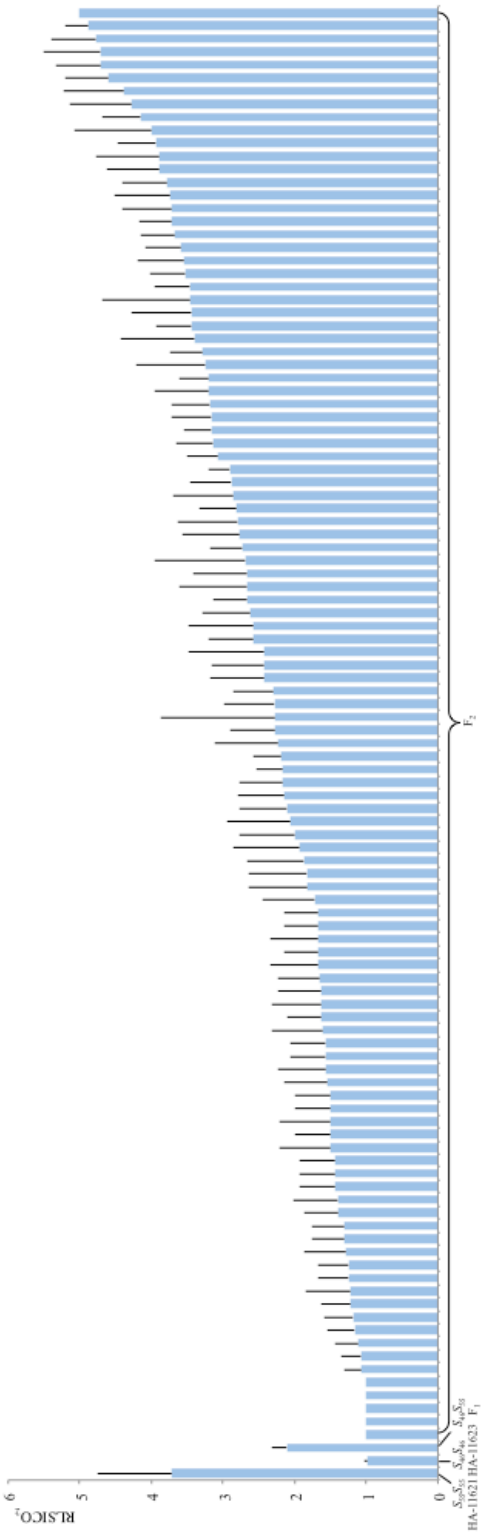

Fig. 1-9. $RLSICO_2$ in HA-11621, HA-11623 lines, F_1 and F_2 progeny based on the number of penetrating pollen tubes after self-pollination under high CO_2 conditions. $RLSICO_2$ is continuously distributed and does not follow a simple one-locus biallelic Mendelian distribution.

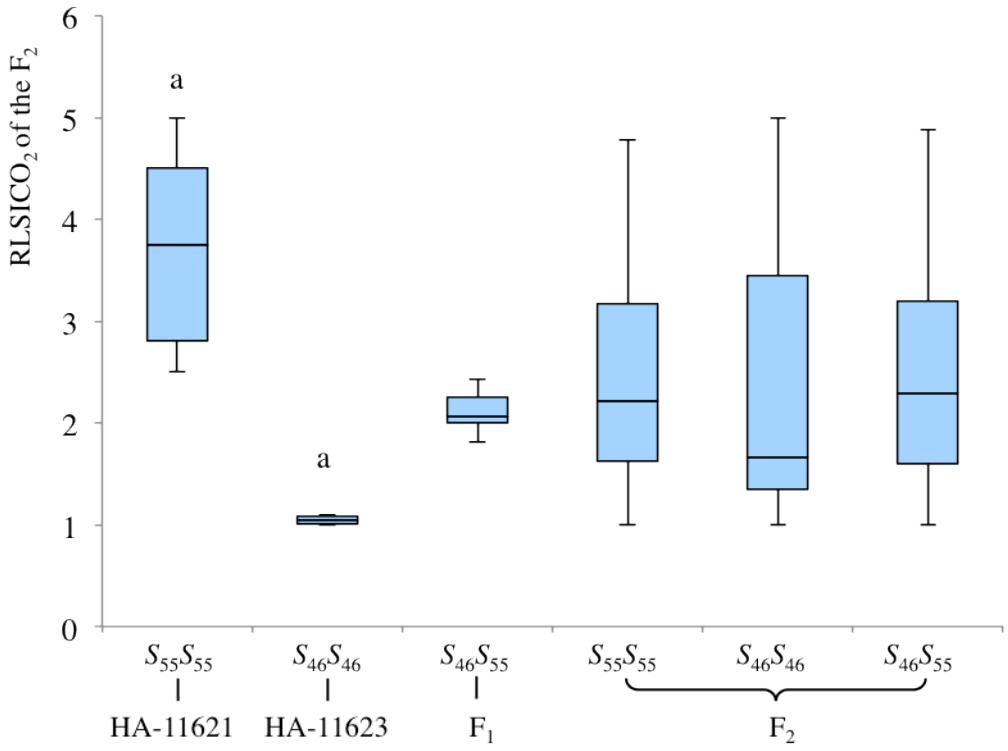

Fig. 1-10. Box plots data of CO_2-sensitivity phenotypes. Data shows distribution of $RLSICO_2$ with 25th, 50th and 75th percentiles (horizontal bars), interquartile ranges (columns) and 1.5 interquartile ranges (error bars) of $RLSICO_2$ from 110 F_2 individuals. a indicates significant difference $p<0.01$ between HA-11621 and HA-11623.

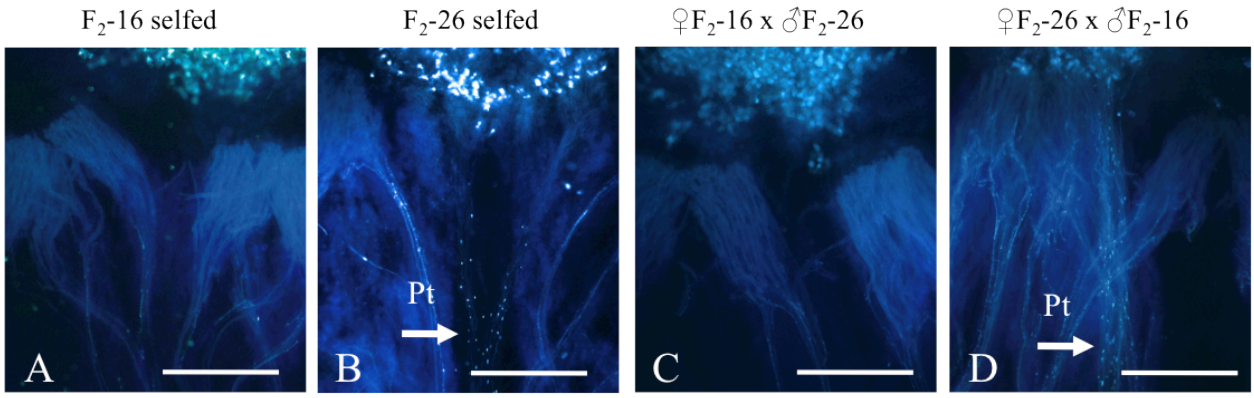

Fig. 1-11. Reciprocal crosses between two S_{46} homozygous individuals with different $RLSICO_2$ selected from the F_2 population.

CO_2-insensitive F_2-16 (A) shows low CO_2-sensitivity when pollinated with pollen from CO_2-sensitive F_2-26 (C), and CO_2-sensitive F_2-26 (B) shows high CO_2-sensitivity when pollinated with pollen from CO_2-insensitive F_2-16 (D). Pt, pollen tubes. n=3.

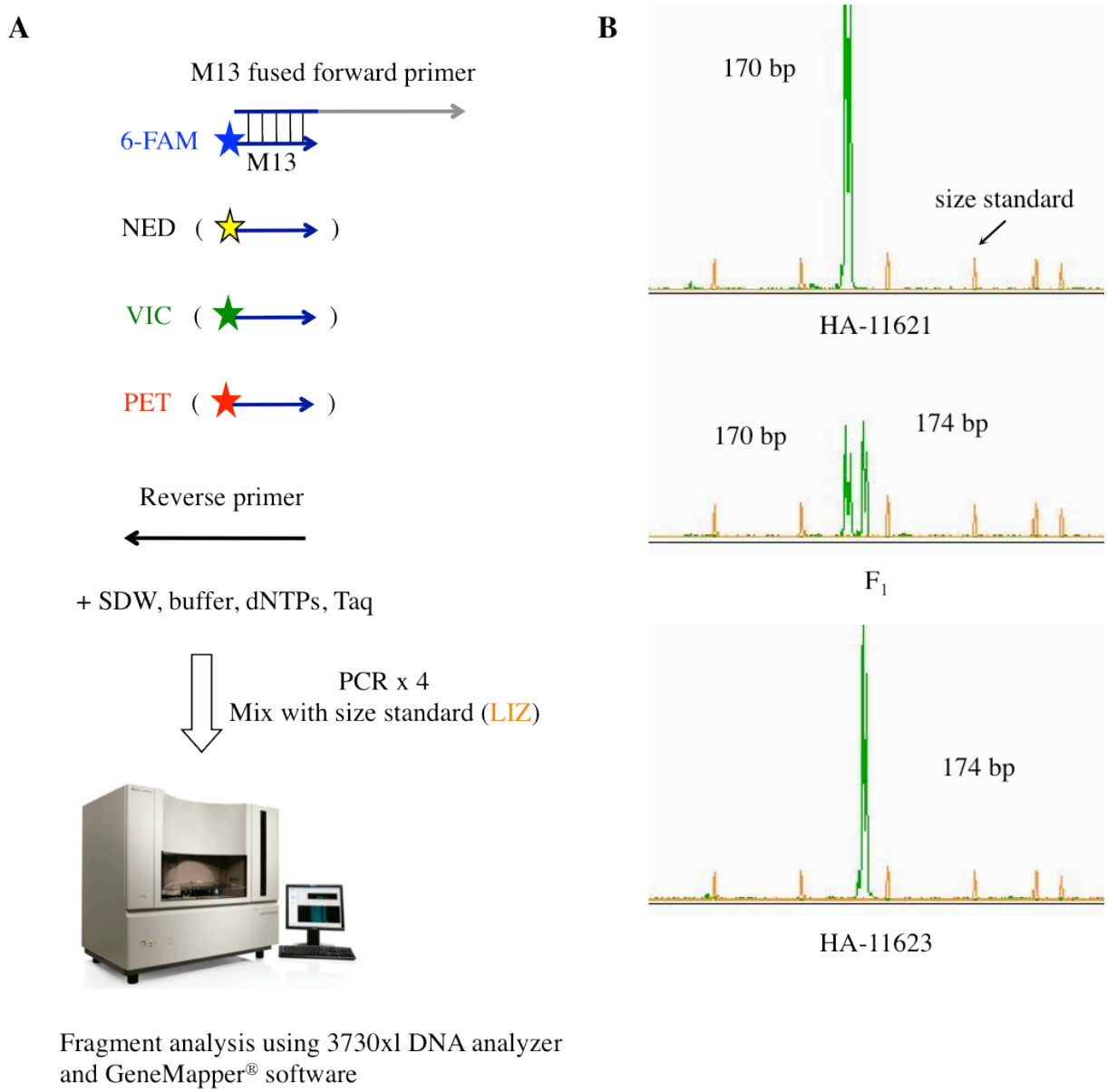

Fragment analysis using 3730xl DNA analyzer and GeneMapper® software

Fig. 1-12. Methodology of SSR marker genotyping using fragment analysis

Forward primer is fused to the M13 (-21) universal primer, which is labeled with one of the fluorescent dyes: 6-FAM (blue), NED (yellow), VIC (green), or PET (red). Four PCR products are mixed together with fluorescent dye LIZ-labeled (orange) size standard for fragment analysis (A) and one example of the genotyped data from PCR with VIC-labeled primer is shown in B.

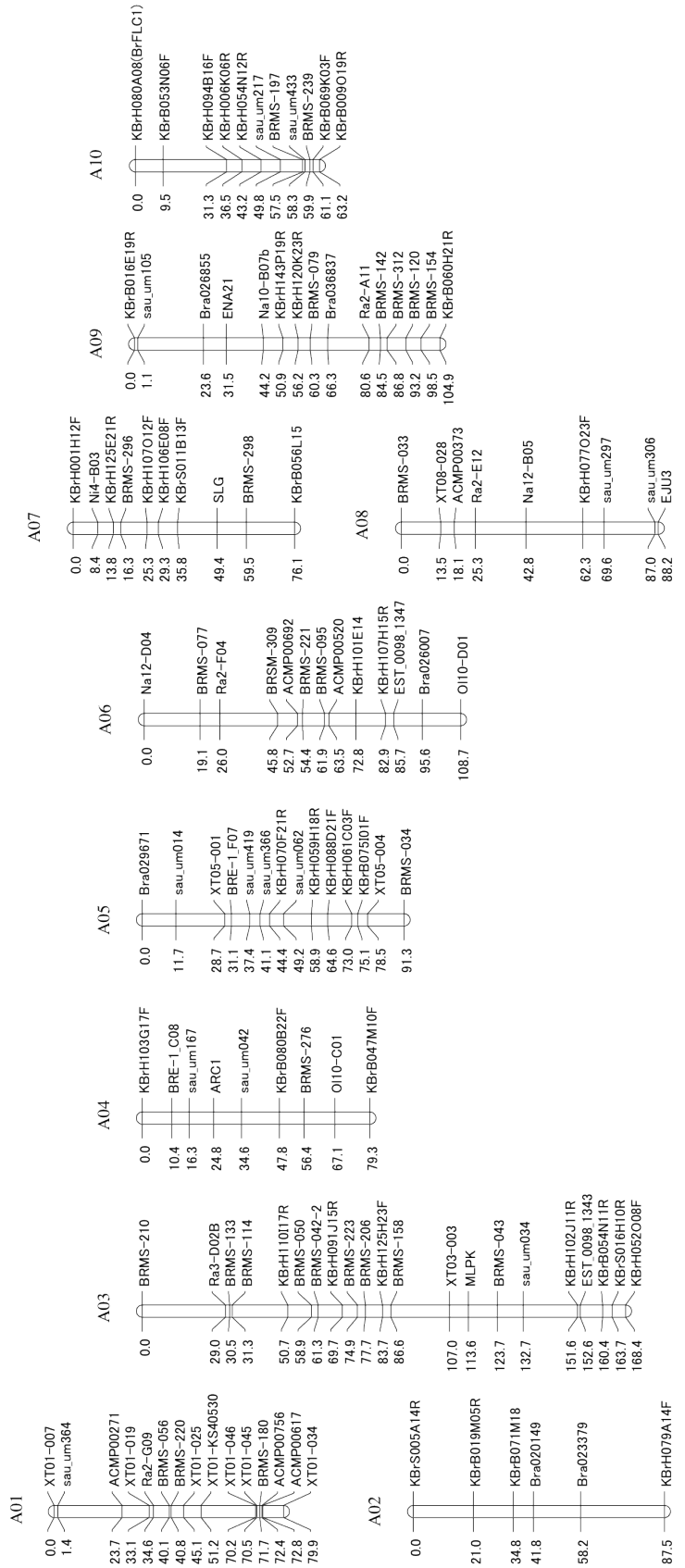

Fig. 1-13. Linkage map with 123 genetic markers

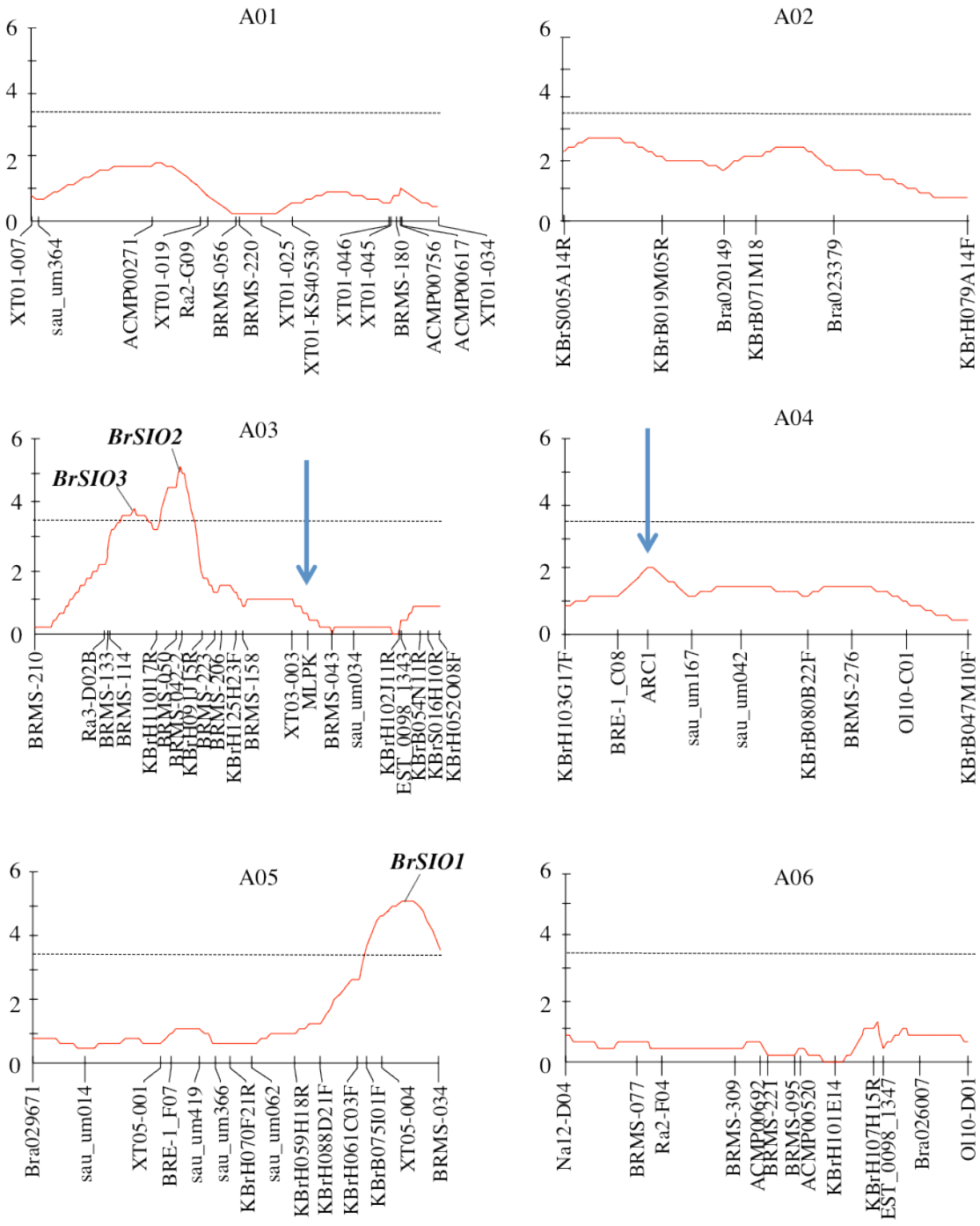
A01
A02
A03
A04
A05
A06
BrSIO1
BrSIO2
BrSIO3
XT01-007
sau_um364
ACMP00271
XT01-019
Ra2-G09
BRMS-056
BRMS-220
XT01-025
XT01-KS40530
XT01-046
XT01-045
BRMS-180
ACMP00756
ACMP00617
XT01-034
KBrS005A14R
KBrB019M05R
Bra020149
KBrB071M18
Bra023379
KBrH079A14F
BRMS-210
Ra3-D02B
BRMS-133
BRMS-114
XT03-003
MLPK
BRMS-043
sau_um034
KBrB054N11R
KBrS016H10R
KBrH052O08F
KBrH103G17F
BRE-1_C08
ARC1
sau_um167
sau_um042
KBrB080B22F
BRMS-276
O110-C01
KBrB047M10F
Bra029671
sau_um014
XT05-001
BRE-1_F07
sau_um419
sau_um366
KBrH070F21R
sau_um062
KBrH059H18R
KBrH088D21F
KBrH061C03F
KBrB075101F
XT05-004
BRMS-034
Na12-D04
BRMS-077
Ra2-F04
BRMS-309
BRMS-095
ACMP00520
KBrH101E14
Bra026007
O110-D01

(continued)

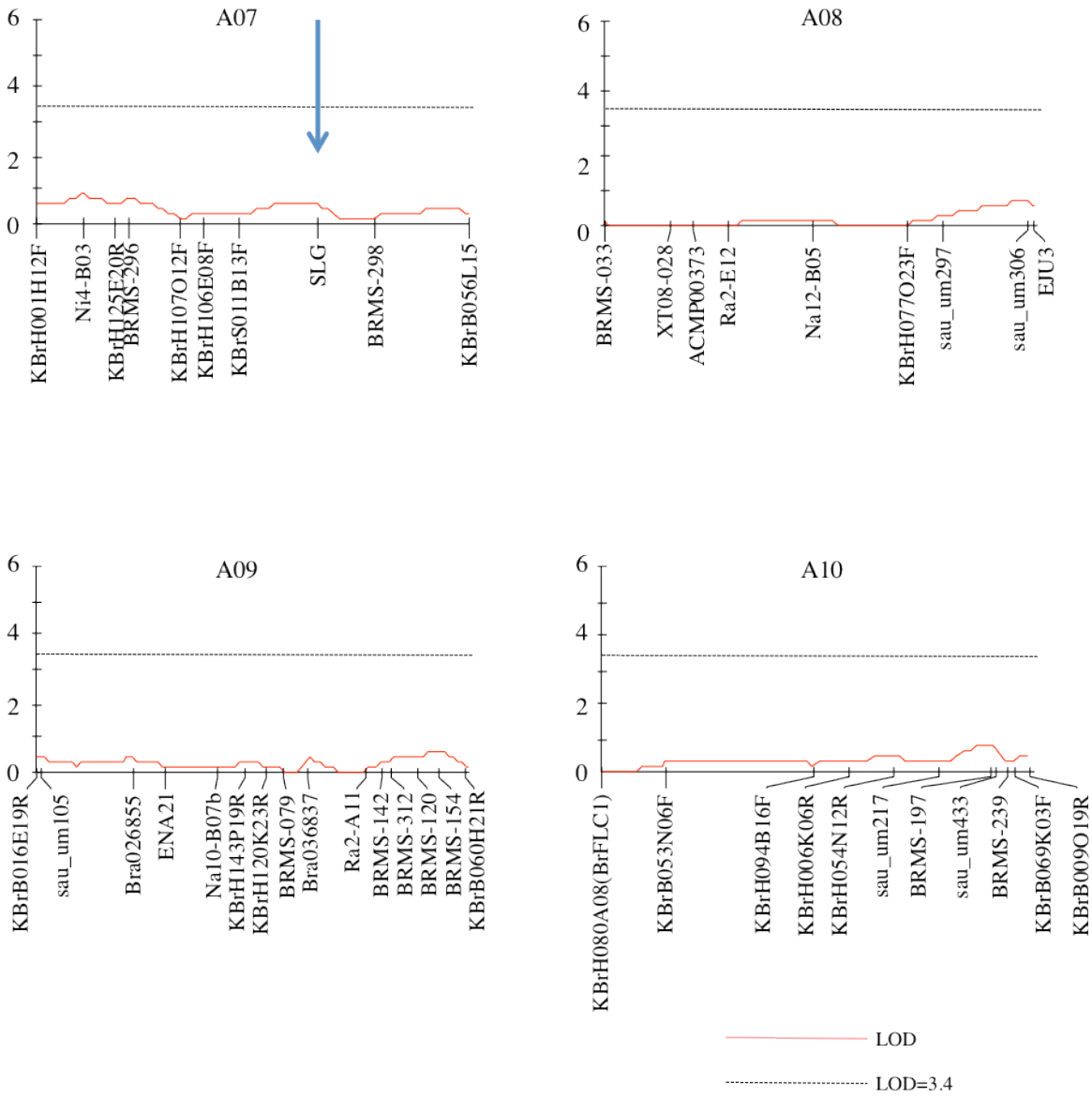

Fig. 1-14. QTL analysis results

Red solid line indicates LOD score and black dotted line indicates QTL threshold decided using 1000 permutation test (p<0.05). X-axis represents each linkage group (cM) and Y-axis indicates QTL score. Two QTL (*BrSIO2*, *3*) are detected in A03 and one in A05 (*BrSIO1*). No QTL was detected at *MLPK*, *ARC1* or *SLG* (*S*-locus) (arrows).

Table 1-1. *S*-haplotype segregation in F_2 population

Nr	Marker	Position (CM)	LG	Forward primer (5'-3')	Rverse primer (5'-3')	Type
1	XT01-007	0.00	A01	TGTAAAACGACGGCCAGTGAGAAGAAGAGAATACCTTTGGAG	GGAGGCACATAGAAGAGTGTGACT	SSR
2	sau_um364	1.36	A01	TGTAAAACGACGGCCAGTTCTACACGACGCACTCTCTCTCT	GAGCGGTAAGGGAAGTTTGAG	SSR
3	ACMP00271	23.67	A01	TGTAAAACGACGGCCAGTCGCAGCTACTCTCATCTCCA	CGTCTCCACCAATGACCATA	SSR
4	XT01-019	33.08	A01	TGTAAAACGACGGCCAGTCTTTGGGAGTTCAGCCGATTCG	CTTTAGTACCATTAAGGTTGG	SSR
5	Ra2-G09	34.63	A01	TGTAAAACGACGGCCAGTACAGCAAGGATGTGTTGACG	GATGAGCCTCTGGTTCAAGC	SSR
6	BRMS-056	40.12	A01	TGTAAAACGACGGCCAGTGATCAAGGCTACGGAGAGAGAG	CGTGACGCTAGAGTAATCGAGT	SSR
7	BRMS-220	40.79	A01	TGTAAAACGACGGCCAGTCCTGAATGTTTTAGGAGTGTACTTC	TTGCTTCAGAAGGAAGGTCAGGAGA	SSR
8	XT01-025	45.11	A01	TGTAAAACGACGGCCAGTGACTCGGTCGCAGAGATACTGC	CCTCCATTGTCAAACCACCTTCATC	SSR
9	XT01-KS40530	51.17	A01	GGAAGGTTTGACATGGTGGAC	GTTGACAGAGTAACCCTCTGGACT	InDel
10	XT01-046	70.24	A01	TGTAAAACGACGGCCAGTGATTTGAACAATTGAAAAGCATGA	AGCAGACCCAACTTTAGGATTGTG	SSR
11	XT01-045	70.49	A01	TGTAAAACGACGGCCAGTCTATTACTTAGGGCATTTATATTGAG	CGTAATCTGAAGCATACATTTATTGG	SSR
12	BRMS-180	71.75	A01	TGTAAAACGACGGCCAGTATTAAAGTCTTTCACTCACCAGCTT	AGTCACTCTATCCGGCTGTACC	SSR
13	ACMP00756	72.35	A01	TGTAAAACGACGGCCAGTTCTCATCTTTGCCGTCTCAC	GGATTGGGTTGGTCTTCTTC	SSR
14	ACMP00617	72.82	A01	TGTAAAACGACGGCCAGTAACTCAATGCTCTTCGCTCA	CCTTCTGCTGCTTCCAAGAT	SSR
15	XT01-034	79.89	A01	GGTTTCGTTGTCCTATCGAGTCAC	AAACATCGAAAACCTCCTTCATGC	InDel
1	KBrS005A14R	0.00	A02	TGTAAAACGACGGCCAGTATTCAAATCCTTTTGGGTTCATGC	GTTTCGGTATTGGTCATACATTGTTCAAG	SSR
2	KBrB019M05R	21.05	A02	TGTAAAACGACGGCCAGTACTGCAAAGCATTGGATCTTCTCT	GTTTCCATTTCGAAGGAGAACAAAAGGA	SSR
3	Bra020149	34.85	A02	CTAATACAGGCTTTGATTTCGC	ATACCACTACTCGAGGCTAAGGAAG	RFLP
4	KBrB071M18	41.75	A02	TGTAAAACGACGGCCAGTACCGTGATTTTCTCGGTAAAGA	GTTTATCCCACAAATGTGCCTCATA	SSR
5	Bra023379	58.25	A02	CTTCGTCTTTCAAAAGAGAGGTATG	ATGAGAGAGTTAAACTGGTGTGACC	InDel
6	KBrH079A14F	87.54	A02	TGTAAAACGACGGCCAGTAGCTTTCCTACCTTTTTCCCCTTC	GTTTGAGTGCGACTTGGAATTTCTCCAT	SSR
1	BRMS-210	0.00	A03	TGTAAAACGACGGCCAGTACTTTCCTGCATGAGATATGGA	TCGGAATTGGATAAGAATTCAA	SSR
2	Ra3-D02B	29.02	A03	TGTAAAACGACGGCCAGTCACAGGAAACCGTGGCTAGA	AACCCAACCTCAACGTCTTG	SSR
3	BRMS-133	30.52	A03	TGTAAAACGACGGCCAGTAATCCCCTCTACCAACCTCATTTCT	GATCTTGCAATAAAACCGACTTTGA	SSR
4	BRMS-114	31.25	A03	TGTAAAACGACGGCCAGTGATCTCTCTTTTCCTCTTCCTTCCT	TGTTCTGTATTTTTATTTTCTCCGG	SSR
5	KBrH110I17R	50.67	A03	TGTAAAACGACGGCCAGTAGCTAAGCTAGAGCTTGCACTGAA	GTTTGCGGAACAAAGAGAAATGGAGAAA	SSR
6	BRMS-050	58.87	A03	TGTAAAACGACGGCCAGTAACTTTGCTTCCACTGATTTTT	TTGCTTAACGCTAAATCCATAT	SSR
7	BRMS-042-2	61.33	A03	TGTAAAACGACGGCCAGTAGCTCCCGACAGCAACAAAAGA	TTCGCTTCCTTTTCTGGGAATG	SSR
8	KBrH091J15R	69.71	A03	TGTAAAACGACGGCCAGTACTTCCCCGCAGATTTGAGTATAA	GTTTACGGTAACATCTTTGAGTAAGGTGA	SSR
9	BRMS-223	74.85	A03	TGTAAAACGACGGCCAGTAGCCTTGTTGCTTTTCAACG	GCTCTCAACTTGTTGTTGAGTGTTA	SSR
10	BRMS-206	77.73	A03	TGTAAAACGACGGCCAGTATTAGACTCTTTCAAAAACGCAAAG	GATGACAACAACTCTTCCTCTGTTA	SSR
11	KBrH125H23F	83.73	A03	TGTAAAACGACGGCCAGTAAAAGACAAAACCATCCAAACACTA	AAGCCTTTTTGAACTTCTCTGTGAT	SSR
12	BRMS-158	86.58	A03	TGTAAAACGACGGCCAGTACCAGTAAAACAACATCACGACCA	GTTTATGATTTACATGCCGCTGCCTC	SSR
13	XT03-003	106.96	A03	TGTAAAACGACGGCCAGTTGAGTTTTCAGATTCCGACAAC	CTCCTATAGGCCTCGTCACCAC	SSR
14	MLPK	113.65	A03	TGTAAAACGACGGCCAGTGCACAAAGCATATTTGAAGAGGATC	TAACTCCGCGTTTGGCTACAGTC	SSR
15	BRMS-043	123.69	A03	TGTAAAACGACGGCCAGTGCGATGTTTTTTCTTCAGTGTC	TTAATCCCTACCCACAATTTCC	SSR
16	sau_um034	132.65	A03	TGTAAAACGACGGCCAGTCGTTCTCTCCATCTTCACTCTCC	CTCAACTGAAGCTGCTCTTCCT	SSR
17	KBrH102J11R	151.59	A03	TGTAAAACGACGGCCAGTAGGCTTTGATCCATTCCCTTAGTG	GTTTCCCATCTCAGCAAACACAGTTACG	SSR
18	EST_0098_1343	152.55	A03	TGTAAAACGACGGCCAGTAGGCTTTGATCCATTCCCTTAGTG	GTTTCCCATCTCAGCAAACACAGTTACG	SSR
19	KBrB054N11R	160.40	A03	TGTAAAACGACGGCCAGTATCCAAACGATTTCAGATCTGCTG	GTTTGCACACACCAATTCTTCTTCG	SSR
20	KBrS016H10R	163.66	A03	TGTAAAACGACGGCCAGTACTTTGCCTGTTTGCTCTAGCGAC	GTTTGTAGCAACCACATTTGCTGCATT	SSR
21	KBrH052O08F	168.42	A03	TGTAAAACGACGGCCAGTAGCAGTAATCACTCTTGTAGCCGC	GTTTCAATCTTTTGTCCGAACCAAATCC	SSR
1	KBrH103G17F	0.00	A04	TGTAAAACGACGGCCAGTACAGACAAAAGCTTCATTGCCACA	GTTTGAGACAAAGGCTGATTCCTCCAAA	SSR
2	BRE-1_C08	10.39	A04	TGTAAAACGACGGCCAGTAGAAATCTATTTTCTTCATCTTCCA	GTTTCATCACCCAAATCGAAAG	SSR
3	ARC1	16.31	A04	CACCATGGCCACTGATTCAGCAATGT	GATCACAGGATCGTTCATGAGGTTG	RFLP
4	sau_um167	24.76	A04	TGTAAAACGACGGCCAGTGGGGAAGGAGAGAGAGTTGC	CGATAGTTCTCCTCGATGTGCT	SSR
5	sau_um042	34.60	A04	TGTAAAACGACGGCCAGTCTCTCCATCATCTTCCTCTCCTC	ATGTTCTTGTGCGGCTTCTC	SSR
6	KBrB080B22F	47.79	A04	TGTAAAACGACGGCCAGTAGCCTTTTGCTTTTTCATCTGCTA	GTTTGGAGCCCAATGAAAGTGGTAGAAA	SSR
7	BRMS-276	56.39	A04	TGTAAAACGACGGCCAGTGACCGTTTTGCATTTTAAGAGCATT	TCACCACCACCAGTATCTTCAACAATCA	SSR
8	OI10-C01	67.05	A04	TGTAAAACGACGGCCAGTATGACTGCTTAAACAGCGCC	CTTCTCCAACAAAAGCTCGG	SSR
9	KBrB047M10F	79.29	A04	TGTAAAACGACGGCCAGTATGCCTTGTTCCATCCTCCATAAC	GTTTGACCATAGTAAAGGCGTTCCG	SSR
1	Bra029671	0.00	A05	CTTCTACTGGATGTGTATAGTCCG	AGCCTATCATTACTCGGAGAGTTC	RFLP
2	sau_um014	11.66	A05	TGTAAAACGACGGCCAGTGAATCTGGTTCCGGTTCAGTCT	CTCCTCATCCACTCCTTCTTCTC	SSR
3	XT05-001	28.65	A05	AGAGTGACTCCTCTCTTTAGCCAAC	CTGATCGTCATCACCTCTATCG	RFLP
4	BRE-1_F07	31.14	A05	TGTAAAACGACGGCCAGTATTATCAAACAGCCAACCAAAA	GTTTAGAGACTGACGGAACCTTTGAA	SSR
5	sau_um419	37.44	A05	TGTAAAACGACGGCCAGTCGCTGAAAAAGGTGGTACTCGT	GGAGCCACGGTTATGAGGATTAG	SSR
6	sau_um366	41.15	A05	TGTAAAACGACGGCCAGTTTCTCCTCGTATCACCACTCCT	GCCTACGTCTTCTACAGCGAGAT	SSR
7	KBrH070F21R	44.43	A05	TGTAAAACGACGGCCAGTAGTTCCAAACATCTGAAACCAGTG	GTTTACTCAAGCTGCGTCCAAAAGC	SSR
8	sau_um062	49.21	A05	TGTAAAACGACGGCCAGTGAACAGCAGCAGGAGGAGAC	CGAACATGGACCAAGAGAGAAC	SSR
9	KBrH059H18R	58.87	A05	TGTAAAACGACGGCCAGTACCCACCTTTTCTAGATCTGTATGA	GTTTCTCCAGCTCTTCCATCTGTTTCC	SSR
10	KBrH088D21F	64.62	A05	TGTAAAACGACGGCCAGTACTTGTGACGGAGGCATAGACTTT	GTTTGTCCCTGGAATGTCAAAGGTT	SSR
11	KBrH061C03F	73.01	A05	TGTAAAACGACGGCCAGTATACCTGCTGCTCTTGTTCCTGTA	GTTTGAGATGGCTGATGCTGAAGAAC	SSR
12	KBrB075I01F	75.08	A05	TGTAAAACGACGGCCAGTACCGTGATTTTCTCGGTAAAGA	GTTTATCCCACAAATGTGCCTCATA	SSR
13	XT05-004	78.50	A05	GCTTTTACCTGGAGCTTCTTCAGG	CTAACCAAGGCCACTCCATCACG	SSR
14	BRMS-034	91.28	A05	TGTAAAACGACGGCCAGTGATCAAATAACGAACGGAGAGA	GAGCCAAGAAAGGACCTAAGAT	SSR

Table 1-1. (continued)

Nr	Marker	Position (CM)	LG	Forward primer (5'-3')	Rverse primer (5'-3')	Type
1	Na12-D04	0.00	A06	TGTAAAACGACGGCCAGTACGGAGTGATGATGGGTCTC	CCTCAATGAAACTGAAATATGTGTG	SSR
2	BRMS-077	19.08	A06	TGTAAAACGACGGCCAGTCCGCCGAATTTATAGTGTTTTTACC	TCGATTAACCAGCTAAAATAATAATG	SSR
3	Ra2-F04	25.99	A06	TGTAAAACGACGGCCAGTCCTACAAACACATAAATAAAGAGAGAG	AACAACATAAAAGATTCATTTCG	SSR
4	BRMS-309	45.76	A06	TGTAAAACGACGGCCAGTCAAGAGCAAGTTTGAAACAAACGAT	CATCAGTTCTTGATATGCTAGGTGA	SSR
5	ACMP00692	52.69	A06	TGTAAAACGACGGCCAGTCGAGTTGCAGAGCCAAGTAG	AACGTAACGCTTCCTCTTCC	SSR
6	BRMS-221	54.39	A06	TGTAAAACGACGGCCAGTAAAGTCCTTGACGTTTGAGGAAGAA	CAGGTTCTTATGAAGGACCATGCAT	SSR
7	BRMS-095	61.95	A06	TGTAAAACGACGGCCAGTGTCATAACCAATGTATGTGTCTGCT	GATCCCTAATCAAAGAGACAGAGAG	SSR
8	ACMP00520	63.48	A06	TGTAAAACGACGGCCAGTCGGGCTTTCTAGTTGGGTAA	CGAGGTCTTACTCGATGCAG	SSR
9	KBrH101E14	72.78	A06	TGTAAAACGACGGCCAGTATTCGAAATCAAATCAAACCGCTC	GTTTCATCCAACCACGTTTTCACAGA	SSR
10	KBrH107H15R	82.90	A06	TGTAAAACGACGGCCAGTACAGCGAGTGGTAGTGACACGAAA	GTTTGCCTATCGTTCTCCTCATCTGCAT	SSR
11	EST_0098_1347	85.71	A06	TGTAAAACGACGGCCAGTATCTCTCTCTCCGAATCCAAAA	GTTTAGCTCTGATGAGACCAGCTCTT	SSR
12	Bra026007	95.57	A06	GTGGTAATGAGAGTTGGGTGTTTC	TTAGATAGAACTGGCTCCCTGAAC	InDel
13	Ol10-D01	108.66	A06	TGTAAAACGACGGCCAGTTCTCTGCCAAAAGCAAATAGC	CTTGGCTCTCTCTCACCACC	SSR
1	KBrH001H12F	0.00	A07	TGTAAAACGACGGCCAGTAGGTGAGTGCTCAGGTTCAGGTAG	GTTTCTCTGTTGCCATTGATTCGGTAA	SSR
2	Ni4-B03	8.37	A07	TGTAAAACGACGGCCAGTTGCTGTTTCTGTGGAATTGTCG	ACTTTCTTTACATTCTAATCGC	SSR
3	KBrH125E20R	13.76	A07	TGTAAAACGACGGCCAGTACATTCACTTGTAGTCCGCTCAGA	GTTTAAATGTTCGAACTGAGGTTTGGGA	SSR
4	BRMS-296	16.30	A07	TGTAAAACGACGGCCAGTCATCCTAATGTTGCTGAGAAAGAGG	TATATGAAACCGATGAAGCTCCTTT	SSR
5	KBrH107O12F	25.34	A07	TGTAAAACGACGGCCAGTACAATGCTGGGAAGAAACTCTGTG	GTTTAGATCTCTCCTCTCGCACCTCAAA	SSR
6	KBrH106E08F	29.28	A07	TGTAAAACGACGGCCAGTATCGATCCTTTGGATCTGCTTGAT	GTTTAACCGCTCCAAAAGCGTTTAATTC	SSR
7	KBrS011B13F	35.78	A07	TGTAAAACGACGGCCAGTAGACCAGCTGCAAATGAGGTTAGA	GTTTAAAAGGGTATACAGGGGGTGCAGT	SSR
8	SLG	49.36	A07	ATGAAAGGCGTAAGAAAAACCTA	CCGTGTTTTATTTTAAGAGAAAGAGCT	RFLP
9	BRMS-298	59.47	A07	TGTAAAACGACGGCCAGTCCACTGTTTTATGACTCCAGTGCTT	TGACCTGGTGAAGTAGTTGTCTCGT	SSR
10	KBrB056L15	76.09	A07	TGTAAAACGACGGCCAGTAGGACATCTTTTTGTAACCCAA	GTTTCACCTCAATTCCTAATTTTGAGA	SSR
1	BRMS-033	0.00	A08	TGTAAAACGACGGCCAGTGCGGAAACGAACACTCCTCCCATGT	CCTCCTTGTGCTTTCCCTGGAGACG	SSR
2	XT08-028	13.50	A08	GACTCCTTGTCTCCTTCTTCCTC	TGACTCCGTGAAATATAGGATCG	SSR
3	ACMP00373	18.08	A08	TGTAAAACGACGGCCAGTGCAAGTTGGGAGATTTGGAT	GCCTCAAAGGTCATCATCAG	SSR
4	Ra2-E12	25.31	A08	TGTAAAACGACGGCCAGTTGTCAGTGTGTCCACTTCGC	AAGAGAAACCCAATAAAGTAGAACC	SSR
5	Na12-B05	42.85	A08	TGTAAAACGACGGCCAGTCAAATATCCGTCATCGGAGC	CCTGCGGGATATTGAAGACC	SSR
6	KBrH077O23F	62.31	A08	TGTAAAACGACGGCCAGTACCTGTAATGTGACCCCCAACAAT	GTTTAGTCAAATGGCTCTCTCGCCAA	SSR
7	sau_um297	69.64	A08	TGTAAAACGACGGCCAGTGGAAACACGAGTTGTCACACTTA	ATGGTGAGATTGTGAAGAGGATG	SSR
8	sau_um306	87.00	A08	TGTAAAACGACGGCCAGTGTCTACTTGGTGGTTGTTAGCCC	GTGTCCTCTTCTTCAGGTTCCTC	SSR
9	EJU3	88.21	A08	TGTAAAACGACGGCCAGTACCTCTTTTAATTCAAACAAGAAATCA	GTTTTCGGACAATGGCAGTGATA	SSR
1	KBrB016E19R	0.00	A09	TGTAAAACGACGGCCAGTATGTTGAGCTGCGAATACGTTCCT	GTTTGAGCAATCTTCACCCTCTTCGTGT	SSR
2	sau_um105	1.05	A09	TGTAAAACGACGGCCAGTCCTTTCTAATGGGAAGCGGTAG	CTCCCTCTTCGAATTGACTCAC	SSR
3	Bra026855	23.56	A09	GAGTGGTGTCTGAGATCATGAGG	CTAGAAGGAAGAGAGACCAGCAAG	InDel
4	ENA21	31.50	A09	TGTAAAACGACGGCCAGTAGAGTGTTTGGAGCAGATGA	GTTGGAGACTTTGCCTTTGTGT	SSR
5	Na10-B07b	44.15	A09	TGTAAAACGACGGCCAGTGCCTTAGATTAGATGGTCGCC	ACTTCAGCTCCGATTTGCC	SSR
6	KBrH143P19R	50.88	A09	TGTAAAACGACGGCCAGTATAGACTCTTCCACCAAGTGGCAT	GTTTCGCATCCCAAATCTTGTTGAAT	SSR
7	KBrH120K23R	56.21	A09	TGTAAAACGACGGCCAGTAGAATTTTGGGGTCTGTACCTGCT	GTTTAACAGACTGGGCGTTACGGAAA	SSR
8	BRMS-079	60.26	A09	TGTAAAACGACGGCCAGTGGGAAGATCCCAATCTAAGAAAATG	AATGACCTTTGTGACCCTATTCGTT	SSR
9	Bra036837	66.33	A09	TGTAAAACGACGGCCAGTTACTGACGTGACGTATACAGATGC	CTCCTTCACGTTTTCATCATTAACC	SSR
10	Ra2-A11	80.64	A09	TGTAAAACGACGGCCAGTGACCTATTTTAATATGCTGTTTTACG	ACCTCACCGGAGAGAAATCC	SSR
11	BRMS-142	84.52	A09	TGTAAAACGACGGCCAGTTACTTTGCTTTATTTGCATGGAAGG	TTGTTTGCATTGCATGTAAGACTTC	SSR
12	BRMS-312	86.81	A09	TGTAAAACGACGGCCAGTCGCAGCAATTAAAAGCTTCACAGTA	ATTTCAACATGTCAGACGCTCTTTC	SSR
13	BRMS-120	93.16	A09	TGTAAAACGACGGCCAGTGTCAGCATACACGGCAAAACTCGCA	GGTACGGCAGTTCTCGGTCGGTTAA	SSR
14	BRMS-154	98.45	A09	TGTAAAACGACGGCCAGTATGTAGACCGAAGAAAACAAAATCA	GGAACTTTCCAGACTTGTACTCCTC	SSR
15	KBrB060H21R	104.91	A09	TGTAAAACGACGGCCAGTATGCACGAGGTTACATTATTGTGTCT	GTTTGTAAGGCCGTGTGAACTCTCT	SSR
1	KBrH080A08(BrFLC1)	0.00	A10	TGTAAAACGACGGCCAGTATGAACCTATTTTAGATTATAGCTGGC	GTTTGATGTTTTCTTCTTCTTTTTCATC	SSR
2	KBrB053N06F	9.46	A10	TGTAAAACGACGGCCAGTAGATCTCCCATGGCTTCTTGATGT	GTTTCCATTATAAGGCCCACGAAACAAA	SSR
3	KBrH094B16F	31.28	A10	TGTAAAACGACGGCCAGTACTTCTTCTCGATCTCACTCTCGG	GTTTCGAACTCCTCCTTGAACGACTC	SSR
4	KBrH006K06R	36.53	A10	TGTAAAACGACGGCCAGTAAGAGAGAGACGACACACACTCGG	GTTTAATCGCAATCCCCAAAAGAGAGA	SSR
5	KBrH054N12R	43.19	A10	TGTAAAACGACGGCCAGTACCATGGTAACATCTGGAAGGTGA	GTTTGTGCAGGCACTTCTACACCAG	SSR
6	sau_um217	49.81	A10	TGTAAAACGACGGCCAGTAACCAGAAACGGTGTCATGC	GTACTCCGGAAGCTCACTAAACG	SSR
7	BRMS-197	57.52	A10	TGTAAAACGACGGCCAGTCTATTACAAGTGCACTAACCCGAAT	GCTCTCAACTTGTTGTTGAGTGTTA	SSR
8	sau_um433	58.30	A10	TGTAAAACGACGGCCAGTAAGAGTCCACAGCAGGAGATTG	GGGATGAGAAAAAGACAGGTGG	SSR
9	BRMS-239	59.95	A10	TGTAAAACGACGGCCAGTAATATTCGTCTGATTATTCGGATTC	TCTCTCTGATGACTCCATACTTTCC	SSR
10	KBrB069K03F	61.12	A10	TGTAAAACGACGGCCAGTAGCATTATTTTGCACAAGAGACGG	GTTTGGGTTGCGTTGTGTAATCC	SSR
11	KBrB009O19R	63.23	A10	TGTAAAACGACGGCCAGTACCCCTGGTCTTCTTAGGTCTTCC	GTTTGAAGCCTGTTGAGGTCTCTC	SSR

Table 1-2. *S*-haplotype segregation in F_2 population

***S*-genotype**	$S_{46}S_{46}$	$S_{46}S_{55}$	$S_{55}S_{55}$	**Total**	**Goodness of fit**		
Observed	22	64	24	110	Ratio	χ^2	*p*
Calculated	27.50	55.00	27.50	110.00	1:2:1	3.02	0.2-0.4
Average of RLSICO$_2$	2.22	2.51	2.49				

Table 1-3. Summary of QTL detected

QTL	LG	Closest marker	QTL peak (cM)[a]	LOD	R^{2}[b]	Additive effect[c]
BrSIO1	A05	XT05-004	83.5	5.17	19.3	0.72
BrSIO2	A03	BRMS-042-2	60.87	4.46	19	0.69
BrSIO3	A03	KBrH110I17R	41.25	3.76	14.5	0.65

[a] QTL peak position, detected by interval mapping, between two markers.
[b] Amount of phenotypic variation explained by the QTL.
[c] Additive effect of the CO_2-sensitive HA-11621 allele on RLSICO_2.

Table 1-4. Statistical analysis on QTL effect

QTL	*BrSIO1*			*BrSIO2*		*BrSIO3*	
Marker[a]	KBrB075I01F	XT05-004	BRMS-034	BRMS-042-2	BRMS-050	KBrH110I17R	BRMS-114
SS	3.12	3.17	3.24	3.10	3.09	3.01	3.01
IS	2.34 ** [b,c]	2.36 **	2.42 **	2.43 **	2.47 **	2.45 **	2.30 *
II	2.02	1.93	2.06	1.87	1.84	1.86	2.03

[a] S, CO_2-susceptible HA-11621 allele; I, CO_2-insusceptible HA-11623 allele
[b] Kruskal-Wallis analysis comparing phenotype between genotype groups with individuals in the same groups,
[c] Significant different level, **, $p<0.01$; *, $p<0.05$

Table 1-5. QTL association for CO_2-sensitivity

Group no.	Marker[a]		No. of individual[b]	Mean RLSICO_2			
	XT05-004	BRMS-042-2					
1	SS	SS	5	3.86			*[c]
2	SS	IS	13	3.23		*	
3	SS	II	5	2.40			
4	IS	SS	13	3.12	*		
5	IS	IS	23	2.37		*	
6	IS	II	13	1.63			
7	II	SS	6	2.42			
8	II	IS	16	1.78			
9	II	II	3	1.71			

[a] S, CO_2-susceptible HA-11621 allele; I, CO_2-insusceptible HA-11623 allele
[b] Genotype unidentified individuals are excluded
[c] Significant different level, *, $p<0.05$

Table 1-6. Annotated genes and *Arabidopsis* homologues in *BrSIO1*

Gene ID	LG	Start	End	AGI	Description	Slide A	Slide B	Slide C	AVE
Bra004778	**A05**	**1802120**	**1804421**	**AT2G43710**	**Encodes a stearoyl-ACP desaturase**	**355.3**	**361.7**	**372.9**	**363.3**
Bra004779	A05	1805009	1805659	AT2G43730	Mannose-binding lectin superfamily protein				
Bra004780	A05	1806494	1807130	AT2G43730	Mannose-binding lectin superfamily protein				
Bra004781	**A05**	**1807522**	**1809777**	**AT2G43750**	**Arabidopsis thaliana O-acetylserine (thiol) lyase (OAS-TL) isoform oasB**	**272.7**	**287.7**	**333.2**	**297.9**
Bra004782	**A05**	**1810520**	**1811050**	**AT2G43760**	**molybdopterin biosynthesis MoaE family protein**	**123.3**	**118.4**	**163.2**	**134.9**
Bra004783	**A05**	**1811154**	**1813258**	**AT2G43770**	**Transducin/WD40 repeat-like superfamily protein**	**225.5**	**203.2**	**203.4**	**210.7**
Bra004784	**A05**	**1814778**	**1816787**	**AT2G43790**	**MAP KINASE 6**	**207.4**	**162.7**	**178.5**	**182.9**
Bra004785	A05	1817117	1818644	AT2G43795	unknown protein				
Bra004786	**A05**	**1822215**	**1825011**	**AT2G43800**	**Actin-binding FH2 (formin homology 2) family protein**	**343.2**	**339.3**	**349.8**	**344.1**
Bra004787	A05	1828516	1830271	AT2G43820	Arabidopsis thaliana salicylic acid glucosyltransferase 1				
Bra004788	A05	1831237	1832659	AT2G43820	Arabidopsis thaliana salicylic acid glucosyltransferase 1				
Bra004789	A05	1837991	1839351	AT2G43880	Pectin lyase-like superfamily protein				
Bra004790	A05	1846616	1848000	AT2G43880	Pectin lyase-like superfamily protein				
Bra004791	A05	1849377	1850884	AT2G43880	Pectin lyase-like superfamily protein				
Bra004792	A05	1851396	1853277	AT2G43910	HARMLESS TO OZONE LAYER 1 (HOL1)				
Bra004793	A05	1857759	1859109	AT2G43910	HARMLESS TO OZONE LAYER 1 (HOL1)				
Bra004794	A05	1860370	1861952	AT2G43945	unknown protein				
Bra004795	**A05**	**1863096**	**1865725**	**AT2G43970**	**RNA-binding protein**	**145.7**	**150.2**	**139.6**	**145.1**
Bra004796	**A05**	**1866075**	**1868706**	**AT2G43980**	**inositol 1,3,4-trisphosphate 5/6-kinase 4 (ITPK4)**	**105.7**	**112.6**	**88.8**	**102.4**
Bra004797	**A05**	**1868986**	**1870488**	**AT2G43990**	**unknown protein**	**26.8**	**25.9**	**26.9**	**26.5**
Bra004798	A05	1871248	1871856	AT2G44000	Late embryogenesis abundant (LEA) hydroxyproline-rich glycoprotein family				
Bra004799	A05	1873482	1873766	AT2G44010	unknown protein				
Bra004800	**A05**	**1874741**	**1876084**	**AT2G44020**	**Mitochondrial transcription termination factor family protein**	**77.3**	**76.5**	**74.7**	**76.2**
Bra004801	**A05**	**1877612**	**1879360**	**AT2G44065**	**Ribosomal protein L2 family**	**209.7**	**234.3**	**228.9**	**224.3**
Bra004802	A05	1881187	1889019	-	-	-	-	-	-
Bra004803	**A05**	**1892847**	**1893176**	**AT2G44080**	**Encodes ARL, a gene similar to ARGOS involved in cell expansion-dependent organ growth**	**98.5**	**114.5**	**104.0**	**105.7**
Bra004804	**A05**	**1894119**	**1896095**	**AT2G44090**	**Ankyrin repeat family protein**	**73.1**	**74.2**	**96.1**	**81.2**
Bra004805	**A05**	**1898162**	**1900945**	**AT2G44100**	**GDP dissociation inhibitor involved in vesicular membrane traffic**	**798.2**	**773.1**	**758.3**	**776.6**
Bra004806	**A05**	**1902291**	**1903374**	**AT2G44120**	**Ribosomal protein L30/L7 family protein**	**1391.5**	**1390.2**	**1443.3**	**1408.3**
Bra004807	A05	1908181	1909470	AT2G44130	Galactose oxidase/kelch repeat superfamily protein				
Bra004808	A05	1909664	1911216	AT2G44140	Peptidase family C54 protein				
Bra004809	**A05**	**1912514**	**1914621**	**AT2G44150**	**Encodes a protein-lysine N-methyltransferase. Located in ER.**	**92.3**	**88.6**	**81.4**	**87.4**
Bra004810	A05	1915442	1918534	AT2G44160	methylenetetrahydrofolate reductase MTHFR2 mRNA, complete				
Bra004811	**A05**	**1919370**	**1921218**	**AT2G44190**	**Encodes a novel microtubule binding protein**	**50.6**	**49.0**	**63.4**	**54.3**
Bra004812	A05	1921741	1923420	AT2G44195	CBF1-interacting co-repressor CIR, N-terminal;Pre-mRNA splicing factor				
Bra004813	A05	1926040	1927962	-	-	-	-	-	-
Bra004815	A05	1933683	1935558	-	-	-	-	-	-
Bra004816	A05	1936960	1939048	-	-	-	-	-	-
Bra004817	**A05**	**1939997**	**1941807**	**AT2G44230**	**Plant protein of unknown function (DUF946)**	**96.2**	**86.0**	**85.8**	**89.3**
Bra004818	A05	1943704	1945964	-	-	-	-	-	-
Bra004819	A05	1947849	1950090	-	-	-	-	-	-
Bra004820	A05	1952417	1954357	-	-	-	-	-	-
Bra004821	A05	1965165	1969541	-	-	-	-	-	-
Bra004822	**A05**	**1970933**	**1973160**	**AT2G44270**	**Encodes ROL5, a repressor of lrx1 mutants that develop aberrant root hairs**	**74.2**	**78.7**	**71.0**	**74.6**
Bra004823	A05	1974209	1976693	AT2G44280	Major facilitator superfamily protein				
Bra004824	A05	1978048	1979340	AT2G44290	Bifunctional inhibitor/lipid-transfer protein/seed storage 2S albumin superfamily protein				
Bra004825	A05	1984033	1984575	AT2G44340	VQ motif-containing protein				
Bra004826	A05	1987355	1988083	AT2G44370	Cysteine/Histidine-rich C1 domain family protein				
Bra004827	A05	1992070	1994016	-	-	-	-	-	-
Bra004828	A05	1995264	1996025	AT2G44370	Cysteine/Histidine-rich C1 domain family protein				
Bra004829	A05	1997885	1999084	AT2G44410	RING/U-box superfamily protein				
Bra004830	**A05**	**1999513**	**2001278**	**AT2G44420**	**protein N-terminal asparagine amidohydrolase family protein**	**41.6**	**42.0**	**44.9**	**42.8**
Bra004831	A05	2002992	2005950	AT2G44430	DNA-binding bromodomain-containing protein				
Bra004832	**A05**	**2006506**	**2008503**	**AT2G44440**	**Emsy N Terminus (ENT) domain-containing protein**	**47.8**	**56.6**	**46.1**	**50.2**
Bra004833	**A05**	**2013630**	**2016348**	**AT2G44450**	**beta glucosidase 15 (BGLU15)**	**64.3**	**60.3**	**68.0**	**64.2**
Bra004834	A05	2020029	2022302	-	-	-	-	-	-
Bra004835	**A05**	**2025706**	**2029646**	**AT2G44450**	**beta glucosidase 15 (BGLU15).**	**64.3**	**60.3**	**68.0**	**64.2**
Bra004836	A05	2035186	2039155	AT2G44450	beta glucosidase 15 (BGLU15				
Bra004837	**A05**	**2042204**	**2066541**	**AT2G44460**	**beta glucosidase 28 (BGLU28)**	**22.6**	**19.5**	**18.7**	**20.3**
Bra004838	A05	2074677	2077758	AT2G44450	beta glucosidase 15 (BGLU15)				
Bra004839	**A05**	**2080458**	**2083229**	**AT2G44490**	**Encodes a glycosyl hydrolase**	**43.2**	**46.4**	**46.5**	**45.4**
Bra004840	A05	2086734	2089770	AT2G44450	beta glucosidase 15 (BGLU15)				
Bra004841	**A05**	**2099727**	**2101689**	**AT2G44500**	**O-fucosyltransferase family protein**	**185.0**	**191.9**	**183.6**	**186.8**
Bra004842	**A05**	**2102608**	**2104660**	**AT2G44520**	**cytochrome c oxidase 10 (COX10)**	**84.6**	**86.9**	**86.4**	**86.0**
Bra004843	**A05**	**2105300**	**2106562**	**AT2G44525**	**Protein of unknown function (DUF498/DUF598)**	**186.7**	**183.3**	**165.9**	**178.6**
Bra004844	A05	2107659	2109389	AT2G44540	glycosyl hydrolase 9B9 (GH9B9)				
Bra004845	A05	2111987	2113709	AT2G44540	glycosyl hydrolase 9B9 (GH9B9)				
Bra004846	A05	2116326	2118247	AT2G44560	glycosyl hydrolase 9B11 (GH9B11)				
Bra004847	A05	2124205	2124642	AT2G44581	RING/U-box superfamily protein				
Bra004848	A05	2125608	2127401	AT2G44580	zinc ion binding				
Bra004849	A05	2129746	2130591	AT2G44600	unknown protein				
Bra004850	**A05**	**2133155**	**2135330**	**AT2G44610**	**Encodes a GTP-binding protein with similarity to yeast YPT6**	**242.5**	**239.0**	**208.8**	**230.1**
Bra004851	**A05**	**2136308**	**2136887**	**AT2G44620**	**Encodes a member of the mitochondrial acyl carrier protein (ACP) family.**	**518.5**	**491.2**	**524.1**	**511.3**
Bra004852	**A05**	**2137601**	**2139679**	**AT2G44640**	**unknown protein**	**184.6**	**186.0**	**177.7**	**182.8**
Bra004853	**A05**	**2139867**	**2141063**	**AT2G44650**	**Encodes a chloroplast-localized chaperonin 10**	**686.8**	**690.6**	**647.1**	**674.8**
Bra004854	A05	2142969	2145037	AT2G44660	ALG6, ALG8 glycosyltransferase family				
Bra004855	**A05**	**2147596**	**2147974**	**AT2G44670**	**Protein of unknown function (DUF581)**	**479.1**	**485.0**	**473.6**	**479.2**
Bra004856	**A05**	**2149090**	**2150324**	**AT2G44680**	**Encodes casein kinase II beta chain, a CK2 regulatory subunit.**	**137.6**	**137.4**	**140.7**	**138.6**
Bra004857	**A05**	**2151542**	**2152819**	**AT2G44690**	**A member of ROP GTPase gene family.**	**34.0**	**40.3**	**29.4**	**34.5**
Bra004858	**A05**	**2153663**	**2157318**	**AT2G44710**	**RNA-binding (RRM/RBD/RNP motifs) family protein**	**61.7**	**79.6**	**77.6**	**73.0**
Bra004859	**A05**	**2158462**	**2159370**	**AT2G44730**	**Alcohol dehydrogenase transcription factor Myb/SANT-like family protein**	**56.2**	**48.3**	**45.6**	**50.0**
Bra004860	A05	2160277	2160909	-	-	-	-	-	-
Bra004861	A05	2161320	2162135	-	-	-	-	-	-
Bra004862	A05	2162865	2164474	-	-	-	-	-	-
Bra004863	**A05**	**2164973**	**2166282**	**AT2G44740**	**cyclin p4;1 (CYCP4;1)**	**102.9**	**110.4**	**121.4**	**111.6**
Bra004864	**A05**	**2169762**	**2171241**	**AT2G44745**	**WRKY family transcription factor**	**20.8**	**33.3**	**26.7**	**27.0**
Bra004865	**A05**	**2176019**	**2177933**	**AT2G44760**	**unknown protein**	**49.5**	**54.5**	**42.4**	**48.8**

Table 1-6. (continued)

Bra004866	A05	2179844	2180803	AT2G44790	UCLACYANIN 2				
Bra004867	A05	2184212	2186273	AT2G44800	2-oxoglutarate (2OG) and Fe(II)-dependent oxygenase superfamily protein				
Bra004868	A05	2204575	2205768	-	-	-	-	-	-
Bra004869	A05	2207070	2208410	AT2G44810	DEFECTIVE ANTHER DEHISCENCE 1				
Bra004870	A05	2217092	2217645	-	-	-	-	-	-
Bra004871	**A05**	**2222111**	**2222983**	**AT2G44820**	**unknown protein**	**186.4**	**184.1**	**191.6**	**187.4**
Bra004872	**A05**	**2228412**	**2231516**	**AT2G44830**	**Protein kinase superfamily protein**	**137.5**	**134.7**	**137.7**	**136.6**
Bra004873	**A05**	**2234840**	**2235538**	**AT2G44840**	**ETHYLENE-RESPONSIVE ELEMENT BINDING FACTOR 13**	**123.2**	**116.5**	**117.9**	**119.2**
Bra004874	**A05**	**2237723**	**2239355**	**AT2G44910**	**ARABIDOPSIS THALIANA HOMEOBOX-LEUCINE ZIPPER PROTEIN 4**	**13.7**	**16.8**	**15.0**	**15.2**
Bra004875	**A05**	**2247722**	**2249159**	**AT2G44920**	**Tetratricopeptide repeat (TPR)-like superfamily protein**	**160.5**	**161.0**	**185.5**	**169.0**
Bra004876	A05	2249958	2250774	-	-	-	-	-	-
Bra004877	A05	2252356	2257044	AT2G44930	Plant protein of unknown function (DUF247)				
Bra004878	**A05**	**2263243**	**2264091**	**AT2G44940**	**encodes a member of the DREB subfamily A-4 of ERF/AP2 transcription factor family.**	**41.0**	**41.9**	**38.6**	**40.5**
Bra004879	**A05**	**2270073**	**2274586**	**AT2G44950**	**encodes one of two orthologous E3 ubiquitin ligases in Arabidopsis**	**71.2**	**78.0**	**73.0**	**74.1**
Bra004880	**A05**	**2275277**	**2277507**	**AT2G44970**	**alpha/beta-Hydrolases superfamily protein**	**131.9**	**125.6**	**123.2**	**126.9**
Bra004881	**A05**	**2278325**	**2283046**	**AT2G44980**	**SNF2 domain-containing protein / helicase domain-containing protein**	**24.5**	**28.6**	**27.1**	**26.7**
Bra004882	A05	2283365	2286657	AT2G45000	EMBRYO DEFECTIVE 2766 (EMB2766)				
Bra004883	**A05**	**2287086**	**2288787**	**AT2G45010**	**PLAC8 family protein**	**129.8**	**144.1**	**126.1**	**133.3**
Bra004884	A05	2290046	2294328	AT2G45030	Translation elongation factor EFG/EF2 protein				
Bra004885	A05	2296232	2297251	AT2G45040	Matrixin family protein				
Bra004886	A05	2302497	2303350	AT2G45050	Encodes a member of the GATA factor family of zinc finger transcription factors.				
Bra004887	**A05**	**2305445**	**2305696**	**AT2G45070**	**Sec61 Beta Subunit**	**932.4**	**956.1**	**1002.5**	**963.7**
Bra004888	**A05**	**2310343**	**2311104**	**AT2G45080**	**cyclin p3;1 (cycp3;1)**	**48.4**	**43.3**	**43.9**	**45.2**
Bra004889	A05	2314366	2315456	AT2G45110	member of BETA-EXPANSINS.				
Bra004890	A05	2323211	2326057	AT2G45110	member of BETA-EXPANSINS.				
Bra004891	A05	2331494	2332478	-	-	-	-	-	-
Bra004892	A05	2332987	2338977	AT2G45220	Plant invertase/pectin methylesterase inhibitor superfamily				
Bra004893	**A05**	**2344666**	**2347543**	**AT2G45240**	**Encodes a cytoplasmic MAP1 like methionine aminopeptidase**	**227.3**	**242.2**	**222.1**	**230.5**
Bra004894	A05	2347927	2349138	AT2G45260	Plant protein of unknown function (DUF641)				
Bra004895	A05	2349797	2352347	AT2G45270	Mitochondrial protein essential for embryo development.				
Bra004896	A05	2353963	2355351	-	-	-	-	-	-
Bra004897	**A05**	**2364883**	**2367127**	**AT2G45280**	**Encodes a protein similar to RAD51C**	**45.2**	**44.9**	**43.2**	**44.4**
Bra004898	**A05**	**2367652**	**2370453**	**AT2G45290**	**Transketolase**	**47.3**	**54.4**	**79.6**	**60.4**
Bra004899	A05	2371226	2378801	AT2G45330	RNA 2'-phosphotransferase/ transferase, transferring phosphorus-containing groups				

Genes listed in BOLD are expressing in carpel based on Microarray data NASCArrays, and signal from 3 individual slides and those average are shown.

Table 1-7. Annotated genes and *Arabidopsis* homologues in *BrSIO2*

Gene ID	LG	Start	End	AGI	Description	Slide A	Slide B	Slide C	AVE
Bra012922	**A03**	**21503679**	**21504755**	**AT3G49790**	**Carbohydrate-binding protein**	**37.5**	**35.7**	**42.1**	**38.4**
Bra012921	A03	21506279	21506569	-	-	-	-	-	-
Bra012920	**A03**	**21506932**	**21509115**	**AT3G49740**	**pentatricopeptide (PPR) repeat-containing protein**	**33.3**	**20.4**	**23.9**	**25.9**
Bra012919	**A03**	**21520607**	**21521649**	**AT3G49850**	**Encodes a telomeric DNA binding protein.**	**42.6**	**40.7**	**33.9**	**39.1**
Bra012918	A03	21522066	21523153	AT3G49860	A member of ARF-like GTPase family				
Bra012917	**A03**	**21525865**	**21527832**	**AT3G49890**	**unknown protein**	**42.3**	**35.4**	**43.1**	**40.2**
Bra012916	**A03**	**21528338**	**21528778**	**AT3G49910**	**Translation protein SH3-like family protein**	**2606.1**	**2733.3**	**2843.0**	**2727.4**
Bra012915	A03	21529958	21531257	AT3G49920	Encodes a voltage-dependent anion channel.				
Bra012914	A03	21533867	21534508	AT3G49930	C2H2 and C2HC zinc fingers superfamily protein				
Bra012913	**A03**	**21541449**	**21542267**	**AT3G49940**	**LOB domain-containing protein 38 (LBD38)**	**62.4**	**54.6**	**67.5**	**61.5**
Bra012912	**A03**	**21549497**	**21550945**	**AT3G49990**	**unknown protein**	**137.9**	**145.5**	**123.6**	**135.6**
Bra012911	A03	21570191	21571431	AT3G50040	unknown protein				
Bra012910	**A03**	**21573956**	**21574837**	**AT3G50060**	**Encodes a member of the R2R3 transcription factor gene family.**	**711.5**	**716.7**	**722.0**	**716.7**
Bra012909	**A03**	**21583387**	**21584617**	**AT3G50070**	**Encode CYCD3;3, a CYCD3 D-type cyclin.**	**481.9**	**467.3**	**473.2**	**474.1**
Bra012908	**A03**	**21588821**	**21591662**	**AT3G50110**	**Encodes a phosphatase with low in vitro tyrosine phosphatase activity**	**55.2**	**47.4**	**47.5**	**50.0**
Bra012907	A03	21592701	21594635	AT3G50120	Plant protein of unknown function (DUF247)				
Bra012906	A03	21597258	21599046	AT3G50130	Plant protein of unknown function (DUF247)				
Bra012905	A03	21600007	21602471	AT3G50140	Plant protein of unknown function (DUF247)				
Bra012904	A03	21609574	21611627	AT3G50120	Plant protein of unknown function (DUF247)				
Bra012903	A03	21620360	21621754	AT3G50390	Transducin/WD40 repeat-like superfamily protein				
Bra012902	A03	21622445	21623207	AT3G50400	GDSL-like Lipase/Acylhydrolase superfamily protein				
Bra012901	**A03**	**21630236**	**21630964**	**AT3G50410**	**Arabidopsis Dof protein containing a single 51-amino acid zinc finger DNA-binding domain**	**70.5**	**79.0**	**81.6**	**77.0**
Bra012900	A03	21631175	21633316	AT3G50420	Pentatricopeptide repeat (PPR) superfamily protein				
Bra012899	A03	21634500	21635632	AT3G50440	Encodes a protein shown to have methyl jasmonate esterase activity in vitro.				
Bra012898	A03	21646727	21647884	AT3G50450	Homolog of RPW8				
Bra012897	**A03**	**21648630**	**21650423**	**AT3G50500**	**encodes a member of SNF1-related protein kinases (SnRK2)**	**178.8**	**185.4**	**183.2**	**182.5**
Bra012896	**A03**	**21650998**	**21654747**	**AT3G50520**	**Phosphoglycerate mutase family protein**	**120.1**	**133.2**	**124.4**	**125.9**
Bra012895	**A03**	**21656123**	**21657262**	**AT3G50620**	**P-loop containing nucleoside triphosphate hydrolases superfamily protein**	**68.7**	**61.8**	**52.5**	**61.0**
Bra012894	**A03**	**21677192**	**21678080**	**AT3G50630**	**Kip-related protein (KRP) gene**	**93.4**	**89.3**	**80.4**	**87.7**
Bra012893	A03	21684916	21686388	AT3G50740	UGT72E1 is an UDPG:coniferyl alcohol glucosyltransferase which specifically glucosylates sinapyl- and coniferyl aldehydes.				
Bra012892	A03	21689260	21690705	AT3G50470	UGT72E1 is an UDPG:coniferyl alcohol glucosyltransferase which specifically glucosylates sinapyl- and coniferyl aldehydes.				
Bra012891	A03	21701000	21701975	AT3G50750	BES1/BZR1 homolog 1 (BEH1)				
Bra012890	**A03**	**21712848**	**21713864**	**AT3G50760**	**Encodes a protein with putative galacturonosyltransferase activity.**	**15.1**	**22.2**	**21.3**	**19.5**
Bra012889	**A03**	**21721289**	**21721900**	**AT3G50770**	**calmodulin-like 41 (CML41)**	**30.1**	**28.6**	**25.1**	**28.0**
Bra012888	A03	21729319	21731296	-	-	-	-	-	-
Bra012887	A03	21731833	21732303	AT3G50800	unknown protein				
Bra012886	**A03**	**21735261**	**21735878**	**AT3G50810**	**Uncharacterised protein family (UPF0497)**	**62.4**	**74.8**	**60.1**	**65.8**
Bra012885	**A03**	**21739425**	**21740448**	**AT3G50830**	**cold acclimation protein WCOR413-like protein beta form**	**176.7**	**172.0**	**166.3**	**171.7**
Bra012884	**A03**	**21743712**	**21744839**	**AT3G50860**	**Clathrin adaptor complex small chain family protein**	**84.4**	**90.3**	**87.9**	**87.6**
Bra012883	**A03**	**21788116**	**21789296**	**AT3G50870**	**Encodes a GATA transcriptional regulator required to position the proembryo boundary in the early embryo.**	**30.0**	**49.1**	**50.4**	**43.2**
Bra012882	**A03**	**21799851**	**21803215**	**AT3G50890**	**homeobox protein 28 (HB28)**	**59.6**	**52.7**	**56.7**	**56.3**
Bra012881	**A03**	**21806412**	**21806831**	**AT3G50900**	**unknown protein**	**12.1**	**29.1**	**14.7**	**18.6**
Bra012880	**A03**	**21808947**	**21810344**	**AT3G50910**	**unknown protein**	**134.8**	**141.5**	**125.2**	**133.8**
Bra012879	**A03**	**21810726**	**21814469**	**AT3G50920**	**Encodes a phosphatidic acid phosphatase that can be detected in chloroplast membrane fractions.**	**119.6**	**123.1**	**135.3**	**126.0**
Bra012878	A03	21819325	21820083	-	-	-	-	-	-
Bra012877	A03	21823544	21825055	AT3G50930	cytochrome BC1 synthesis (BCS1)				
Bra012876	**A03**	**21825545**	**21827016**	**AT3G50960**	**Encodes a protein that functions in microtubule assembly.**	**107.8**	**113.2**	**114.5**	**111.8**
Bra012875	**A03**	**21827741**	**21828842**	**AT3G51000**	**alpha/beta-Hydrolases superfamily protein**	**74.0**	**67.9**	**87.4**	**76.4**
Bra012874	**A03**	**21829127**	**21830246**	**AT3G51010**	**unknown protein**	**361.5**	**373.1**	**367.8**	**367.5**
Bra012873	A03	21830934	21831338	AT3G51020	unknown protein				
Bra012872	**A03**	**21833447**	**21834370**	**AT3G51030**	**encodes a cytosolic thioredoxin**	**108.0**	**118.5**	**120.6**	**115.7**
Bra012871	**A03**	**21835581**	**21841120**	**AT3G51050**	**FG-GAP repeat-containing protein**	**224.6**	**241.3**	**233.2**	**233.0**
Bra012870	**A03**	**21842601**	**21844033**	**AT3G51090**	**Protein of unknown function (DUF1640)**	**47.3**	**38.6**	**41.7**	**42.5**
Bra012869	**A03**	**21844794**	**21846222**	**AT3G51100**	**unknown protein**	**174.9**	**164.3**	**172.6**	**170.6**
Bra012868	**A03**	**21848187**	**21853892**	**AT3G51120**	**DNA binding;zinc ion binding;nucleic acid binding;nucleic acid binding**	**105.9**	**101.4**	**99.0**	**102.1**
Bra012867	**A03**	**21860025**	**21864871**	**AT3G51130**	**unknown protein**	**194.6**	**215.8**	**198.9**	**203.1**
Bra012866	**A03**	**21867468**	**21874187**	**AT3G51150**	**ATP binding microtubule motor family protein**	**70.3**	**73.0**	**68.9**	**70.7**
Bra012865	**A03**	**21874550**	**21875635**	**AT3G51160**	**Catalyzes the first step in the de novo synthesis of GDP-L-fucose.**	**143.6**	**139.1**	**144.0**	**142.2**
Bra012864	A03	21879896	21880840	AT3G51190	Ribosomal protein L2 family				
Bra012863	A03	21882120	21882813	AT3G51220	Plant protein of unknown function (DUF827)				
Bra012862	**A03**	**21884085**	**21885545**	**AT3G51240**	**Encodes flavanone 3-hydroxylase that is coordinately expressed with chalcone synthase and chalcone isomerases.**	**821.2**	**840.4**	**864.6**	**842.1**
Bra012861	**A03**	**21887206**	**21888537**	**AT3G51260**	**20S proteosomal alpha subunits. Interacts with SnRK, SKP1/ASK1 during proteasomal binding of an SCF ubiquitin ligase.**	**425.4**	**398.9**	**393.3**	**405.9**
Bra012860	**A03**	**21889549**	**21892303**	**AT3G51270**	**protein serine/threonine kinases;ATP binding;catalytics**	**55.4**	**57.8**	**59.5**	**57.6**
Bra012859	**A03**	**21892762**	**21894206**	**AT3G51280**	**Tetratricopeptide repeat (TPR)-like superfamily protein**	**130.2**	**136.3**	**136.0**	**134.2**
Bra012858	**A03**	**21895239**	**21896289**	**AT3G51300**	**Encodes a pollen-specific Rop GTPase, member of the Rho family of small GTP binding proteins that interacts with RIC3 and RIC4 to control tip growth in pollen tubes.**	**61.6**	**52.6**	**63.6**	**59.2**
Bra012857	A03	21896574	21899299	AT3G51330	Eukaryotic aspartyl protease family protein				
Bra012856	**A03**	**21904574**	**21904843**	**AT3G51370**	**Protein phosphatase 2C family protein**	**153.8**	**151.7**	**137.4**	**147.7**
Bra012855	A03	21907338	21907726	AT3G51380	IQ-domain 20 (IQD20)				
Bra012854	A03	21909542	21910375	AT3G51400	Arabidopsis protein of unknown function (DUF241)				
Bra012853	A03	21913022	21913759	AT3G51410	Arabidopsis protein of unknown function (DUF241)				
Bra012852	**A03**	**21916802**	**21917020**	**AT3G51500**	**unknown protein**	**48.2**	**50.3**	**62.4**	**53.6**
Bra012851	**A03**	**21917365**	**21918998**	**AT3G51520**	**diacylglycerol acyltransferase family**	**122.5**	**119.7**	**125.3**	**122.5**
Bra012850	**A03**	**21919767**	**21922457**	**AT3G51550**	**FERONIA**	**376.0**	**401.5**	**400.2**	**392.6**
Bra012849	**A03**	**21923814**	**21925904**	**AT3G51580**	**unknown protein**	**51.3**	**49.3**	**50.9**	**50.5**
Bra012848	A03	21927444	21928521	AT3G51590	Encodes a member of the lipid transfer protein family.				
Bra012847	**A03**	**21930765**	**21931269**	**AT3G51600**	**Predicted to encode a PR (pathogenesis-related) protein.**	**445.7**	**451.8**	**490.3**	**462.6**
Bra012846	**A03**	**21935886**	**21938732**	**AT3G51620**	**Tautomerase/MIF superfamily protein**	**86.5**	**92.4**	**95.1**	**91.3**
Bra012845	A03	21943489	21944494	AT3G51660	Tautomerase/MIF superfamily protein				
Bra012843	**A03**	**21956417**	**21961018**	**AT3G51670**	**SEC14 cytosolic factor family protein / phosphoglyceride transfer family protein**	**479.7**	**485.7**	**485.2**	**483.5**

Table 1-7. (continued)

Bra012844	A03	21958056	21958801	-	-	-	-	-	-
Bra012842	A03	21966018	21967077	AT3G51680	NAD(P)-binding Rossmann-fold superfamily protein				
Bra012841	A03	21972702	21974345	AT3G51710	D-mannose binding lectin protein with Apple-like carbohydrate-binding domain				
Bra012840	**A03**	**21975321**	**21976436**	**AT3G51730**	**saposin B domain-containing protein**	**572.7**	**536.3**	**516.2**	**541.7**
Bra012839	A03	21976993	21977610	AT3G51750	unknown protein				
Bra012838	**A03**	**21979034**	**21982030**	**AT3G51770**	**Encodes a negative regulator of 1-aminocyclopropane-1-carboxylic acid synthase5(ACS5)**	**43.9**	**44.7**	**33.4**	**40.6**
Bra012837	**A03**	**21987354**	**21988859**	**AT3G51780**	**A member of Arabidopsis BAG (Bcl-2-associated athanogene) proteins, plant homologs of mammalian regulators of apoptosis.**	**143.2**	**143.7**	**135.0**	**140.6**
Bra012836	**A03**	**21989642**	**21991826**	**AT3G51800**	**putative nuclear DNA-binding protein G2p (AtG2) mRNA,**	**910.4**	**862.2**	**1000.7**	**924.4**
Bra012835	**A03**	**21999149**	**22001348**	**AT3G51850**	**member of Calcium Dependent Protein Kinase**	**335.9**	**298.4**	**278.9**	**304.4**
Bra012834	A03	22012543	22013294	-	-	-	-	-	-
Bra012833	**A03**	**22014395**	**22021133**	**AT3G51860**	**cation exchanger 3 (CAX3)**	**189.0**	**184.3**	**180.4**	**184.6**
Bra012832	**A03**	**22021830**	**22022840**	**AT3G51880**	**Encodes a protein belonging to the subgroup of HMGB (high mobility group B) proteins that have a distinctive DNA-binding motif, the HMG-box domain.**	**218.6**	**213.7**	**212.6**	**215.0**
Bra012831	**A03**	**22023678**	**22028202**	**AT3G51895**	**Encodes a sulfate transporter.**	**363.7**	**386.5**	**370.0**	**373.4**
Bra012830	A03	22038200	22038427	-	-	-	-	-	-
Bra012829	**A03**	**22040320**	**22041629**	**AT3G51910**	**member of Heat Stress Transcription Factor (Hsf) family**	**143.2**	**140.4**	**129.7**	**137.8**
Bra012828	**A03**	**22042610**	**22048354**	**AT3G51910**	**member of Heat Stress Transcription Factor (Hsf) family**	**143.2**	**140.4**	**129.7**	**137.8**
Bra012827	**A03**	**22058579**	**22060504**	**AT3G51950**	**Zinc finger (CCCH-type) family protein / RNA recognition motif (RRM)-containing protein**	**667.3**	**644.2**	**633.5**	**648.3**
Bra012826	A03	22062557	22062958	AT3G52000	serine carboxypeptidase-like 36 (scpl36)				
Bra012824	A03	22064355	22067631	AT3G52030	F-box family protein with WD40/YVTN repeat doamin				
Bra012825	**A03**	**22066539**	**22066980**	**AT3G52040**	**unknown protein**	**294.8**	**274.3**	**316.8**	**295.3**
Bra012823	A03	22068270	22070117	-	-	-	-	-	-
Bra012822	A03	22071617	22074763	AT3G52080	encodes a cation:proton exchanger expressed in pollen				
Bra012821	**A03**	**22075262**	**22075790**	**AT3G52090**	**Non-catalytic subunit common to nuclear DNA-dependent RNA polymerases II, IV and V**	**560.5**	**596.4**	**607.7**	**588.2**
Bra012820	A03	22076368	22080442	AT3G52100	RING/FYVE/PHD-type zinc finger family protein				
Bra012819	A03	22081654	22082025	AT3G52130	Bifunctional inhibitor/lipid-transfer protein/seed storage 2S albumin superfamily protein				
Bra012818	**A03**	**22086290**	**22087251**	**AT3G52155**	**Phosphoglycerate mutase family protein**	**50.6**	**51.5**	**50.1**	**50.7**
Bra012817	A03	22087520	22089021	AT3G52160	Encodes KCS15, a member of the 3-ketoacyl-CoA synthase family involved in the biosynthesis of VLCFA (very long chain fatty acids).				
Bra012816	**A03**	**22089446**	**22091224**	**AT3G52170**	**DNA binding**	**106.1**	**92.3**	**79.6**	**92.7**
Bra012815	A03	22093983	22101222	AT3G52250	Encodes a protein with a putative role in mRNA splicing.				
Bra012814	**A03**	**22101545**	**22105804**	**AT3G52260**	**Pseudouridine synthase family protein**	**42.8**	**38.5**	**30.9**	**37.4**
Bra012813	A03	22106896	22108296	AT3G52270	Transcription initiation factor IIF, beta subunit				
Bra012812	A03	22109374	22110381	-	-	-	-	-	-
Bra012811	A03	22110751	22111510	AT3G52270	Transcription initiation factor IIF, beta subunit				
Bra012810	A03	22111762	22113450	AT3G52280	Bromodomain containing nuclear-localized protein involved in leaf development.				
Bra012809	**A03**	**22114190**	**22115517**	**AT3G52300**	**ATP synthase D chain, mitochondrial (ATPQ)**	**1087.3**	**1063.0**	**1107.4**	**1085.9**
Bra012808	A03	22115961	22117190	AT3G52320	F-box and associated interaction domains-containing protein				
Bra012807	**A03**	**22126348**	**22127526**	**AT3G52380**	**chloroplast RNA-binding protein**	**152.6**	**179.9**	**187.9**	**173.5**
Bra012806	**A03**	**22129315**	**22130605**	**AT3G52400**	**syntaxin protein**	**15.8**	**20.7**	**27.1**	**21.2**
Bra012805	A03	22131668	22137432	AT3G52430	Encodes a lipase-like gene that is important for salicylic acid signaling and function in resistance (R) gene-mediated and basal plant disease resistance.				
Bra012804	A03	22138538	22139263	AT3G52440	Dof-type zinc finger DNA-binding family protein				
Bra012803	A03	22146966	22148237	AT3G52450	Encodes a cytoplasmically localized U-box domain E3 ubiquitin ligase protein				
Bra012802	A03	22152538	22153290	AT3G52460	hydroxyproline-rich glycoprotein family protein				
Bra012801	**A03**	**22156349**	**22156975**	**AT3G52470**	**Late embryogenesis abundant (LEA) hydroxyproline-rich glycoprotein family**	**220.8**	**233.8**	**221.0**	**225.2**
Bra012800	**A03**	**22160012**	**22163072**	**AT3G52490**	**Double Clp-N motif-containing P-loop nucleoside triphosphate hydrolases superfamily protein**	**47.6**	**44.7**	**42.6**	**45.0**
Bra012799	**A03**	**22174322**	**22175740**	**AT3G52500**	**aspartyl protease family protein**	**209.0**	**230.1**	**198.8**	**212.6**
Bra012798	A03	22183180	22183584	AT4G15215	PDR13, ATPDR13; PDR13; ATP binding / ATPase/ nucleoside-triphosphatase/ nucleotide binding				
Bra012797	A03	22187168	22194238	AT4G15215	PDR13, ATPDR13; PDR13; ATP binding / ATPase/ nucleoside-triphosphatase/ nucleotide binding				
Bra012796	**A03**	**22195037**	**22197102**	**AT4G15240**	**Protein of unknown function (DUF604)**	**21.5**	**23.4**	**17.0**	**20.6**
Bra012795	A03	22203115	22204539	AT4G15260	UDP-Glycosyltransferase superfamily protein				
Bra012794	A03	22205236	22207291	AT4G15400	Encodes BIA1, a member of the BAHD acyltransferase family.				
Bra012793	A03	22233686	22236995	AT4G15300	a member of the cytochrome P450 gene family. molecular function unknown.				
Bra012792	A03	22241320	22244656	AT4G15300	a member of the cytochrome P450 gene family. molecular function unknown.				
Bra012791	**A03**	**22246023**	**22247577**	**AT4G15410**	**serine/threonine protein phosphatase 2A 55 kDa regulatory subunit B prime gamma (PUX5)**	**183.5**	**144.8**	**163.7**	**164.0**
Bra012790	**A03**	**22248592**	**22250134**	**AT4G15415**	**B' regulatory subunit of PP2A (AtB'gamma)**	**83.6**	**89.2**	**79.0**	**84.0**
Bra012789	A03	22254261	22255793	AT4G15417	RNAse II-like 1 (RTL1)				
Bra012788	**A03**	**22266555**	**22270612**	**AT4G15440**	**Encodes a hydroperoxide lyase. Also a member of the CYP74B cytochrome p450 family.**	**356.1**	**370.4**	**378.1**	**368.2**
Bra012787	A03	22270987	22271322	AT4G15460	glycine-rich protein				
Bra012786	**A03**	**22278433**	**22279696**	**AT4G15470**	**Bax inhibitor-1 family protein**	**689.0**	**687.9**	**695.2**	**690.7**
Bra012785	**A03**	**22283402**	**22285899**	**AT4G15475**	**F-box/RNI-like superfamily protein**	**131.0**	**127.0**	**124.0**	**127.3**
Bra012784	**A03**	**22287411**	**22288883**	**AT4G15480**	**Encodes a protein that might have sinapic acid:UDP-glucose glucosyltransferase activity**	**33.9**	**46.0**	**37.1**	**39.0**
Bra012783	A03	22290158	22293884	-	-	-	-	-	-
Bra012782	**A03**	**22298207**	**22299235**	**AT4G15520**	**tRNA/rRNA methyltransferase (SpoU) family protein**	**98.2**	**94.1**	**101.8**	**98.1**
Bra012781	A03	22299647	22303813	AT4G15530	Encodes a dual-targeted protein believed to act as a pyruvate, orthophosphate dikinase.				
Bra012780	A03	22306772	22309183	AT4G15550	UDP-glucose:indole-3-acetate beta-D-glucosyltransferase				
Bra012779	**A03**	**22312343**	**22315209**	**AT4G15560**	**Encodes a protein with 1-deoxyxylulose 5-phosphate synthase activity involved in the MEP pathway.**	**799.0**	**835.5**	**836.8**	**823.8**
Bra012778	A03	22315983	22316959	-	-	-	-	-	-
Bra012777	A03	22325280	22326834	AT4G15610	Uncharacterised protein family (UPF0497)				
Bra012776	A03	22337080	22337502	-	-	-	-	-	-
Bra012775	A03	22340095	22341323	AT4G15610	Uncharacterised protein family (UPF0497)				
Bra012774	A03	22343131	22344328	AT4G15650	unknown protein				
Bra012773	A03	22347565	22347873	AT4G15660	Thioredoxin superfamily protein				
Bra012772	A03	22351554	22353392	AT4G15720	Tetratricopeptide repeat (TPR)-like superfamily protein				
Bra012771	A03	22356457	22357317	-	-	-	-	-	-
Bra012770	A03	22357795	22359108	-	-	-	-	-	-
Bra012769	A03	22360932	22361857	AT4G15180	SET domain protein 2 (SDG2)				

Table 1-7. (continued)

Bra012768	A03	22362305	22362934	AT4G15740	Calcium-dependent lipid-binding (CaLB domain) family protein				
Bra012767	A03	22363915	22365639	AT4G15760	Encodes a protein with similarity to monooxygenases that are known to degrade salicylic acid (SA).				
Bra012766	A03	22366090	22366604	-	-	-	-	-	-
Bra012765	**A03**	**22368082**	**22368645**	**AT4G15770**	**RNA binding**	**353.9**	**365.7**	**342.7**	**354.1**
Bra012764	**A03**	**22371466**	**22371801**	**AT4G15800**	**Member of a diversely expressed predicted peptide family**	**268.7**	**228.6**	**254.2**	**250.5**
Bra012763	A03	22373442	22374391	AT4G15802	Encodes a protein with similarity to heat shock factor binding proteins. Involved in negative regulation of heat shock response. Becomes nuclear localized upon heat treatment.				
Bra012762	**A03**	**22377334**	**22379165**	**AT4G15820**	**unknown protein**	**26.9**	**26.1**	**32.6**	**28.5**
Bra012761	**A03**	**22380010**	**22383776**	**AT4G15840**	**BTB/POZ domain-containing protein**	**65.5**	**69.7**	**68.0**	**67.7**
Bra012760	A03	22385679	22386306	-	-	-	-	-	-
Bra012759	A03	22390060	22390823	-	-	-	-	-	-
Bra012758	**A03**	**22391541**	**22395768**	**AT4G15880**	**EARLY IN SHORT DAYS 4**	**154.0**	**158.8**	**153.0**	**155.3**
Bra012757	A03	22397979	22400200	-	-	-	-	-	-
Bra012756	A03	22403280	22404812	-	-	-	-	-	-
Bra012755	A03	22407515	22411960	AT4G15885	kinesin motor protein-related				
Bra012754	**A03**	**22414390**	**22419755**	**AT4G15890**	**unknown protein**	**53.7**	**41.1**	**50.5**	**48.4**
Bra012753	**A03**	**22425046**	**22428376**	**AT4G15900**	**Encodes a nuclear WD40 protein that is imported into the nucleus.**	**197.5**	**193.1**	**195.5**	**195.4**
Bra012752	**A03**	**22429268**	**22432153**	**AT4G15920**	**Nodulin MtN3 family protein**	**103.0**	**107.0**	**93.8**	**101.3**
Bra012751	**A03**	**22435198**	**22435729**	**AT4G15930**	**Dynein light chain type 1 family protein**	**638.5**	**609.4**	**587.3**	**611.7**
Bra012750	A03	22436076	22437330	-	-	-	-	-	-
Bra012749	**A03**	**22439592**	**22441476**	**AT4G16060**	**unknown protein**	**155.9**	**142.3**	**159.0**	**152.4**
Bra012748	A03	22450559	22450975	AT4G15990	unknown protein				
Bra012747	A03	22457311	22458730	AT4G15955	alpha/beta-Hydrolases superfamily protein				
Bra012746	A03	22459058	22460791	-	-	-	-	-	-
Bra012745	A03	22466885	22470221	AT4G16070	Mono-/di-acylglycerol lipase, N-terminal;Lipase, class 3				
Bra012744	**A03**	**22475667**	**22477136**	**AT4G16100**	**Protein of unknown function (DUF789)**	**94.4**	**92.9**	**106.9**	**98.0**
Bra012743	**A03**	**22487567**	**22490721**	**AT4G16110**	**ARR2; ARR2 (ARABIDOPSIS RESPONSE REGULATOR 2)**	**36.1**	**43.0**	**32.9**	**37.3**
Bra012742	A03	22492421	22493134	AT4G16141	sequence-specific DNA binding / transcription factor/ zinc ion binding				
Bra012741	A03	22494519	22496253	AT4G16143	Protein interacts with Agrobacterium proteins VirD2 and VirE2.				
Bra012740	**A03**	**22500143**	**22500935**	**AT4G16143**	**IMPA-2; IMPA-2 (IMPORTIN ALPHA ISOFORM 2); binding / protein transporter**	**221.7**	**212.0**	**198.1**	**210.6**
Bra012739	A03	22501816	22504975	AT4G16144	Encodes AMSH3, a deubiquitinating enzyme.				
Bra012738	**A03**	**22513582**	**22514946**	**AT4G16155**	**dihydrolipoyl dehydrogenases**	**162.3**	**151.2**	**133.9**	**149.1**
Bra012737	A03	22515311	22516483	AT4G16160	Homologous to pea OEP16 and barley pPORA (OEP16)				
Bra012736	A03	22517140	22518706	-	-	-	-	-	-
Bra012735	A03	22521491	22522159	-	-	-	-	-	-
Bra012734	**A03**	**22522902**	**22527685**	**AT4G16170**	**unknown protein**	**199.0**	**169.5**	**274.6**	**214.4**
Bra012733	**A03**	**22527988**	**22529356**	**AT4G16190**	**Papain family cysteine protease**	**645.4**	**620.6**	**587.7**	**617.9**
Bra012732	A03	22529512	22529985	AT4G16195	Plant self-incompatibility protein S1 family				
Bra012731	**A03**	**22530232**	**22531190**	**AT4G16210**	**enoyl-CoA hydratase/isomerase A (ECHIA)**	**117.9**	**125.7**	**122.7**	**122.1**
Bra012730	A03	22533528	22533827	-	-	-	-	-	-
Bra012729	A03	22536974	22537435	-	-	-	-	-	-
Bra012728	A03	22538822	22540554	AT4G16220	GDSL-like Lipase/Acylhydrolase superfamily protein				
Bra012727	A03	22543908	22545481	-	-	-	-	-	-
Bra012726	A03	22547001	22550278	-	-	-	-	-	-
Bra012725	**A03**	**22553701**	**22554823**	**AT4G16360**	**5'-AMP-activated protein kinase beta-2 subunit protein**	**177.7**	**164.7**	**170.6**	**171.0**
Bra012724	A03	22559834	22560680	AT4G16380	Heavy metal transport/detoxification superfamily protein				
Bra012723	**A03**	**22562218**	**22562475**	**AT4G16400**	**unknown protein**	**24.5**	**16.0**	**22.0**	**20.8**
Bra012722	A03	22562648	22563190	AT4G16410	unknown protein				
Bra012721	**A03**	**22563364**	**22565755**	**AT4G16420**	**Transcriptional co-activator.**	**172.5**	**159.9**	**179.9**	**170.8**
Bra012720	**A03**	**22567864**	**22569234**	**AT4G16430**	**basic helix-loop-helix (bHLH) DNA-binding superfamily protein**	**127.5**	**111.8**	**131.9**	**123.7**
Bra012719	**A03**	**22569490**	**22570500**	**AT4G16442**	**Uncharacterised protein family (UPF0497)**	**249.2**	**250.2**	**237.2**	**245.5**
Bra012718	**A03**	**22571225**	**22572303**	**AT4G16444**	**unknown protein**	**125.8**	**127.0**	**127.3**	**126.7**
Bra012717	**A03**	**22575731**	**22576108**	**AT4G16447**	**unknown protein**	**278.0**	**286.4**	**333.6**	**299.3**
Bra012716	**A03**	**22577486**	**22577899**	**AT4G16450**	**unknown protein**	**947.1**	**960.7**	**972.2**	**960.0**
Bra012715	A03	22579876	22580573	AT4G16460	unknown protein;				
Bra012714	**A03**	**22584641**	**22586548**	**AT4G16480**	**Encodes a high affinity H+:myo-inositol symporter.**	**57.0**	**49.2**	**59.1**	**55.1**
Bra012713	**A03**	**22587234**	**22588685**	**AT4G16490**	**ARM repeat superfamily protein**	**133.3**	**134.0**	**110.1**	**125.8**
Bra012712	**A03**	**22604200**	**22604541**	**AT4G16500**	**Cystatin/monellin superfamily protein**	**580.8**	**537.6**	**599.4**	**572.6**
Bra012711	**A03**	**22607186**	**22607431**	**AT4G16515**	**Encodes a root meristem growth factor (RGF).**	**102.2**	**122.4**	**119.1**	**114.5**
Bra012710	**A03**	**22608868**	**22609702**	**AT4G16520**	**autophagy 8f (ATG8F)**	**458.1**	**485.4**	**532.9**	**492.1**
Bra012709	A03	22615941	22616609	AT4G16530	Family of unknown function (DUF577)				
Bra012708	A03	22617874	22618839	AT4G16540	Heat shock protein HSP20/alpha crystallin family				
Bra012707	A03	22621584	22622508	AT4G16540	Heat shock protein HSP20/alpha crystallin family				
Bra012706	A03	22624845	22627299	AT4G16540	Heat shock protein HSP20/alpha crystallin family				
Bra012705	A03	22629378	22632850	AT4G16540	Heat shock protein HSP20/alpha crystallin family				
Bra012704	A03	22635782	22636458	AT4G16540	Heat shock protein HSP20/alpha crystallin family				
Bra012703	**A03**	**22642127**	**22650605**	**AT4G16566**	**Encodes a protein that has an unexpected bifunctional capability in vitro.**	**62.2**	**77.3**	**71.1**	**70.2**
Bra012702	**A03**	**22652381**	**22656889**	**AT4G16590**	**encodes a gene similar to cellulose synthase**	**55.7**	**43.2**	**51.8**	**50.2**
Bra012701	**A03**	**22662703**	**22663347**	**AT4G16610**	**C2H2-like zinc finger protein**	**96.5**	**117.7**	**105.8**	**106.7**
Bra012700	A03	22666240	22667907	AT4G16620	nodulin MtN21-like transporter family protein				
Bra012699	A03	22674172	22675266	AT4G16640	Matrixin family protein				
Bra012698	A03	22678821	22683532	-	-	-	-	-	-
Bra012697	**A03**	**22687071**	**22689558**	**AT4G16650**	**O-fucosyltransferase family protein**	**74.8**	**85.9**	**72.3**	**77.7**
Bra012696	**A03**	**22690909**	**22694777**	**AT4G16660**	**heat shock protein 70 (Hsp 70) family protein**	**186.7**	**177.7**	**208.6**	**191.0**
Bra012695	A03	22696243	22696489	-	-	-	-	-	-
Bra012694	**A03**	**22697449**	**22699659**	**AT4G16720**	**Ribosomal protein L23/L15e family protein**	**1979.6**	**2029.6**	**2110.4**	**2039.9**
Bra012693	**A03**	**22708404**	**22708937**	**AT4G16750**	**encodes a member of the DREB subfamily A-4 of ERF/AP2 transcription factor family.**	**15.6**	**15.5**	**17.8**	**16.3**
Bra012692	A03	22713752	22714072	-	-	-	-	-	-
Bra012691	A03	22714414	22717327	AT4G16765	2-oxoglutarate (2OG) and Fe(II)-dependent oxygenase superfamily protein				
Bra012690	A03	22722231	22723763	AT4G16820	Encodes a lipase that hydrolyzes phosphatidylcholine, glycolipids as well as triacylglycerols.				
Bra012689	**A03**	**22724348**	**22730873**	**AT4G16860**	**RECOGNITION OF PERONOSPORA PARASITICA 4, RPP4**	**12.7**	**12.4**	**16.4**	**13.8**
Bra012688	**A03**	**22731251**	**22737169**	**AT4G16860**	**RECOGNITION OF PERONOSPORA PARASITICA 4, RPP4**	**12.7**	**12.4**	**16.4**	**13.8**
Bra012687	A03	22740665	22742204	-	-	-	-	-	-
Bra012686	A03	22744793	22746772	-	-	-	-	-	-
Bra012685	A03	22748498	22749631	AT4G17200	F-box and associated interaction domains-containing protein				
Bra012684	A03	22750594	22753322	AT4G17030	Encodes EXLB1 (expansin-like B1), a member of the expansin family.				

Table 1-7. (continued)

Bra012683	**A03**	**22757906**	**22760123**	**AT4G17040**	**encodes the ClpR4 subunit of the chloroplast-localized Clp protease complex.**	**688.4**	**676.2**	**687.5**	**684.0**
Bra012682	A03	22760487	22762906	AT4G17050	Encodes a protein with ureidoglycine aminohydrolase activity.				
Bra012681	A03	22770001	22771524	-	-	-	-	-	-
Bra012680	A03	22775981	22781437	-	-	-	-	-	-
Bra012679	A03	22791386	22792132	-	-	-	-	-	-
Bra012678	A03	22794839	22798551	-	-	-	-	-	-
Bra012677	A03	22803983	22804240	AT4G17085	Putative membrane lipoprotein				
Bra012676	**A03**	**22804681**	**22806581**	**AT4G17090**	**Encodes a beta-amylase targeted to the chloroplast.**	**204.9**	**208.2**	**206.1**	**206.4**
Bra012675	**A03**	**22808866**	**22811066**	**AT4G17100**	**unknown protein**	**131.5**	**149.5**	**158.7**	**146.6**
Bra012674	A03	22814475	22815042	AT4G17160	RAB GTPase homolog B1A (RABB1a)				
Bra012673	A03	22826220	22826735	AT4G17215	Pollen Ole e 1 allergen and extensin family protein				
Bra012672	A03	22831432	22833660	AT4G17250	unknown protein				
Bra012671	**A03**	**22834749**	**22835871**	**AT4G17260**	**Lactate/malate dehydrogenase family protein**	**308.5**	**295.5**	**291.2**	**298.4**
Bra012670	**A03**	**22837875**	**22839995**	**AT4G17270**	**Mo25 family protein**	**146.9**	**145.6**	**147.0**	**146.5**
Bra012669	**A03**	**22841667**	**22843315**	**AT4G17350**	**Protein of unknown function DUF828**	**72.5**	**66.7**	**76.2**	**71.8**
Bra012668	**A03**	**22843726**	**22845379**	**AT4G17370**	**Oxidoreductase family protein**	**22.0**	**21.9**	**27.4**	**23.8**
Bra012667	**A03**	**22846092**	**22847568**	**AT4G17390**	**Ribosomal protein L23/L15e family protein**	**1970.2**	**1845.4**	**2065.0**	**1960.2**
Bra012666	A03	22850241	22851492	-	-	-	-	-	-
Bra012665	A03	22854496	22855661	-	-	-	-	-	-
Bra012664	A03	22858877	22859704	AT4G17440	Protein of unknown function (DUF1639)				
Bra012663	**A03**	**22870234**	**22871338**	**AT4G17460**	**Encodes a class II HD-ZIP protein that regulates meristematic activity in different tissues**	**404.1**	**411.8**	**389.1**	**401.7**
Bra012662	A03	22872072	22873607	AT4G17470	alpha/beta-Hydrolases superfamily protein				
Bra012661	**A03**	**22874242**	**22875107**	**AT4G17486**	**PPPDE putative thiol peptidase family protein**	**126.5**	**129.9**	**135.4**	**130.6**
Bra012660	**A03**	**22876088**	**22877555**	**AT4G17510**	**ubiquitin C-terminal hydrolase 3 (UCH3)**	**189.9**	**192.1**	**200.9**	**194.3**
Bra012659	**A03**	**22878123**	**22879891**	**AT4G17520**	**Hyaluronan / mRNA binding family**	**261.8**	**283.4**	**308.7**	**284.6**
Bra012658	**A03**	**22880314**	**22881657**	**AT4G17530**	**AtRabD2c encodes a Rab GTPase**	**315.9**	**309.6**	**320.7**	**315.4**
Bra012657	**A03**	**22886426**	**22889023**	**AT4G17550**	**Encodes a member of the phosphate starvation-induced glycerol-3-phosphate permease gene family**	**22.9**	**27.3**	**28.9**	**26.3**
Bra012656	**A03**	**22890900**	**22892842**	**AT4G17600**	**Encodes Lil3:1 (light-harvesting-like) protein.**	**260.8**	**278.2**	**262.2**	**267.1**
Bra012655	**A03**	**22897484**	**22899346**	**AT4G17615**	**Member of AtCBL (Calcineurin B-like Calcium Sensor Proteins) family.**	**94.4**	**89.8**	**95.8**	**93.3**
Bra012654	A03	22899921	22901861	AT4G17616	Pentatricopeptide repeat (PPR) superfamily protein				
Bra012653	**A03**	**22902680**	**22905495**	**AT4G17620**	**glycine-rich protein**	**156.9**	**176.7**	**181.3**	**171.6**
Bra012652	**A03**	**22906024**	**22908683**	**AT4G17640**	**Encodes casein kinase II beta (regulatory) subunit.**	**262.7**	**227.1**	**242.2**	**244.0**
Bra012651	**A03**	**22909790**	**22910427**	**AT4G17670**	**Protein of unknown function (DUF581)**	**396.6**	**379.8**	**388.2**	**388.2**
Bra012650	A03	22915403	22927293	AT4G17680	SBP (S-ribonuclease binding protein) family protein				
Bra012649	**A03**	**22933529**	**22933996**	**AT4G17690**	**Peroxidase superfamily protein**	**13.7**	**9.7**	**9.4**	**10.9**
Bra012648	A03	22947960	22948367	AT4G17718	Encodes a defensin-like (DEFL) family protein.				
Bra012647	**A03**	**22949396**	**22951220**	**AT4G17720**	**RNA-binding (RRM/RBD/RNP motifs) family protein**	**139.3**	**143.8**	**164.9**	**149.3**
Bra012646	**A03**	**22957393**	**22958909**	**AT4G17720**	**RNA-binding (RRM/RBD/RNP motifs) family protein**	**139.3**	**143.8**	**164.9**	**149.3**
Bra012645	**A03**	**22959734**	**22961071**	**AT4G17730**	**member of SYP2 Gene Family**	**193.5**	**195.7**	**188.8**	**192.7**
Bra012644	**A03**	**22961454**	**22964005**	**AT4G17740**	**Peptidase S41 family protein**	**102.7**	**112.1**	**126.6**	**113.8**
Bra012643	**A03**	**22965905**	**22967302**	**AT4G17760**	**damaged DNA binding;exodeoxyribonuclease IIIs**	**19.2**	**14.0**	**17.2**	**16.8**

Genes listed in BOLD are expressing in carpel based on Microarray data NASCArrays, and signal from 3 individual slides and those average are shown.

CHAPTER 2

Responses to CO_2 in self-incompatibility of different *Arabidopsis thaliana* accessions

2.1 Introduction

SI is a genetic system to assure cross-fertilization. Yet despite the clear benefits (reviewed by Charlesworth, 2003), the loss of the functioning SI system is very common (Weller and Sakai, 1999). The model plant *Arabiposis thaliana* belongs to the Brassicaceae family and loss-of-function mutations in genes that are required for SI make it a highly self-fertile species with an outcrossing rate less the 1% (Abbott and Gomes, 1989). The evolution from SI-based outcrossing to a self-fertilization system is one of the important transitions in flowering plants. As *Arabidopsis* is widely distributed in Europe, America, Africa and Asia, and over 750 natural accessions have been collected and well studied by researchers around the world, the molecular mechanism of SI and functional polymorphisms at the *S*-locus have been extensively described (Nasrallah *et al*., 2004; Sherman-Broyles *et al*., 2008; Shimizu *et al*., 2008, Guo *et al*., 2011). Recent research shows that a mutation in *SP11/SCR* (hereafter *SCR*) is the first mutation which disrupted SI in *Arabidopsis* (Tsuchimatsu *et al*., 2010). *Arabis alpina* is a distant cousin of *A. thaliana*, which is also self-compatible, possibly because of a mutation in *SCR*, but interestingly, populations in Italy are almost self-sterile and there are variations in the level of SI stability. (Tedder *et al*., 2011).

Transformation of *A. thaliana* with the *S*-locus from *A. lyrata*, an obligate outbreeder that diverged from *A. thaliana* ~5 million years ago (Koch *et al*., 2000), can restore the self-incompatible phenotype in some accessions such as C24, Cvi-0, Kashmir, Shahkdara and Hodja-Obi-Garm, (Nasrallah *et al*., 2002, Boggs *et al*., 2009). A self-incompatible *A. thaliana* in C24 accession (SI-C24) was successfully generated in my laboratory harboring both SRK_b and SCR_b fused in one construct (hereafter SRK_b+SCR_b), and it is known that this SI-C24 line is CO_2 sensitive and has many seeds formed under a high CO_2 condition (Takehisa, 2009). However, there is no information on CO_2-sensitivity in other accessions, thus, it is unclear that whether there is genetic variation in SI response to CO_2 in SI *Arabidopsis*.

Accessions like Mt-0, RLD, No, Nd-0, WS-0, and Col-0, in which both *SRK* and *SCR* are pseudogenized (Kusaba *et al*., 2001) show a pseudo-self-compatible phenotype (i.e. self-fertile in mature flower) after the *S*-locus transformation (Nasrallah *et al*., 2004). But by crossing them to the SI-C24, F_1 hybrids show stable SI, demonstrating that the dominant

nature of self-incompatible phenotype, and that accession C24 harbors dominant functional alleles at SI-modifier loci required for the stable SI (Nasrallah *et al*., 2004, Boggs *et al*., 2009). However no SI-modifier genes have been functionally identified so far. As Col-0 is the reference accession, this SI hybrid could be an ideal material to investigate its CO_2-sensitivity and compare it with that of SI-C24. Meanwhile, I also focused on accession Cvi-0, which lives at an elevation of 1,200 m of the tropical Cape Verde Islands (Lobin 1983), as it has some different response to biotic and abiotic stresses such as several biotic pathogens (Aguilar *et al*., 2002; Perchepied *et al*., 2010), ozone (Rao and Davis, 1999; Brosché *et al*., 2010; Overmyer *et al*., 2003), and UV irradiation (Cooley *et al*., 2001). Moreover, Cvi-0 has an irregular stomatal closure under high CO_2 and low humidity (Monda *et al*., 2011). I generated SI-C24 x Cvi-0 hybrids and investigated the SI stability and its CO_2-sensitivity.

2.2 Materials and methods

2.2.1 Plant materials

All accessions of *Arabidopsis thaliana* (C24, Col-0, Cvi-0) were grown in a growth chamber with 16-hr light and 8-hr dark growth conditions at 22 °C.

2.2.2 F_1 hybrid generation and reciprocal crosses

To prevent self-pollination, stamens were removed at flower stage-13 (mature bud) (Smyth *et al*., 1990) from flower that used as female organ. Between stages 14 and 15, pollen was hand pollinated. Pollen tube visualization was performed as described in 1.2.4, except the softening time in 1 N NaOH was 30 min.

2.2.3 Genomic DNA extraction and genotyping

DNAs extraction was performed as described in 1.2.6. Tail-PCR (Liu *et al*., 1995) was performed to define the insertion site of the insertion site of transgene SRK_b+SCR_b. A T-DNA border-specific primer and a pool of three arbitrary degenerate (AD) primers (AD1, 5′-NGTCGASWGANAWGAA-3′; AD2, 5′-GTNCGASWCANAWGTT-3′; AD3, 5′-WGTG NAGWANCANAGA-3′) were used per round of Tail-PCR cycling. The T-DNA border primers used were as follows: RB1 (5′-TCCAAACGTAAAACGGCTTGTCCCG-3′), RB2 (5′-GGGTCATAACGTGACTCCCTTAATTC-3′), or RB3 (5′-CGCTCATGATCAGATTGT CGTTTCC-3′). Three rounds of Tail-PCR cycling were performed in Applied Biosystems® 9700 thermocycler. The final concentration of the pooled primers AD1, AD2, AD3 were as follows: 5.0/4.0/4.0 μM (primary /secondary/ tertiary round). T-DNA border primers were at a final concentration of 0.2 μM.

Cycling parameters for the primary round were as follows: (1) 94 °C for 1 min and 95 °C for 1 min; (2) 5 cycles of 94 °C for 30 sec, 62 °C for 1 min, and 72 °C for 2.5 min; (3) 94 °C for 30 sec, 25 °C for 3 min (50% ramp), and 72 °C for 2.5 min (32% ramp); (4) 14 cycles of 94 °C for 10 sec, 68 °C for 1 min, 72 °C for 2.5 min, 94 °C for 10 sec, 68 °C for 1 min, 72 °C for 2.5 min, 94 °C for 10 sec, 44 °C for 1 min, and 72 °C for 2.5 min; and (5) 72 °C for 5 min. Cycling parameters for the second round were as follows: (1) 94 °C for 1

min and 95 °C for 1 min; (2) 5 cycles of 94 °C for 10 sec, 64 °C for 1 min, and 72 °C for 2.5 min; (3) 12 cycles of 94 °C for 10 sec, 64 °C for 1 min, 72 °C for 2.5 min, 94 °C for 10 sec, 64 °C for 1 min, 72 °C for 2.5 min, 94 °C for 10 sec, 44 °C for 1 min, and 72 °C for 2.5 min; and (4) 72 °C for 5 min. Cycling parameters for the tertiary round were as follows: (1) 94 °C for 3 min; (2) 20 cycles of 94 °C for 10 sec, 44 °C for 1 min, 72 °C for 2.5 min; and (3) 72 °C for 5 min. ExTaq polymerase was used for all amplifications. The primary Tail reaction contained 10 ng of genomic DNA.

Final amplified DNA fragment was sequenced and the SRK_b+SCR_b insertion was mapped to Chromosome 1, in At1g74020. Primers for insertion genotyping was designed based on this result: right genomic primer, 5'-CAGTACAGTCACGACTTTGGTCG-3'; left genomic primer, 5'-GTCCACCCGTAAAAGAATTCATG-3'; right border primer of the insertion, 5'-CGCTCATGATCAGATTGTCGTTTCC-3' (RB3). PCRs were performed in a 10 μL reaction volume containing 10 ng of template DNA, 1 μM of forward primer and reverse primer, 1x PCR buffer, 1x dNTP, and 0.5 U of ExTaq. Conditions for PCR were as follows: (1) 94 °C for 5 min; (2) 35 cycles of 94 °C for 30 sec, 55 °C for 30 sec, 72 °C for 1.5 min; and (3) 72 °C for 5 min. Amplified DNAs were electrophoresed in a 1.5% agarose gel.

2.2.4 Real-time PCR analysis

RNA was extracted from five stigmas at stage-13 or 14 using Plant RNeasy Mini kit (Qiagen). 10 μL of RNase-free water was used to elute RNA. 1 μL of each RNA sample was used as template. Following primers for SRK_b: forward primer, 5'-TGCTCAGGAGTGA AACAGAAACC-3' and reverse primer, 5'-AGGTGATTTGGTTAACCGTACAG-3'; and for *GAPDH*: forward primer, 5'-GACCTTACTGTCAGACTCGAG-3' and reverse primer, 5'-CGGTGTATCCAAGGATTCCCT-3' were used.

QuantiFast SYBR Green RT-PCR kit was used and real-time analysis was performed with the LightCycler®480 System II (Roche). The real-time PCR was performed in a 10 μL reaction volume containing 1 μL of template RNA, 1 μM of each forward and reverse primer, 1x QuantiFast SYBR Green RT-PCR Master Mix, 0.1 μL QuantiFast RT Mix. Real-time cycler conditions were as follows: reverse transcription at 50 °C for 30 min, PCR initial activation step at 94 °C for 5 min followed by 45 cycles of combined annealing/extension

two-step cycling at 94 °C for 10 sec, 60 °C for 30 sec.

2.2.5 CO_2 treatment for *Arabidopsis*

Whole plants were put into the CO_2 incubator in the morning between 8 and 10 a.m., with the same conditions as in Chapter 1, except the treatment time was 8 hr. CO_2-sensitivity was defined by seed formation.

2.3 Results

2.3.1 SI of *Arabidopsis* hybrids

SI-C24 established in my lab is homozygous for transgenic SRK_b+SCR_b and the insertion site was mapped to the third exon of At1g74020 with the Tail-RCR method. I crossed this SI-C24 with a wild type Col-0. Six F_1 hybrids between SI-C24 and Col-0 showed no significant difference compared to the Col-0 parent except for a delay of flowering. Almost all siliques were full and self-incompatible phenotype could not be confirmed in any SI-C24 x Col-0 hybrids (Fig. 2-1B). My result did not show a consistent result with previous study reporting that C24 has dominant functional alleles to stabilize SI (Nasrallah *et al*., 2004). On the contrary, hybrid with Cvi-0 and SI-C24 showed a very stable SI (Fig. 2-1C).

In order to know whether SRK_b and SCR_b were functional in the SI-C24 x Col-0 hybrid, I performed reciprocal crosses and found that SI was ineffective when SI-C24 x Col-0 hybrid was pollinated with SI-C24 pollen (Fig. 2-2). This result suggests that the SI signaling pathway was disrupted because SRK_b or other downstream components could not work functionally in the SI-C24 x Col-0 hybrid stigma.

2.3.2 SI of F_2 progenies of SI-C24 x Col-0 hybrid

An F_2 population from a randomly chosen self-pollinated SI-C24 x Col-0 hybrid was used to examine whether the self-incompatible phenotype would segregate. Transgenic SRK_b+SCR_b of 56 F_2 individuals were genotyped and the segregation ratio was 9:29:18 (-/-:+/-:+/+) (See Materials and methods 2.2.3). Within the 47 individuals that harboring SRK_b+SCR_b, only two F_2 (#17 and #47) showed partial SI. It is difficult to explain this abnormal segregation ratio without considering other effects such as gene silencing.

2.3.3 *SRK* expression of SI-C24 x Col-0 hybrid and its F_2 progenies

Expression of the SRK_b transgene was analyzed in F_1 hybrid and two homozygous SRK_b+SCR_b F_2 progenies (#59 and #60). Col-0 and C24 wild type plants were used as negative controls. RNA was extracted from stigmas at stage-13 and stage-14. Three replicates were prepared for each RNA sample and the results were analyzed with LightCycler®480 System II (Roche) and

GAPDH was used as an internal control. Relative SRK_b expression was recalculated compared to SRK_b expression in SI-C24 at stage-13. Results were shown in Fig. 2-3. In SI-C24, SRK_b expression at stage-13 was slightly higher than at stage-14, as it is necessary to start SRK_b protein synthesis before pollination. Therefore, SRK_b expression at stage-13 was compared and I found its expression decreased by 80% in F_1. In both F_2 plants, the SRK_b was expressed but the expression level was less than 5% compared to SI-C24. These results suggest that SI breakdown could be caused by the remarkable decrease of SRK_b expression in the SI-C24 x Col-0 hybrid and F_2 progeny, perhaps due to an epigenetic silencing system which may be activated when Col-0 and C24 genomes are crossed and which could be maintained afterward.

2.3.4 CO_2-sensitivity of SI-C24 and Cvi-0 x SI-C24 hybrid

Unlike the SI-C24 x Col-0 hybrid, SI-C24 x Cvi-0 hybrid showed stable and complete SI. This SI-C24 x Cvi-0 hybrid and SI-C24 were then treated with CO_2 to determine whether there is difference in the SI responses to CO_2 in these two lines. Because pollen can be deposited onto self-stigma in *A. thaliana*, hand-pollination was not needed, and the small plants fit into the CO_2 incubator, so the whole plant was treated and seed formation was observed. Although *Arabidopsis* mostly flowers in the morning, there is some variability in timing such that all flowers do not flower at the same time, so treatment was started in the morning (before 10 a.m.) and stopped after eight hours. As shown in Fig. 2-4C, with CO_2 treatment, many long siliques with seeds were formed in SI-C24 (white arrows), and no seeds formed without CO_2 treatment (red arrows). Few seeds were formed and no significant difference could be observed after CO_2 treatment in the SI-C24 x Cvi-0 hybrid (Fig. 2-4B, D), suggesting that there is a genetic variation in different *A. thaliana* accessions; SI-C24 is CO_2-sensitive while its hybrid with Cvi-0 is CO_2-insensitive.

2.3.5 Backcross of SI-C24 x Cvi-0 with C24 wild type and CO_2-sensitivity segregation

Self-incompatible Cvi-0 cannot be generated due to the unsuccessful transformation of Cvi-0. Though I could not compare CO_2-insensitivity of SI Cvi-0 to that of SI-C24 x Cvi-0 hybrid, it could be genes that control the different CO_2-sensitivities in accession C24 and Cvi-0. I backcrossed this hybrid with C24 wild type, and obtained two plants showing CO_2-sensitive

phenotype from six BC_2 (Table 2-1). One of the four CO_2-insensitive BC_2 was then backcrossed again. In BC_3, four CO_2-sensitive and two CO_2-insensitive plants were obtained together with two showing a weaker CO_2-sensitive phenotype with a few seeds (Table 2-1). Again, one of the CO_2-insensitive BC_3 was backcrossed and 15 BC_4 was analyzed (Table 2-1). Six of them showed CO_2-insensitive phenotype, seven showed CO_2-sensitive phenotype and two with weaker CO_2-sensitive phenotype. These are preliminary and more thorough evaluation of more plants is needed to quantify the CO_2-sensitivity, but it is clear that there is phenotype segregation, and the ratio was close to 1:1, suggesting that one dominant gene in Cvi-0 controls the CO2-insensitive phenotype. Other minor factors could be involved, and I hypothesize that after few more backcrossing, NIL lines with CO_2-insensitive phenotype due to a heterozygous responsible gene could be obtained and could be used in responsible gene identification.

2.4 Discussion

SI overcome by CO_2 treatment is a well-known phenomenon in *Brassica*, and it is known that in *A. thaliana*, SI-C24 is CO_2-sensitive. Though the reference line Col-0 is pseudo-self-compatible after *S*-genes transformation, Nasrallah *et al*. (2004) reported that SI-C24 and Col-0 hybrid shows stable SI, and I tried to use this hybrid to investigate the variation of CO_2 response in different *A. thaliana* accessions. However, the result was not reproduced in my experiment, SI-C24 x Col-0 hybrid was self-compatible, and so were the F_2 progenies (Fig. 2-1, 2-2). Instead, my results indicated that the SI was broken down in the hybrid, which may be due to a remarkable decrease of SRK_b gene expression at the mature bud stage (Fig. 2-3).

The *S*-locus in *A. thaliana* has three haplotypes. Col-0 and C24 belong to haplotype A. The structure of the *S*-locus in Col-0 and C24 has been well sequenced and compared (Liu *et al*., 2007). In haplotype A there is a ~1kb inverted repeat region including the *SRK* sequence (Guo *et al*., 2011). It is clear that in *B. rapa,* 24-nt small RNAs can silence *SP11* expression (Tarutani *et al*., 2010). This region may be responsible for small RNA production and the SRK_b gene silencing in SI-C24 x Col-0 hybrid. Further transformation studies using different functional *SRK* sequences are required to prove whether RNAi-induced gene silencing is involved in the loss of SI in the hybrid.

The SI-C24 x Cvi-0 hybrid, on the contrary, had stable SI and differed from SI-C24, its SI could not be overcome by CO_2 treatment (Fig. 2-1C, Fig. 2-4), suggesting that there is genetic variation of CO_2-sensitivity in different *A. thaliana* accessions. In Cvi-0, from the segregation ratio (Table 2-1), one major dominant gene together with some minor responsible genes seem to control its low CO_2-sensitivity phenotype. In order to identify this major responsible gene, I used the backcross method to transfer the responsible Cvi-0 allele to the C24 background, and this line could be subjected to a next generation sequencer to identify the responsible gene.

Interestingly, recent research showed that Cvi-0 has irregular stomatal movements with a constitutive stomatal opening when treated with high CO_2 (Monda *et al*., 2011). It is known that stomatal pores regulate the flow of gas in and out of plants. A pair of guard cells forms

these pores and they respond to environmental signals such that increased CO_2 typically stimulates stomatal closure (Assmann, 1993). The recent model of this CO_2-regulated stomatal closure is shown in Fig. 2-5. HT1 (high leaf temperature 1) is the first functionally and molecularly isolated protein kinase that mediates CO_2-induced stomatal movements. It acts as a negative regulator of the CO_2 response pathway (Hashimoto *et al*., 2006). β-carbonic anhydrase 1 and 4 catalyzing the reversible reaction of $CO_2+H_2O \Leftrightarrow HCO_3^- + H^+$ function early in the CO_2 signaling pathway, at downstream of HT1 (Hu *et al*., 2009). Anion channel SLAC1 (slow anion channel-associated 1) is activated in high CO_2 condition, resulting in the efflux of anions such as Cl^- and NO_3^- to decrease the osmotic pressure in the guard cells (Negi *et al*., 2008; Vahisalu *et al*., 2008). Water then flows out of the guard cells to close the stomatal pores. OST1 (open stomata kinase 1) was originally identified as a mediator in ABA signal transduction (Mustilli *et al*., 2002). Studies have shown that OST1 can activate SLAC1 (Lee *et al*., 2009; Vahisalu *et al*., 2010) and OST1 loss-of-function mutant also shows strong impaired CO_2-induced stomatal closing (Xue *et al*., 2011), indicating its involvement in the CO_2 response pathway. I have noticed there is some similarity between this CO_2-induced stomatal closure and CO_2-induced SI breakdown, as in both pathways, water is transported out from cells in a high CO_2 condition. Cvi-0 plants are CO_2-insensitive in its stomatal movement and CO_2-insensitive in SI breakdown as well. Cvi-0 has irregular anion homeostasis, which could explain the constitutive stomatal opening under high CO_2 condition (Monda *et al*., 2011) but the molecular mechanisms are still unclear and further work is expected to provide new insights into these two pathways and possible relationships between them.

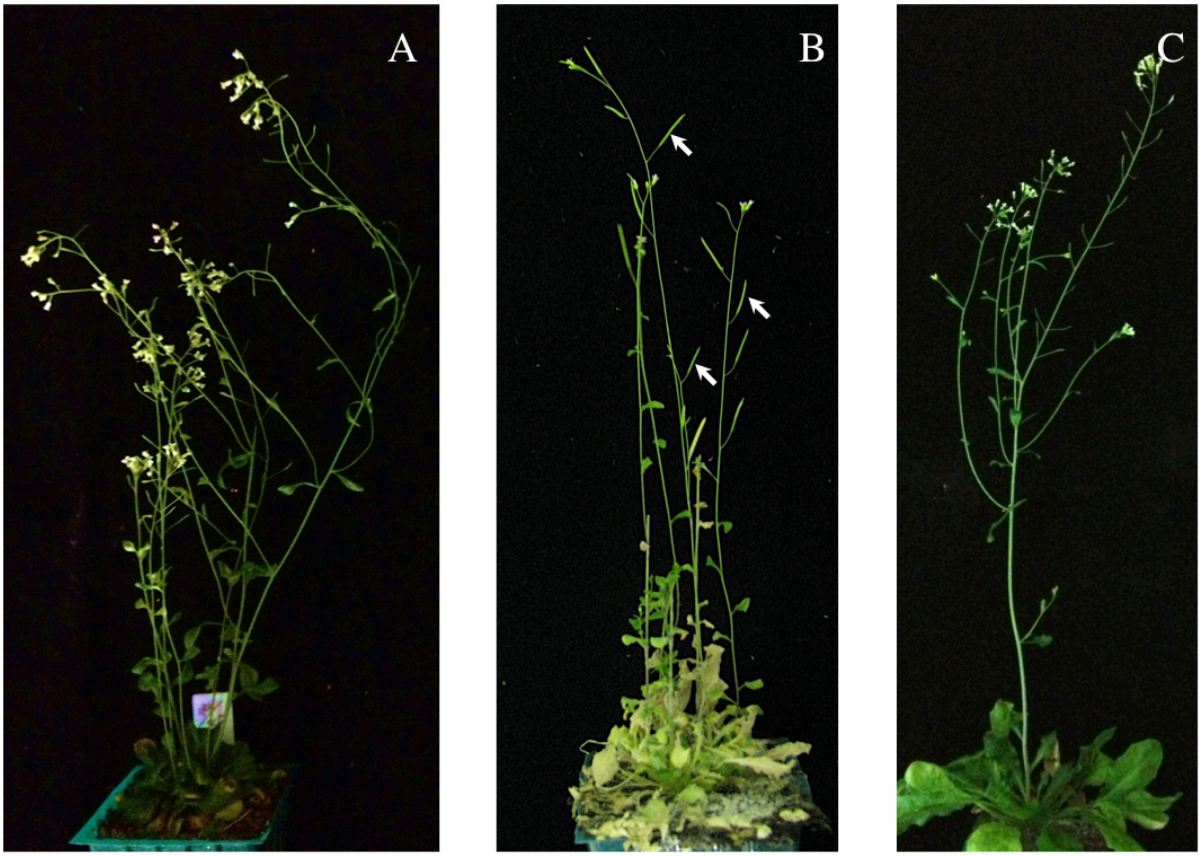

Fig. 2-1. Phenotype of transgenic plants *A. thaliana*

C24 accession habouring SRK_b and SCR_b (SI-C24) (A); F_1 hybrids with accession Col-0, siliques full with seeds are formed (arrows) (B); F_1 hybrids with accession Cvi-0 (C).

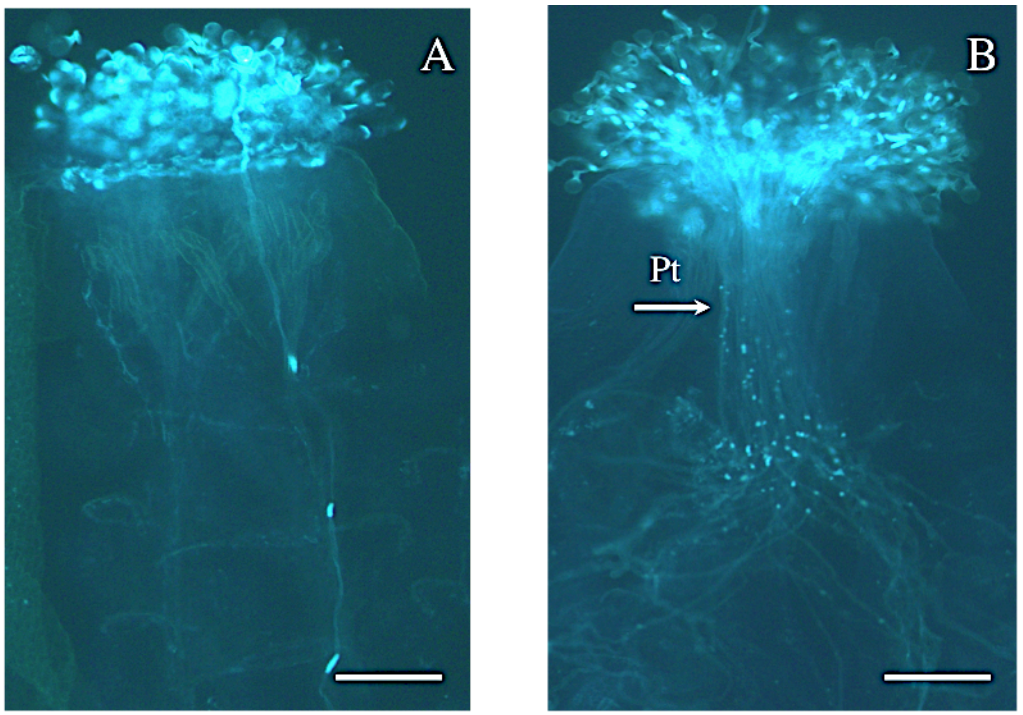

♀SI-C24 x ♂ SI-C24 x Col-0 hybrid ♀SI-C24 x Col-0 hybrid x ♂SI-C24

Fig. 2-2. Reciprocal crosses with SI-C24 and SI-C24 x Col-0 hybrid

SI-C24 x Col-0 hybrid pollen grains are rejected on SI-C24 pistil (A); SI-C24 pollen grains are germinated and penetrated into stigma of SI-C24 x Col-0 hybrid pistil (B). Pt, Pollen tubes.

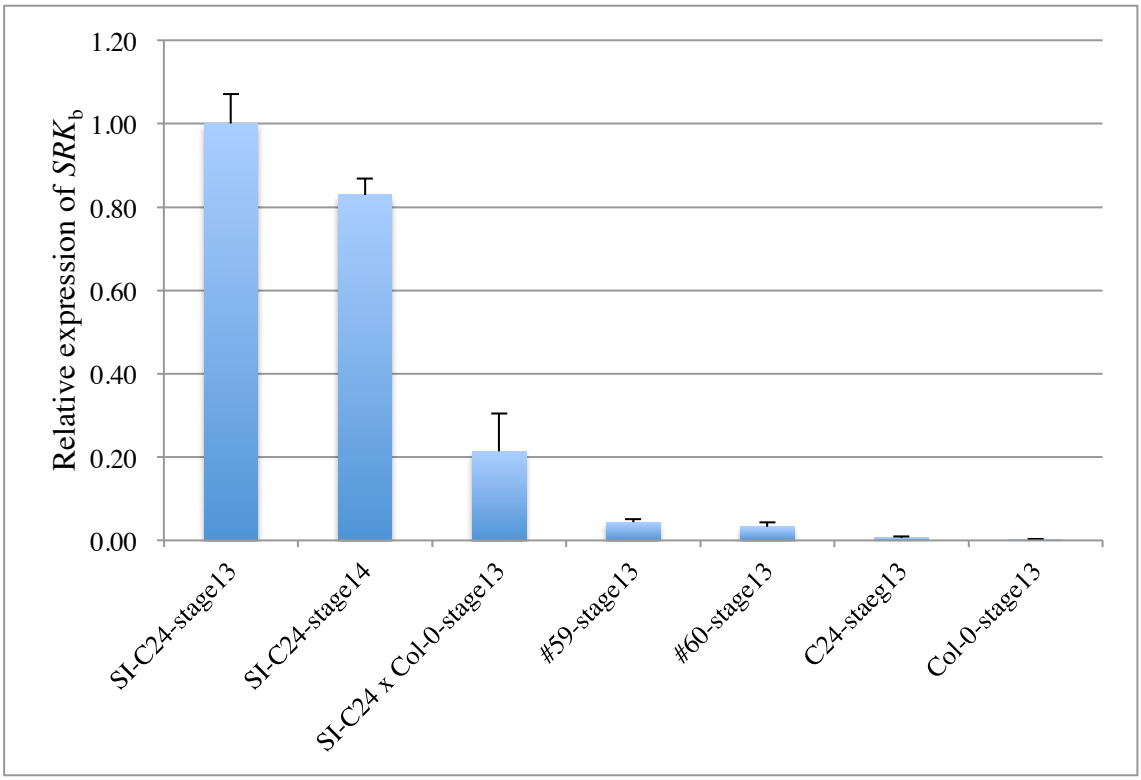

Fig. 2-4. *SRK*$_b$ expression in SI-C24 x Col-0 hybrid and its F_2

In SI-C24, *SRK*$_b$ is expressed in stage-13 and 14, and the expression is higher in stage-13. *SRK*$_b$ expression in SI-C24 x Col-0 hybrid decreases by ca. 80% compared to SI-C24, and in two F_2 individuals (#59 and # 60), its expression level is lower than 5% compared to SI-C24.

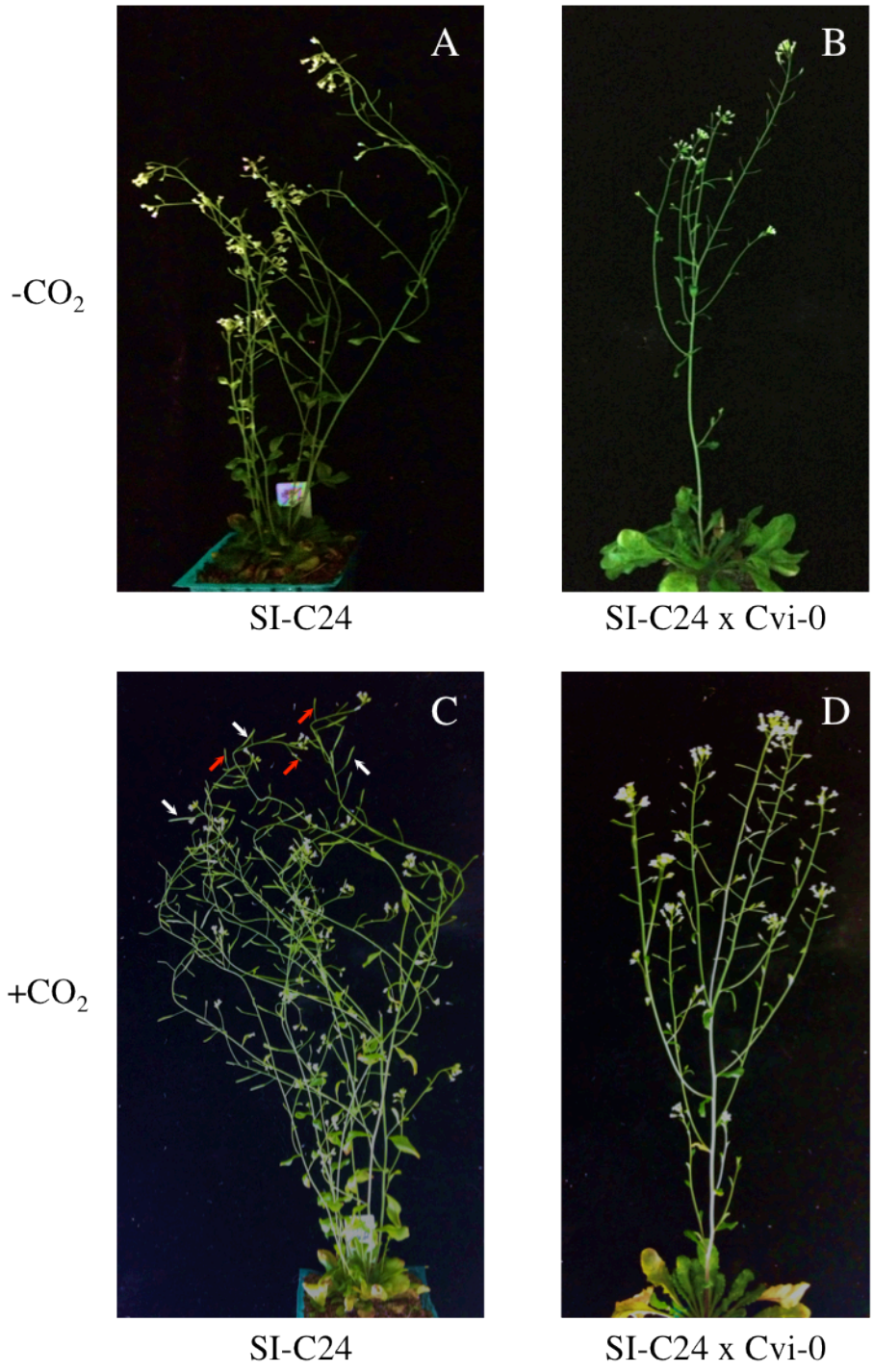

Fig. 2-5. CO_2-sensitivity phenotype in SI-C24 and SI-C24 x Cvi-0 hybrid

SI-C24 and SI-C24 x Cvi-0 hybrid before CO_2 treatment (A, B) and one week after CO_2 treatment (C, D). SI breakdown occurred and many siliques with seeds are observed in SI-C24 (C, white arrows), flowers that flowered after the treatment remain SI (C, red arrows). No significant difference is observed in SI-C24 x Cvi-0 hybrid (B, D).

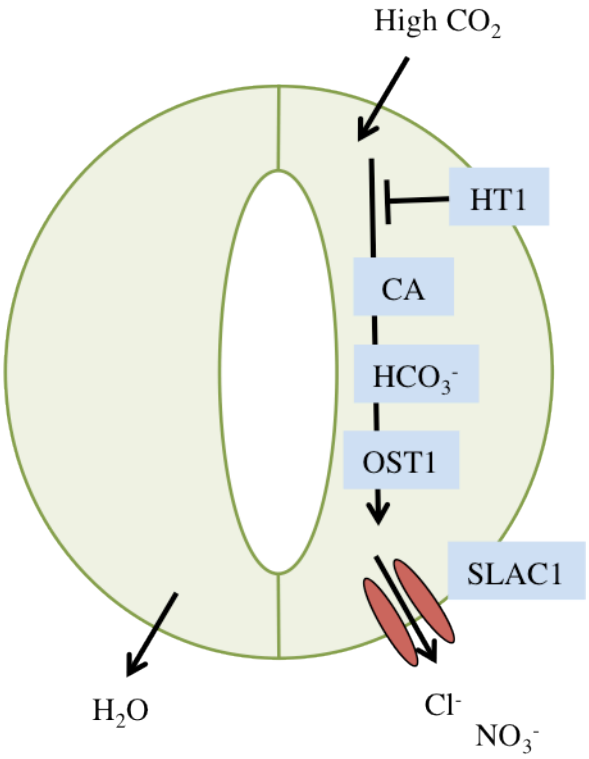

Fig. 2-6. Model for the CO_2-induced stomatal movements (Xue *et al*., 2011 modified)

HT1 (high leaf temperature 1) works as a negatively regulator, βCA (carbonic anhydrase) and OST1 (open stomata kinase 1) work downstream to activate SLAC1 (slow anion channel-associated 1), resulting the efflux of anions like Cl^- and NO_3^-. Decreased osmatic pressure inside the guard cells result in water flows out of the guard cells to close the stomata pore.

Table 2-1. CO_2-suscepibility of backcrossed plants from SI-C24 x Cvi-0

BC_n	SI overcome	Weak overcome	No overcome
BC_2	2	0	4
BC_3	4	2	2
BC_4	7	2	6

CHAPTER 3

Mutant screening of downstream components of SI pathway

3.1 Introduction

To understand CO_2-sensitivity and SI breakdown system in the Brassicaceae, it would be helpful to have a SI pathway in detail. However, although the SI mechanism has been deeply studied for many years, still, little is known about the downstream pathway triggered by the SRK-SP11/SCR binding.

Mutation induction is a powerful tool for the analysis of signal transduction. Mutagens such as ethyl methane sulfonate (EMS), X-rays and γ-rays are especially popular in plant science to discovery and identify many novel genes. Recently, heavy-ion mutagenesis has been accepted as a new powerful technology to generate mutants, especially in higher plants. Heavy-ion beams have high linear energy transfer (LET), and based on radiobiological considerations, high-LET irradiation causes large structural rearrangements (deletions/insertions, translocations, or inversions) due to double-strand breaks whose damaged ends are difficult to be repaired (Hagen, 1994; Ward, 1994). LET-dependent effects of heavy-ion beams have been studied in *Arabidopsis thaliana* with different kind of ions. A LET of 30 keV/μm was the most effective for inducing mutants in the M_2 generation from dry seeds of *A. thaliana* and C ions with LET_{max} showed high mutation efficiency and predominantly induced null mutations like base substitutions (SNP) or small deletions/insertions (Kazama *et al*., 2008; 2011). With the well-developed databases and other genetic resources of *A. thaliana*, it is believed heavy-ion mutagenesis could be benefit for forward genetic approach, combined with next-generation sequencing technologies to identify causal genes responsible for phenotypes of interest.

After the successfully restore the SI in *A. thaliana*, it is believed that this model plant could be used in gene identification with forward genetic approaches such as mutant screening. To search components involved in SI signaling, I performed a mutant screen using the heavy-ion beams treated SI-C24 seeds. I obtained one candidate line showing stable self-compatible phenotype, and analyzed the fundamental characteristics of this mutant.

3.2 Materials and methods

3.2.1 Plant materials

Arabidopsis thaliana (C24) was grown in a growth chamber with the same condition as mentioned in Chapter 2.

3.2.2 Heavy-ion beam and mutant screening

Dry seeds from SI-C24 were sent to RIKEN RI Beam Factory for treatment. They were irradiated with $^{12}C^{6+}$ ion with a dose of 400 Gy. Ion was accelerated up to 1.62 GeV, and the LET was 30 keV/μm. After irradiation, seeds were germinated on MS-medium and transplanted to soil after three weeks. Self-incompatible M_1 plants were treated with dry ice in a closed container overnight to obtained self-pollinated seeds. M_2 seeds were harvested separately from each M_1 plant. These seeds were sown on soil directly after being soaked in a germination aid solution for four days and transferred to the growth chamber. Plants displaying wild-type morphologies were selected as candidate mutants and were backcrossed to wild type C24 plants to analyze genetic characteristics such as the penetrance rate of phenotypes and mode of inheritance.

3.2.3 Library preparation for genome sequencing

After nuclear fractions were prepared using the 'Semi-pure Preparation of Nuclei Procedures' of the CelLytic PN Isolation/Extraction Kit (Sigma-Aldrich), genomic DNA was isolated using Plant DNeasy Mini kit (Qiagen). Isolated genomic DNA was sheared using Covaris S2 (Covaris) at 400 bp setting. Microfluidic chip electrophoresis on an Agilent 2100 Bioanalyzer (DNA High sensitivity kit; Agilent) indicated that Covaris S2 shearing produced a broad peak from 200 to 800 bp.

Library preparation for paired-end sequencing from sheared DNAs was performed using Paired-End DNA Sample Preparation Kit (Illumina). "A" base addition and ligation of adapters were performed according to the protocol developed by Illumina for preparing DNA samples for paired-end sequencing. Briefly, DNAs were end repaired for 30 min at 20 °C in a total volume of 100 μL of 1 x T4 DNA ligase buffer with 10 mM ATP, 4 μL 10 mM dNTP

mix, 5 μL T4 DNA polymerase, 1 μL Klenow enzyme, and 5 μL T4 PNK. After incubation, DNAs were purified with a QIAquick PCR Purification Kit (Qiagen) and eluted with 32 μL EB buffer (Qiagen). "A" bases then were added to the 3′ ends of blunt-ended DNA fragments. DNAs were incubated at 37 °C for 30 min in 1x Klenow buffer, 10 μL 1 mM dATP and 3 μL Klenow exo (3′ to 5′ exo minus). After incubation, DNAs were purified with a QIAquick MinElute Purification Kit (Qiagen) and eluted with 10 μL EB buffer (Qiagen). Illumina PE adapters then were ligated to DNA fragments at 20 °C for 15 min in a total volume of 50 μL reaction containing 1x DNA ligase buffer, 1 μL PE adapter oligo mix and 5 μL DNA ligase. After incubation, DNAs were purified with a QIAquick PCR Purification kit (Qiagen) and eluted with 30 μL EB buffer (Qiagen). Ligated DNAs then were loaded on a 10000-fold diluted SYBR Safe (Invitrogen) contained 2% low range ultra agarose gel (Bio-rad) in the presence of low molecular weight DNA ladder (New England Biolabs) for size selection. After running the gel for 40 min, a 400-500 bp DNA smear was cut out and purified with the QIAquick Gel Extraction kit (Qiagen). DNA was eluted with 30 μL EB buffer (Qiagen). After ligation of Illumina adapters and gel-based size selection of the 400-500 bp ligated DNA fragments, a PCR amplification step was performed in a 50 μL reaction with 10 μL of size-selected DNA, Paired-End (PE) PCR primer 1.0 and 2.0 and 1 x Phusion DNA Polymerase (Finnzymes Oy). PCR conditions were: 30 sec at 98°C, followed by 20 rounds of 10 sec at 98 °C, 30 sec at 65 °C, 30 sec at 72 °C, and a final extension step of 5 min at 72 °C. After PCR enrichment, DNAs were purified with a QIAquick PCR Purification Kit (Qiagen) then subjected to a second round of gel-based size selection using conditions similar to the ones described above. After microfluidic chip electrophoresis, libraries were confirmed containing a narrow range of DNA fragments at about 400-500 bp which were diluted to 10 nM after absolute quantification using KAPA library quantification kit (KAPA Biosystems).

3.2.4 Deep-sequencing using Illumina technologies and output of structural variations

Prepared libraries were deep-sequenced using an Illumina Genome Analyzer IIx. One 8-lane paired-end flow cell was used (three lanes were used for SI-C24, two lanes were used for wild type C24 and mutant, receptively; and one for positive control). 35 bp x 2 sequencing was carried out and Avadis NGS v.1.3.1 (Strand Life Sciences) was used for data analysis.

3.3 Results

3.3.1 Mutant candidate screening

For a better understanding of the downstream pathway of SI that may be involved in CO_2-sensitivity, a mutant candidate screening was performed using heavy-ion beam treatment of a SI-C24 seed pool (Fig. 3-1). M_2 seeds were collected from each individual M_1 line and 20 of each M_2 plant was grown for phenotype observation. A total of 250 M_1 lines were screened and one candidate with a self-compatible phenotype was obtained (M_2-#9) (Fig. 3-2A).

3.3.2 Phenotypic analysis of the self-compatible mutant line

F_1 plants obtained by crossing M2-#9 with a wild-type C24 plant (BC_1F_1) showed a self-incompatible phenotype (Fig. 3-2B), indicating that the SI transgenes (*SRK*$_b$+*SCR*$_b$) remain functional after the heavy-ion beam treatment, and that the mutated gene(s) was recessive.

Reciprocal crosses were then carried out to investigate the organ whose function was affected by the mutation. When SI-C24 pistil was pollinated with the mutant line, the mutant pollen was rejected from SI-C24 stigma, but when the mutant pistil was pollinated with SI-C24 pollen, the SI-C24 pollen could penetrate into the mutant pistil (Fig. 3-2C, D). This result indicates that the mutated gene(s) is responsible for the SI function in the femele organ.

For further identification of the gene(s), it is important to know whether this self-compatible phenotype is controlled by a single gene or multiple genes. To investigate the segregation ratio, self-pollinated seeds were obtained from several BC_1F_1 using CO_2 treatment (mixed population). The *SRK*$_b$+*SCR*$_b$ transgene contains a kanamycin-resistance gene, so seeds were germinated on a plate with kanamycin and 336 plants (BC_1F_2) were selected. Among these BC_1F_2, 56 individuals showed complete self-compatible phenotype, giving a ratio of self-compatibility: self-incompatibility (SC:SI)=1:5. However, it is difficult to provide a proper explanation for this ratio. I examined the segregation again with a BC_2F_2 population. I randomly chose a self-compatible BC_1F_2 progeny and backcross it with wild type C24. The BC_2F_1 again showed stable self-incompatible phenotype and then one BC_2F_1 plant was chosen to generate a BC_2F_2 population after CO_2 treatment. From this F_2 population

that derived from one F_1, I obtained a SC:SI=15:42 (1:3) ratio, suggesting that self-compatible phenotype of this population could be caused by a single gene mutation.

3.3.3 Paired-end sequencing

The 56 individuals with self-compatible phenotype from BC_1F_2 population were collected and genomic DNA was isolated from a pool of them. Genomic DNAs of SI-C24 and C24 wild type were extracted as well. These samples were then deep-sequenced using an Illumina Genome Analyzer IIx. Avadis NGS v.1.3.1 was used for data analysis.

The crude sequences obtained were aligned to the public data of the reference Col-0 genome (TAIR10). The conditions achieved are showed in Table 3-1. The coverage range was from 15x to 45x. All mapped reads were used in large structural variants (SV) and single-nucleotide polymorphism (SNP) analysis. With the SV analysis, deletions, insertions, inversions, translocations, inverted translocations were detected from SI-C24, C24 wild type and M_2-#9 mutant. Because the mutation was recessive, all heterozygous SVs were removed and then SVs only detected in mutant line was extracted. 64 genes that had deletion, 490 genes that had insertion, 5569 genes that had inversion, 1363 genes that had translocation and 67 genes that had inverted translocation were extracted (translocation and inverted translocation include inter-chromosomal translocation and intra-chromosomal translocation), and neither the SNP analysis could show a SNP enrichment region and single out the candidate gene.

3.4 Discussion

To discover novel downstream components involved in the SI signaling pathway, both forward and reverse genetic approaches currently underway in my laboratory. In this chapter, I performed a mutant screening from a heavy-ion beam treated SI-C24 seed pool.

For the treatment, dry seeds of SI-C24 were sent to RIKEN and the mutation induction was performed using C ion with LET_{max} (30keV/μm). With this condition, the irradiation can give high mutation efficiency and predominantly induced base substitutions or small deletion/insertions, which could be determined by single-nucleotide polymorphism (SNP) detection systems (Kazama *et al*., 2011).

One line, M_2-#9, was obtained from 250 M_1 lines. I backcrossed it with the wild type C24 and the completely restored SI of BC_1F_1 confirmed the functionality of the transgenic *S*-locus genes (Fig. 3-1). A genomic DNA pool from all segregated self-compatible BC_1F_2 was subjected to Illumina Genome Analyzer IIx for the paired-end sequencing. Unlike G/C-to-A/T transitions in EMS, heavy-ion mutagenesis can induce a broad range of mutations including insertion/deletions, inversions and translocations (Shikazono *et al*., 2005; Kazama *et al*., 2011), both SV and SNP analysis were performed, however, from the sequencing data, gene responsible for the mutant phenotype could not be singled out. As the segregation ratio is an important factor in this identification process, and the ratio of the BC_1F_2 population was abnormal (SC:SI=1:5), I did the backcross again to generate a BC_2F_2 population derived from single F_1. I obtained SC:SI =15:42 (1:3) ratio, indicating that the self-compatible phenotype is controlled by a single gene with no linkage relationship with inserted *S* genes, and possibly, there could be some other random mutations were removed with backcrossing, which directly or indirectly effect the segregation ratio in the mixed BC_1F_2 population. Therefore, gene identification using segregants of BC_2F_2 or BC_3F_2 derived from one self-pollinated plant would possibly generate a smaller and candidates list or reduce the noise for a clear SNP enrichment region from the sequence data. It seems that reducing the false positive from the sequencing data could be an important step to reduce the candidate numbers and identify the casual gene. Another possible way is combined the sequence data with the mapping approach using mutant line and accession Cvi-0, as the hybrid shows a stable self-incompatible

phenotype that I mentioned in Chapter 2, and the gene identification could possibly lead to a novel SI involved component discovery.

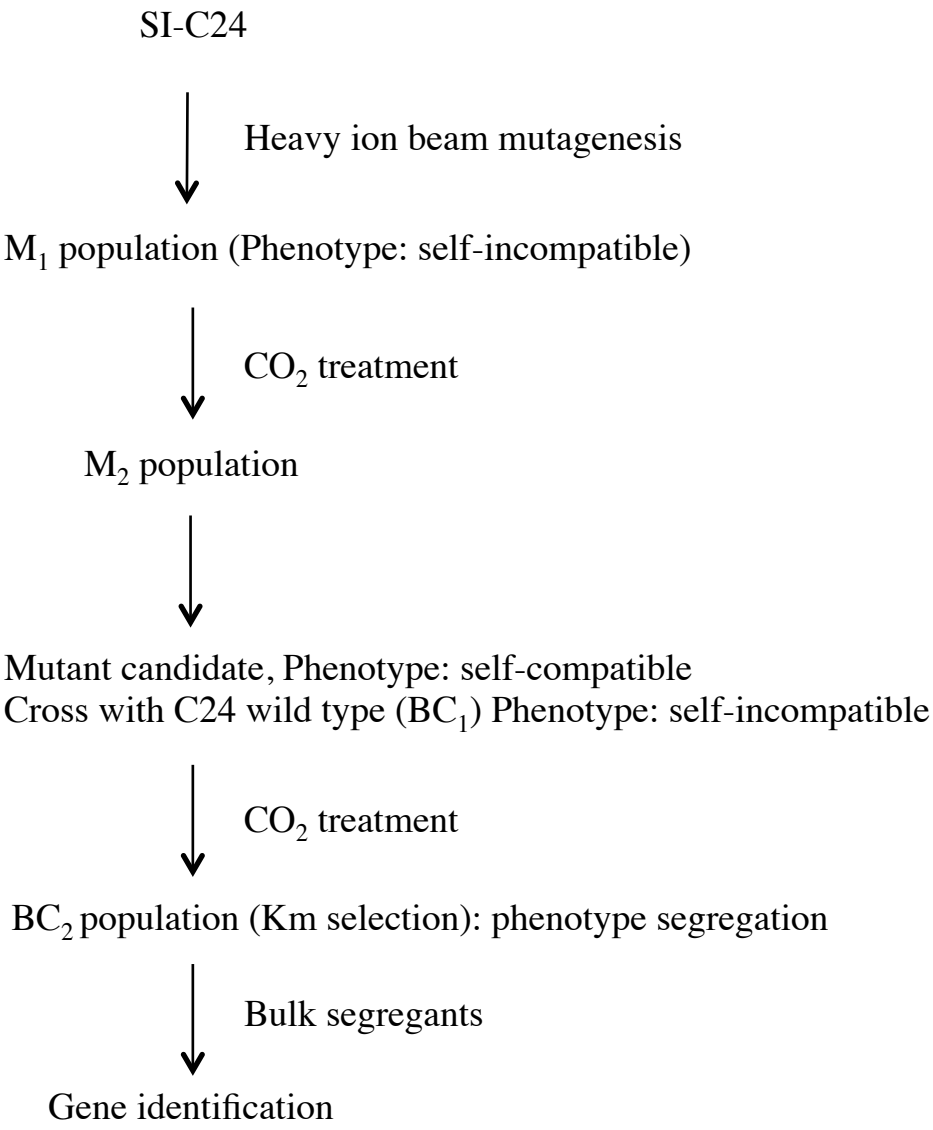

Fig. 3-1. Methodology of mutant screening for the downstream component involved in SI signaling pathway.

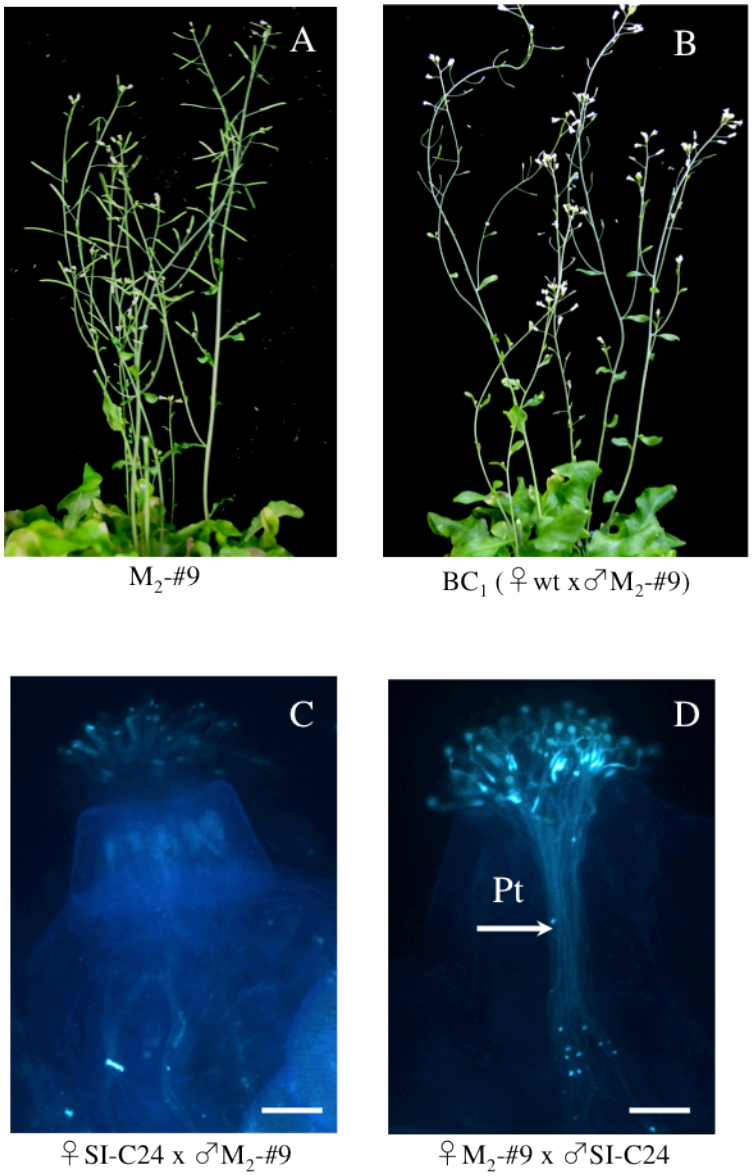

Fig. 3-2. Mutant candidate phenotype and Reciprocal crosses

Mutant candidate (M_2-#9) shows a self-compatible phenotype (A), which can be completely restored after a cross with C24 wild type (B). When M_2-#9 pollen is pollinated to SI-C24, SI reaction occurs and mutant pollen is rejected at SI-C24 stigma (C), when mutant line is pollinated with SI-C24 pollen, pollen grains germinate and penetrate (D). Pt, pollen tubes.

Table 3-1. Summary of the achieved conditions from PE sequencing

Sample	Chromosome	Total no. of bases	Mean coverage
SI-C24	Chr1	823,039,910	27.0
	Chr2	829,637,970	42.1
	Chr3	1,076,787,635	45.9
	Chr4	654,497,305	35.2
	Chr5	849,423,610	31.5
wild type	Chr1	454,960,135	15.0
	Chr2	447,468,315	22.7
	Chr3	608,441,260	25.9
	Chr4	363,736,975	19.6
	Chr5	465,393,495	17.3
M_2-#9	Chr1	450,634,030	14.8
	Chr2	477,490,090	24.2
	Chr3	609,558,740	26.0
	Chr4	363,264,055	19.5
	Chr5	465,380,895	17.3

Conclusion

SI of the Brassicaceae family can be overcome by a CO_2 gas treatment. This method is very useful in obtaining inbred seeds for breeding; however, the molecular mechanism has not been elucidated for over 40 years.

In this study, I focused on *B. rapa* and *A. thaliana* to obtain new insights into the mechanism of CO_2-induced SI breakdown. In Chapter 1, with cryo-SEM observation and X-ray analysis, I observed a high Ca accumulation on self-pollinated CO_2-sensitive papilla surface after CO_2 treatment, as well as Ca^{2+} exporting to self-pollen which was hydrated with CO_2 treatment. My results indicate that CO_2 treatment could activate a certain self-compatible pathway-like cascade to release Ca^{2+} from papilla cell and overcome SI. From the genetic analysis, CO_2-sensitivity could be controlled by more than one responsible gene and I successfully identified two major QTL (*BrSIO1* and *2*) controlling the high CO_2-sensitivity phenotype. Though further genetic analysis is needed to narrow down the responsible genes, because these QTL are independent with SI-stability-related loci, my results could be useful for the marker-assisted selection (MAS) of parental lines with both characteristics of stable SI and high CO_2-sensitivity in breeding. In Chapter 2, I found different CO_2-sensitivities exist in different accessions of *A. thaliana*. SI-C24 could be overcome by CO_2 treatment but SI-C24 x Cvi-0 hybrid showed low CO_2-sensitivity. SI-C24 x Cvi-0 was backcrossed with C24 wild type and the progenies showed a close to 1:1 (CO_2-insensitive: CO_2-sensitive) segregation ratio, suggesting that there could be a major gene controlling the CO_2-sensitivity. A NIL harboring a heterozygous gene from Cvi-0 in C24 background could be used to identify the responsible gene.

At the same time, in Chapter 3, I obtained a mutant line (M_2-#9) with self-compatible phenotype from the heavy-ion beam treated SI-C24 pool. This line could be used in physiological studies such as Ca^{2+} dynamics and it would provide us new insight into the SI pathway when the responsible gene could be finally identified.

Acknowledgments

I would like to give an extremely warm and heartfelt thank you to my supervisor, Prof. Seiji Takayama, who provided me with full training in doing science during these four years.

I thank Dr. Satoshi Niikura for providing seeds of *B. rapa,* and Dr. Keita Suwabe for his help and advices with linkage map construction and QTL analysis. I thank Dr. Tomoko Abe and Dr. Yusuke Kazama for heavy-ion beam mutagenesis in *A. thaliana* and Dr. Tetsuya Kurata and Dr. Tomoaki Sakamoto for the Illumina deep-sequencing and data analysis. I thank current and former lab staff, especially Ass. Prof. Megumi Iwano and Dr. Mitsuru Kakita (now postdoc in NIBB) for their guidance and insightful discussions. I thank Rina Nagai, Yuko Yoshimura, Toshie Ryokume, Momoko Okamura, Hitomi Ishikawa and Mana Abe for their excellent technical assistances and help. I also express my appreciation to my committee members, Prof. Takashi Hashimoto and Prof. Masaaki Umeda, for their time and constructive comments.

Many thanks to Tong Niu, Shuo Zhang, Tamaki Furuichi, Yukari Gobara, Seiko Fukushima, Haruka Saito, Takahiro Hiramatsu, Kosuke Matsuura, Kosei Tsukahara, Kazuko Toki, Kanae Ito, Kie Kajihara, Sayuri Hino, Tomomi Kotoku, Dr. Cecilia Hung, Maliha Masroor Hilaly, Yoshito Ogawa, Shigeyuki Ota, Ikushisa Nishida, Maximilian Krichenbauer, Keigo Sasaki, Tomoya Hioki, Zobaer MD Hasan and Dr. Yuichi Imura, for being with me went through all the happiness and difficulties; through thick and thin. Their priceless friendship supported me to finish this thesis.

I am grateful to all staff in International Student Affair in NAIST for their supports of my study in Japan.

Last but not least, special thanks to my dearest family, my aunt Akane Kitamura and my lovely cousins Kohaku, Sumie and Keika, with their love that I could survive graduate school.

References

Abbott, R. J., and Gomes, M. F. (1989). Population genetic structure and outcrossing rate of *Arabidopsis thaliana* (L.) Heynh. Heredity 62, 411-418.

Aneja, M., and Gianfagna, T. (1994). Carbon dioxide treatment partially overcomes self-incompatibility in a Cacao genotype. HortScience 29, 15-17.

Aguilar, I., Alamillo J. M., García-Olmedo, F., and Rodríguez-Palenzuela, P. (2002). Natural variability in the Arabidopsis response to infection with *Erwinia carotovora* subsp. *carotovora*. Planta 215, 205-209.

Ajisaka, H., Kuginuki, Y., Yui, S., Enomoto, S., and Hirai, M. (2001). Identification and mapping of a quantitative trait locus controlling extreme late bolting in Chinese cabbage (*Brassica rapa* L. ssp. *pekinensis* syn. *campestris* L.) using bulked segregant analysis: A QTL controlling extreme late bolting in Chinese cabbage. Euphytica. 118, 75-81.

Assmann, S. M. (1993). Signal transduction in guard cells. Annu. Rev. Cell Biol. 9, 345-375.

Black, M., and Charlwood, B. (1995). The physiology and biochemistry of plant cell walls. (Chapman & Hall, London).

Brewbaker, J.L., and Kwack, B.H. (1963). The essential role of calcium ion in pollen germination and pollen tube growth. Am J Bot. 50, 859-865.

Boggs, N. A., Nasrallah, J. B., and Nasrallah, M. E. (2009). Independent *S*-locus mutations caused self-fertility in *Arabidopsis thaliana*. PLoS Genet. 5, e1000426.

Brosché, M., Merilo, E., Mayer, F., Pechter, P., Puzõrjova, I., Brader, G., Kangasjärvi, J., and Kollist, H. (2010). Natural variation in ozone sensitivity among *Arabidopsis thaliana* accessions and its relation to stomatal conductance. Plant Cell Environ. 33, 914-925.

Charlesworth, D. (2003). Effects of inbreeding on the genetic diversity of populations. Philosophical Transactions of the Royal Society of London Series B – Biological Sciences 358, 1051-1070.

Cheng, F., Liu, S., Wu, J., Fang, L., Sun, S., Liu, B., Li, P., Hua, W., and Wang, X. (2011). BRAD, the genetics and genomics database for Brassica plants. BMC Plant Biol. 11, 136.

Choi, S. R., Teakle, G. R., Plaha, P., Kim, J. H., Allender, C. J., Beynon, E., Piao, Z. Y., Soengas, P., Han, T. H., King, G. J., Barker, G. C., Hand, P., Lydiate, D. J., Batley, J., Edwards, D., Koo, D. H., Bang, J. W., Park, B. S., and Lim, Y. P. (2007). The reference genetic linkage map for the multinational *Brassica rapa* genome sequencing project. Theor. Appl. Genet. 115, 777-792.

de Nattancourt, D. (2001). Incompatibility and incongruity in wild and cultivated plants, 2nd edition. Springrt-Verlag, Berlin Herdelberg New York.

Dhaliwal, A. S., Malik, C. P., and Singh, M. B. (1981). Overcoming incompatibility in *Brassica campestris* L. by carbon dioxide, and dark fixation of the gas by self- and cross-pollinated pistils. Ann. Bot. 48, 227-233.

Eisen, M. B., Spellman, P. T., Brown, P. O, and Botstein, D. (1998). Cluster analysis and display of genome-wide expression patterns. Proc. Natl. Acad. Sci. USA 95, 14863-14868.

Elleman, C. J., and Dickinson, H. G. (1986). Pollen stigma interactions in *Brassica*. IV. Structural reorganization in the pollen grains during hydration. J. Cell. Sci. 80, 141-157.

Elleman, C. J., and Dickinson, H. G. (1990). The role of the exine coating in pollen-stigma interactions in *Brassica oleracea* L. New Phytol. 114, 511-518.

Elleman, C. J., Franklin, T. V., and Dickinson, H. G. (1992). Pollination in species with dry stigmas: The nature of the early stigmatic response and the pathway taken by pollen tubes. New Phytol. 121, 413-424.

Ge, Y., Ramchiary, N., Wang, T., Liang, C., Wang, N., Wang, Z., Choi, S. R., Lim, Y. P., and Piao, Z. Y. (2011). Development and linkage mapping of unigene-derived microsatellite markers in *Brassica rapa* L. Breed. Sci. 61, 160-167.

Gu, T., Mazzurco, M., Sulaman, W., Matias, D. D., and Goring, D. R. (1998). Binding of an arm repeat protein to the kinase domain of the *S*-locus receptor kinase. Proc. Natl. Acad. Sci. USA 95, 382-387.

Guo, Y. L., Zhao, X., Lanz, C., and Weigel, D. (2011). Evolution of the S-Locus Region in Arabidopsis Relatives. Plant Physiol. 157, 937-946.

Hagen, H. (1994). Mechanisms of induction and repair of DNA double-strand breaks by ionizing radiation: Some contradictions. Radiat. Environ. Biophys. 33, 45-61.

Hashimoto, M., Negi, J., Young, J., Israelsson, M., Schroeder, J. I., and Iba, K. (2006). *Arabidopsis* HT1 kinase controls stomatal movements in response to CO_2. Nat. Cell Biol. 8, 391-397.

Hatakeyama, K., Horisaki, A., Niikura, S., Narusaka, Y., Abe, H., Yoshiaki, H., Ishida, M., Fukuoka, H., and Matsumoto, S. (2010). Mapping of quantitative trait loci for high level of self-incompatibility in *Brassica rapa* L. Genome 53, 257-265.

Hepler, P. K., and Winship, L. J. (2010). Calcium at the cell wall-cytoplast interface. J. Integr. Plant Biol. 52, 147-160.

Horisaki, A., and Niikura, S. (2008). Developmental and environmental factors affecting level of self-incompatibility response in *Brassica rapa* L. Sex. Plant Reprod. 21, 123-132.

Hu, H., Boisson-Dernier, A., Israelsson-Nordstrom, M., Bohmer, M., Xue, S., Ries, A., Godoski, J., Kuhn, J. M., and Schroeder, J. I. (2010). Carbonic anhydrases are upstream regulators of CO_2-controlled stomatal movements in guard cells. Nat. Cell Biol. 12, 87-93.

Hyun, J. Y., Gothandam, K. M., Baek, N. K., Wang, G., and Chung, Y. Y. (2007). Dominance relationship between two self-incompatible *Brassica campestris* haplotypes in response to CO_2 gas. J. Plant Biol. 50, 161-166.

Iwano, M., Wada, M., Morita, Y., Shiba, H., Takayama, and S., Isoga, A. (1999). X-ray microanalysis of papillar cells and pollen grains in the pollination process in *Brassica* using a variable-pressure scanning electron microscope. J. Electron. Microsc. 48, 909-917.

Kakita, M., Murase, K., Iwano, M., Matsumoto, T., Watanabe, M., Shiba, H., Isogai, A., and Takayama, S. (2007). Two distinct forms of MLPK localize to the plasma membrane and interact directly with SRK to transduce self-incompatibility signaling in *Brassica rapa*. Plant Cell 19, 3961-3973.

Kanatani, A. (2008). アブラナ科植物の自家不和合性における情報伝達系の解析. 修士論文（奈良先端科学技術大学院大学）.

Kazama, Y., Saito, H., Yamamoto, Y. Y., Hayashi, Y., Ichida, H., Ryuto, H., Fukunishi, N., and Abe, T. (2008). LET-dependent effects of heavy-ion beam irradiation in *Arabidopsis thaliana*. Plant Biotechnol. 25, 113-117.

Kazama, Y., Hirano, T., Saito, H., Liu, Y., Ohbu, S., Hayashi, Y., and Abe, T. (2011). Characterization of highly efficient heavy-ion mutagenesis in *Arabidopsis thaliana*. BMC Plant Biol. 11, 161.

Koch, M. A., Haubold, B., and Mitchell-Olds, T. (2000). Comparative evolutionary analysis of chalcone synthase and alcohol dehydrogenase loci in *Arabidopsis*, *Arabis*, and related genera (Brassicaceae) Mol. Biol. Evol. 17, 1483-98.

Kosambi, D. D. (1944). The estimation of map distance from recombination values. Annals of Eugenics. 12, 172-175.

Kusaba, M., Dwyer, K., Hendershot, J., Vrebalov, J., Nasrallah, J. B., and Nasrallah, M. E. (2001). Self-incompatibility in the genus *Arabidopsis*: Characterization of the *S* locus in the outcrossing *A. lyrata* and its autogamous relative *A. thaliana*. Plant Cell 13, 627-644.

Kwun, M., Choi, Y., Yoon, H., Park, B. S., Kang, B. J., and Chung, Y. Y. (2004). Expression analysis of the pistil genes in controlling self-incompatibility of *Brassica campestris* by CO_2 gas using microarray. Mol. Cells. 18, 94-99.

Lee, S. C., Lan, W., Buchanan, B. B., and Luan, S. (2009). A protein kinase-phosphatase pair interacts with an ion channel to regulate ABA signaling in plant guard cells. Proc. Natl. Acad. Sci. USA. 106, 21419-21424.

Lee, S. H., Hong, M. Y., Kim, S., Lee, J. S., Kim, B. D., Min, B. H, Baek, N. K., and Chung, Y. Y. (2001). Controlling self-incompatibility by CO_2 gas treatment in *Brassica campestris*: structural alteration of papillae cell and differential gene expression by increased CO_2 gas. Mol. Cells 11, 186-191.

Lewis, D. (1949). Incompatibility in flowering plants. Biol. Rev. 24, 472-496.

Liu, P., Sherman-Broyles, S., Nasrallah, M. E., and Nasrallah, J. B. (2007). A cryptic modifier causing transient self-incompatibility in *Arabidopsis thaliana*. Curr. Biol. 17, 734-740.

Liu, Y. G., Mitsukawa, N., Oosumi, T., and Whittier, R. F. (1995). Efficient isolation and mapping of *Arabidopsis thaliana* T-DNA insert junctions by thermal asymmetric interlaced PCR. Plant J. 8, 457-463.

Lobin, W. (1983). The occurrence of *Arabidopsis thaliana* in the Cape Verde Islands. Arab. Info. Ser. 20, 119-123.

Lowe, A. J., Moule, C., Trick, M., and Edwards, K. J. (2004). Efficient large-scale development of microsatellites for marker and mapping applications in *Brassica* crop species. Theor. Appl. Genet. 108, 1103-1112.

Mather, K. (1943). Specific differences in *Petunia*. I. Incompatibility J. Genet. 45, 215-235.

Matsubara, S. (1980). Overcoming self-incompatibility in *Raphanus sativus* L. with high temperature. J. Am. Soc. Hort. Sci. 105, 842-846.

Matsumoto, A. (2012). アブラナ科植物の和合受粉で機能する雌ずい因子の探索. 修士論文（奈良先端科学技術大学院大学）.

Monda, K., Negi, J., Iio, A., Kusumi, K., Kojima, M., Hashimoto, M., Sakakibara, H., and Iba, K. (2011). Environmental regulation of stomatal response in the *Arabidopsis* Cvi-0 ecotype. Planta 234, 555-563.

Monterio, A. A., and Gabelman, W. H. (1988). Use of sodium chlorid solution to overcome self-incompatibility in *Brassica campestris*. HortScience 23, 876-877.

Murase, K., Shiba, H., Iwano, M., Che, F. S., Watanabe, M., Isogai, A., and Takayama, S. (2004). A membrane-anchored protein kinase involved in *Brassica* self-incompatibility signaling. Sciense 303,1516-1519.

Murray, H. G., and Thompson, W. F. (1980). Rapid isolation of high molecular weight DNA. Nucleilc. Acids. Res. 8, 4321-4325.

Mustilli, A. C., Merlot, S., Vavasseur, A., Fenzi, F., and Giraudat, J. (2002). Arabidopsis OST1 protein kinase mediates the regulation of stomatal aperture by abscisic acid and acts upstream of reactive oxygen species production. Plant Cell. 14, 3089-3099.

Nakanishi, T., Esashi, Y., and Hinata, K. (1969). Control of self-incompatibility by CO_2 gas in *Brassica*. Plant Cell Physiol. 10, 925-927.

Nakanishi, T., and Hinata, K. (1973). An effective time for CO_2 gas trestment in overcoming self-incompatibility in *Brassica*. Plant Cell Physiol. 14, 873-879.

Nakanishi, T., and Hinata, K. (1975). Self-seed production by CO_2 gas treatment in self-incompatible cabbage. Euphytica. 24, 117-120.

Nasrallah, J. B., Kao, T. H., Chen, C. H., Goldberg, M. L., and Nasrallah, M. E. (1987). Aminoacid sequence of glycoproteins encoded by three alleles of the *S* locus of *Brassica oleracea*. Nature 326, 617-619.

Nasrallah, M. E., Liu, P., and Nasrallah, J. B. (2002). Generation of self-incompatible *Arabidopsis thaliana* by transfer of two *S* locus genes from *A. lyrata*. Science 297, 247-249.

Nasrallah, M. E., Liu, P., Sherman-Broyles, S., Boggs, N. A., and Nasrallah, J. B. (2004). Natural variation in expression of self-incompatibility in *Arabidopsis thaliana*: implications for the evolution of selfing. Proc. Natl. Acad. Sci. USA 101, 16070-16074.

Negi, J., Matsuda, O., Nagasawa, T., Oba, Y., Takahashi, H., Kawai-Yamada, M., Uchimiya, H., Hashimoto, M., and Iba, K. (2008). CO_2 regulator SLAC1 and its homologues are essential for anion homeostasis in plant cells. Nature 452, 483-486.

Niikura, S., and Matsuura, S. (2000). Genetic analysis of the reaction level of self-incompatibility to a 4% CO_2 gas treatment in the radish (*Raphanus sativus* L.). Theor. Appl. Genet. 101, 1189-1193.

Nishio, T., M. Kusaba, M. Watanabe, and K. Hinata, (1996). Registration of S alleles in *Brassica campestris* L. by the restriction fragment sizes of *SLG*s. Theor. Appl. Genet. 92, 388-394.

Nou, I.S., Watanabe, M., Isogai, A., and Hinata, K. (1993). Comparison of *S*-alleles and *S*-glycoproteins between two wild populations of *Brassica campestris* in Turkey and Japan. Sex Plant Repord. 6, 79-86.

Obayashi, T., Kinoshita, K., Nakai, K., Shibaoka, M., Hayashi, S., Saeki, M., Shibata, D., Saito, K., and Ohta, H. (2007). ATTED-II: a database of co-expressed genes and *cis* elements for identifying co-regulated gene groups in *Arabidopsis*. Nucleilc. Acids. Res. 35, D863-869.

Ockendon, D. J. (1978). Effects of hexan and humidity on self-incompatibility in *Brassica oleracea*. Theor. Appl. Genet. 52, 113-117.

Ockendon, D. J. (1985). Genetics and physiology of self-incompatibility in *Brassica*. In Plant Cell/Cell Interactions, I. Sussex, A. Ellingboe, M. Crouch and R. Malmberg, eds. (New York: Cold Spring Harbor Press).

Ohara, K. (2010). アブラナ科植物の受粉過程で機能する乳頭細胞内発現遺伝子の探索. 修士論文（奈良先端科学技術大学院大学）.

Okazaki, K., and Hinata, K. (1987). Repressing the expression of self-incompatibility in crucifers by short-term high temperature treatment. Theor. Appl. Genet. 73, 496-500.

Overmyer, K., Brosché, M., and Kangasjärvi, J. (2003). Reactive oxygen species and hormonal control of cell death. Trends Plant Sci. 8, 335-342.

Palloix, A., Herve, Y., Knox, R. B., and Dumas, C. (1985). Effect of carbon dioxide and relative humidity on self-incompatibility in cauliflower, *Brassica oleracea*. Theor. Appl. Genet. 70, 628-633.

Paran, I., and Zamir, D. (2003). Quantitative traits in plants: beyond the QTL Trends Genet. 19, 303-306.

Perchepied, L., Balagué, C., Riou, C., Claudel-Renard, C., Rivière, N., Grezes-Besset, B., and Roby, D. (2010). Nitric oxide participates in the complex interplay of defense-related signaling pathways controlling disease resistance to *Sclerotinia sclerotiorum* in *Arabidopsis thaliana*. Mol. Plant Microb. Interact. 23, 846-860.

Rao, M. V., and Davis, K. R. (1999). Ozone-induced cell death occurs via two distinct mechanisms in *Arabidopsis*: the role of salicylic acid. Plant J. 17, 603-614.

Ramchiary, N., Nguyen, V. D., Li, X., Hong, C. P., Dhandapani, V., Choi, S. R., Yu, G., Piao, Z. Y., and Lim, Y. P. (2011). Genic microsatellite markers in *Brassica rapa*: Development, characterization, mapping, and their utility in other cultivated and wild *Brassica* relatives DNA Res. 18, 305-320.

Schopfer, C. R., Nasrallah, M. E., and Nasrallah, J. B. (1999). The male determinant of self-incompatibility in *Brassica*. Science 286, 1405-1412.

Schranz, M. E., Lysak, M. A., and Mitchell-Olds, T. (2006). The ABC's of comparative genomics in the Brassicaceae: building blocks of crucifer genomes. Trends Plant Sci. 11, 535-542.

Sherman-Broyles, S., Boggs, N., Farkas, A., Liu, P., Vrebalov, J., Nasrallah, M. E., and Nasrallah, J. B. (2007). *S* locus genes and the evolution of self-fertility in *Arabidopsis thaliana*. Plant Cell 19, 94-106.

Shikazono, N., Suzuki, C., Kitamura, S., Watanabe, H., Tano, S., and Tanaka, A. (2005). Analysis of mutations induced by carbon ions in *Arabidopsis thaliana*. J. Exp. Bot. 56, 587-596.

Shimizu, K. K., Shimizu-Inatsugi, R., Tsuchimatsu, T., and Purugganan, M. D. (2008). Independent origins of self-compatibility in *Arabidopsis thaliana*. Mol. Ecol.17, 704-714.

Smyth, D. R., Bowman, J. L., and Meyerowitz, E. M. (1990). Early flower development in *Arabidopsis*. Plant cell 2, 755-767.

Stead, A. D., Roberts, I. N., and Dickinson, H. G.（1980）. Pollen-Stigma interaction in *Brassica oleracea*: the role of stigmatic proteins in pollen grain adhesion. J. Cell. Sci. 42, 417-423.

Stone, S. L., Arnoldo, M., and Goring, D. R. (1999). A breakdown of *Brassica* self-incompatibility in ARC1 antisense transgenic plants. Science 286, 1729-1731.

Stone, S. L., Anderson, E. M., Mullen, R. T., and Goring, D. R. (2003). ARC1 is an E3 ubiquitin ligase and promotes the ubiquitination of proteins during the rejection of self-incompatible *Brassica* pollen. Plant Cell 15, 885-898.

Suwabe, K., Iketani, H., Nunome, T., Kage, T., and Hirai, M. (2002). Isolation and characterization of microsatellites in *Brassica rapa* L. Theor. Appl. Genet. 104, 1092-1098.

Suwabe, K., Iketani, H., Nunome, T., Ohyama, A., Hirai, M., and Fukuoka, H. (2004). Characteristics of microsatellites in *Brassica rapa* genome and their potential. Utilization for comparative genomics in Cruciferae. Breed. Sci. 54, 85-90.

Suwabe, K., Tsukazaki, H., Iketani, H., Hatakeyama, K., Kondo, M., Fujimura, M., Nunome, T., Fukuoka, H., Hirai, M., and Matsumoto, S. (2006). Simple sequence repeat-based comparative genomics between *Brassica rapa* and *Arabidopsis thaliana*: the genetic origin of clubroot resistance. Genetics 173, 309-319.

Suwabe, K., Morgan, C., and Bancroft, I. (2008). Integration of Brassica A genome genetic linkage map between *Brassica napus* and *B. rapa*. Genome 51, 169-176.

Takahashi, H. (1975). Effect of CO2 on self-incompatibility in *Petunia hybrida*. Japan J. Breed. 25, 93-95.

Takasaki, T., Hatakeyama, K., Suzuki, G., Watanabe, M., Isogai, A., and Hinata, K. (2000). The *S* receptor kinase determines self-incompatibility in *Brassica* stigma. Nature 403, 913-916.

Takayama, S., Isogai, A., Tsunemoto, C., Ueda, Y., Hinata, K., Okazaki, K., and Suzuki, A. (1987). Sequences of *S*-glycoproteins, products of the *Brassica campestris* self-incompatibility locus. Nature 326, 102-104.

Takayama, S., Shiba, H., Iwano, M., Shimosato, H., Che, F.S., Kai, N., Watanabe, M., Suzuki, G., Hinata, K., and Isogai, A. (2000). The pollen determinant of self-incompatibility in *Brassica campestris*. Proc. Natl. Acad. Sci. USA 97, 1920-1925.

Takayama, S., Shimosato, H., Shiba, H., Funato, M., Che, F.S., Watanabe, M., Iwano, M., and Isogai, A. (2001). Direct ligand-receptor complex interaction controls *Brassica* self-incompatibility. Nature 413, 534-538.

Takehisa, M. (2009). シロイヌナズナを用いたアブラナ科植物自家不和合情報伝達機構の解析. 修士論文（奈良先端科学技術大学院大学）.

Tanaka, M. (2011). アブラナ科植物の和合・不和合受粉時における乳頭細胞内のCa^{2+}変動解析とCa^{2+}輸送体の薬理学的解析. 修士論文（奈良先端科学技術大学院大学）.

Tao, G., and Yang, R. (1986). Use of CO_2 and salt solution to overcome self-incompatibility of Chinese cabbage (*B. campestris* ssp. *pekinensis*). Eucarpia. Cruciferae Newsl. 11, 75-76.

Tarutani, Y., Shiba, H., Iwano, M., Kakizaki, T., Suzuki, G., Watanabe, M., Isogai, A., and Takayama, S. (2010). Trans-acting small RNA determines dominance relationships in *Brassica* self-incompatibility. Nature 466, 983-986.

Tatebe, T. (1968). Studies on the physiological mechanism of self-incompatibility in Japanese radish. II. Breakdown of self-incompatibility by chemical treatments. J. Jpn. Soc. Hortic. Sci 37, 43-46.

Tateyama, T. (2010). カルシウムイメージング系を利用したアブラナ科植物の受粉・受精機構の解明. 修士論文（奈良先端科学技術大学院大学）.

Tedder, A., Ansell, S. W., Lao, X., Vogel, J. C., and Mable, B. K. (2011). Sporophytic self-incompatibility genes and mating system variation in *Arabis alpina* Ann. Bot. 108, 699-713.

Tsuchimatsu, T., Suwabe, K., Shimizu-Inatsugi, R., Isokawa, S., Pavlidis, P., Städler., Suzuki, G., Takayama, S., Watanabe, M., and Shimizu, K. K. (2010). Evolution of self-compatibility in *Arabidopsis* by a mutation in the male specificity gene. Nature 464, 1342-1346.

Xue, S., Hu, H., Ries, A., Merilo, E., Kollist, H., and Schroeder, J. I. (2011). Central functions of bicarbonate in S-type anion channel activation and OST1 protein kinase in CO_2 signal transduction in guard cell. EMBO J. 30, 1645-1658.

Upton, G., and Cook, I. (1996). Understanding Statistics. Oxford University Press. pp. 55.

Vahisalu, T., Kollist, H., Wang, Y., Nishimura, N., Chan, W., Valerio, G, Lamminmäki, A., Brosché, M., Moldau, H., Desikan, R., Schroeder, J.I., and Kangasjärvi, J. (2008). SLAC1 is required for plant guard cell S-type anion channel function in stomatal signalling. Nature 452, 487-491.

Vahisalu, T., Puzõrjova, I., Brosché, M., Valk, E., Lepiku, M., Moldau, H., Pechter, P., Wang, Y. S., Lindgren, O., Salojärvi, J., Loog, M., Kangasjärvi, J., and Kollist, H. (2010). Ozone-triggered rapid stomatal response involves the production of reactive oxygen species, and is controlled by SLAC1 and OST1. Plant J. 62, 442-453.

Van Ooijen, and J. W. (2006). JoinMap® 4, software for the calculation of genetic linkage maps in experimental populations. Kyazma B.V., Wageningen, Netherlands.

Van Ooijen, and J. W. (2009). MapQTL® 4, software for the mapping of quantitative trait loci in experimental populations of diploid species. Kyazma B.V., Wageningen, Netherlands.

Ward, J. F. (1994). The complexity of DNA damage: relevance to biological consequences. Int. J. Radiat. Biol. 66, 427-432.

Weller, S. G., and Sakai, A. K. (1999). Using phylogenetic approaches for the analysis of plant breeding system evolution. Annu. Rev. Ecol. Ecolsys. 30, 167-199.